Abstract

KUNBERGER, TANYA MARIE KING. Remediation of Soil – Sorbed Cesium Through the Process of Clay Fines Dispersion and Piping. (Under the direction of Dr. M. A. Gabr.)

One of the principle results in the search for the ideal energy source is the insufficient storage and inadequate disposal practices of power generation by-products, which leads to widespread contamination of the subsurface environment. Although regulations have been established controlling current and future storage and transport, as well as addressing the need to remediate contaminated sites; these regulations provide only the desired goal or performance expectations, not a roadmap of how to accomplish remediation.

The research presented herein addressed dispersion and piping of clay fines – colloid mobilization – as a means of remediating subsurface contamination. Prior colloid mobility research has focused on mitigating colloidal movement in order to reduce contamination transport. To date, limited work has been performed to evaluate remediation efficiency associated with the removal of clay-sized (colloidal) particles and related sorbed contamination.

The experimental program consisted of laboratory work, modeling, and a field case study. Laboratory work included fifty flow – through tests on five different soils. Testing was conducted at three ionic strength levels and three induced hydraulic gradients. Thirty-six tests comprised the cesium contamination batch program, which utilized three individual soil types and three ionic strength test levels. Post testing analysis is comprised of mass balance checks for individual testing, grain – size distribution testing, and microscopic analysis of removed colloidal particles. Modeling was applied to link laboratory testing with existing field situations in order to determine the viability of testing at specific field sites. The

proposed model includes a three – phase system, of water, soil, and colloids. After development and application to laboratory results, the model was utilized in conjunction with field data to predict remediation capabilities of colloid mobilization applied through Well Injection Depth Extraction (WIDE) to an actual site contaminated with radioactive cesium.

Results of testing showed the potential of initiating and maintaining clay dispersion and piping. Beneficial effects of increased hydraulic gradients and increased ionic strength are influenced by soil properties such as cation exchange capacity, clay content, and average pore diameter. The tested hydraulic gradient increases resulted in decreased colloidal removal efficiencies for 1:1 clay mineral colloids. Tested hydraulic gradient increases resulted either in continuous increases (10% bentonite) or initial increases then decreases (15% bentonite and natural soil) in colloidal removal efficiencies for 2:1 clay minerals.

Ionic strength effects for the kaolinite and sand combinations were suppressed with increases in hydraulic gradient – although overall trends within each sample were consistent for all ionic strengths and hydraulic gradients. Ionic strength effects for the bentonite and sand combinations and the natural soil were more effective and moderate levels (0.1 M) over elevated levels (1.0 M) for virtually all hydraulic gradients (natural low gradient the exception).

In general, colloid mobilization is hampered by the concept of "more is not always better" – in that extreme levels of mobilization typically result in particle trapping and an overall reduction in colloidal removal. The dispersion and piping of clay fines as a remediation method for the removal of sorbed contamination has the potential to reduce remediation times, as well as reduce some of the health and safety concerns associated with site remediation, relative to methods currently in practice.

Remediation of Soil – Sorbed Cesium Through the Process of

Clay Fines Dispersion and Piping

by

Tanya Marie King Kunberger

A dissertation submitted to the Graduate Faculty of
North Carolina State University
in partial fulfillment of the
requirements for the Degree of
Doctor of Philosophy

CIVIL ENGINEERING

Raleigh, North Carolina

2007

APPROVED BY:

Roy H. Borden, Ph.D., P.E.	Detlef Knappe, Ph.D.
Mohammed A. Gabr, Ph.D., P.E. Chair of Advisory Committee	Dean L. Hesterberg, Ph.D. Co-chair of Advisory Committee

Biography

Born in 1975, Tanya Marie King Kunberger grew up in the mountains of North Carolina with her parents, David and Mary Ann King, and her younger brother Kevin. After graduating as valedictorian from her high school, Tanya moved to Atlanta, Georgia to pursue her studies at Georgia Institute of Technology. She "got out" (graduated) cum laude in 1999 with a Bachelor of Civil Engineering degree and a certificate in Geochemistry, as well as having successfully completed the co-operative education program. Tanya then began her graduate education at North Carolina State University; where she received a MS in Civil Engineering with a minor in Soil Science and then continued on to receive a Doctorate in Civil Engineering. During the course of her graduate work she married her husband, Jeff, and they had two children – Alexander and Annastasia.

Upon graduation Tanya will continue in the academic world as an Assistant Professor in the Department of Environmental and Civil Engineering in the U.A. Whitaker School of Engineering at Florida Gulf Coast University.

Acknowledgements

The author would like to begin by thanking her advisor, Dr. Gabr. His constant support and understanding was a defining factor in the completion of this work. The author would also like to gratefully acknowledge the assistance of her other committee members, Dr. Hesterberg from the Soil Science department and co-chair of her committee, Dr. Borden from the geotechnical group, and Dr. Knappe from the environmental group, both from the Department of Civil, Construction, and Environmental Engineering.

Many, many, many thanks go to Kim Hutchinson in the Soil Science department for all of her assistance in soil mineralogical and contamination testing.

Special thanks to Young Jin for "mobilizing" the colloids in my defense, and to Nadia, Wan Soo, and Hyeseon for enduring the trial runs.

On a personal note – more thanks than can be written go to my mother for living in a tiny bedroom instead of her castle with her King for 18 months while helping raise two energetic (to say the least) little ones. I would have lost it long ago if it weren't for her. And thanks to my father for allowing me to kidnap his queen.

Last, but by no means least, thanks go to my husband. When he signed up "for better or for worse" he had no idea what he was getting himself into. Hopefully the former outweighs the latter, and the balance will continue to shift in that direction. This work is dedicated to him.

Table of Contents

List of Figures

List of Tables

Chapter 1. Introduction

1.1 Background

Since the advent of technology, the acquisition of new and better methods of producing power has propelled the use of natural resources ever higher in search of the ideal energy source. In many cases, however, this trend has resulted in insufficient storage and inadequate disposal practices of power generation by – products leading to widespread contamination of the subsurface environment. Beginning in the 1970's, the United States EPA has established a number of regulations controlling current and future storage, transport, and disposal of waste and addressing the need to remediate existing contaminated sites. However, regulations provide only the desired goal or performance expectations, not a roadmap of how to accomplish remediation. It falls then, to professionals in academia and industry to devise techniques effective in reducing or eliminating contamination levels at sites of concern.

In general, effective in situ remediation at a given site may be hampered by two main factors: 1) contaminant characteristics and 2) subsurface geologic factors including heterogeneity. The first contaminant characteristic of note is the type of contamination. Light Non-Aqueous Phase Liquids (LNAPLs), Dense Non-Aqueous Phase Liquids (DNAPLs), heavy metals, and radioactive elements are the most common; and many sites are tainted with a combination of types. Many of the current clean-up techniques are effective only on certain types of contamination, and some target only specific phases but are ineffective at sites where multiple contamination types and/or multiple phases of contamination exist. Often at sites that fall into this category, compound remediation

measures involving high costs and extended remediation times are required in order to reach acceptable remediation levels.

The second factor hindering remediation is that of subsurface geologic heterogeneity. This factor, while possibly easier to understand, is often more difficult to address. The difficulty arises from the inability to often do little more than simply understand the complexity of the geologic profile. This complexity is the result of a multitude of soil layers, with varying soil types, layer thicknesses, and hydraulic conductivities combined with a groundwater table that often fluctuates seasonally and may possess a hydraulic gradient sufficient to transport contamination significant distances from the source. While some remediation techniques can affect multiple types of contamination with a single method, the only current technique that could be considered to change the subsurface is that of excavation and replacement. This inability to affect change to any degree of significance has forced researchers to develop measures that address some of the more pertinent concerns.

1.2 Problem Statement

Prior research has focused mostly on the desire to mitigate colloid mobility in order to reduce contamination movement or prevent piping that may undermine geotechnical stability. To date, limited work has been performed to evaluate the remediation efficiency associated with the removal of clay – sized (colloidal) particles and related sorbed contamination. Additionally, although many models have been developed that assist in predicting the rate and magnitude of colloidal mobility in various subsurface environments, most again focus on the suppression of colloidal mobility as a means of contamination containment rather than augmenting mobility for site remediation.

1.3 Objectives

Research efforts presented herein will be focused on enhancing colloid mobility in order to facilitate removal of the associated contamination. The primary research objectives are as follows:

1. To evaluate the effectiveness of dispersion and piping on the removal of clay – sized (colloidal) particles and associated contamination from the subsurface environment
    a. Physical Focus: To asses the effect various hydraulic gradients have on dispersion and subsequent removal of colloidal particles
    b. Chemical Focus: To investigate the effect variations in ionic strength have on the dispersion and subsequent removal of colloidal particles
2. To assess the processes associated with seepage forces overcoming shear resistance at grain interfaces to mobilize colloids deposited on larger – sized particles.
3. To quantify how adjustments in the ionic strength of the flushing solution influence the mobilization of colloids through manipulation of clay chemistry.
4. To explain colloidal removal as a function of quantifiable soil properties such as clay content, effective pore diameter, permeability, induced hydraulic gradient, and comparative cation exchange capacities.

1.4 Scope of Work

The proposed research considers utilizing dispersion and piping to remove colloidal particles and the associated contamination from the subsurface environment. While the

majority of previous research in colloidal mobility seeks to limit, rather than enhance, movement; this research desires to promote dispersion and encourage colloidal movement. The use of hydraulic gradient variations has the potential to maximize colloidal removal while minimizing liquid extraction, while the ionic strength manipulation can optimize the time – dependent aspects of colloidal release. The combination of laboratory testing and modeling can give a fairly complete picture of the benefits associated with remediation from colloidal removal.

The work scope for this research consists of four main areas: 1) characterization and concept investigation, 2) performance testing, 3) modeling, and 4) field case study. Characterization and concept investigation involves the compilation of laboratory testing necessary for the advancement of stated research goals. This testing includes basic soil characterization testing, hydraulic conductivity testing, and for any natural soil samples select mineralogical characterization testing. Considering these properties on an individual basis, to the extent possible, facilitates a greater understanding of the contamination issue and possible treatment options / limitations.

A flow chart illustrating the general research program and model development is presented in Figure 1.1. The primary focus areas are in laboratory testing and modeling, with the field study serving as a large – scale justification of modeling based on previous and current research and calibrated from laboratory testing. Laboratory work associated with the field study is necessary in order to obtain relevant model input parameters. Post – testing analysis of laboratory work contributes to the quality assurance / quality control of laboratory testing, but is not required in order to calibrate and test the developed model.

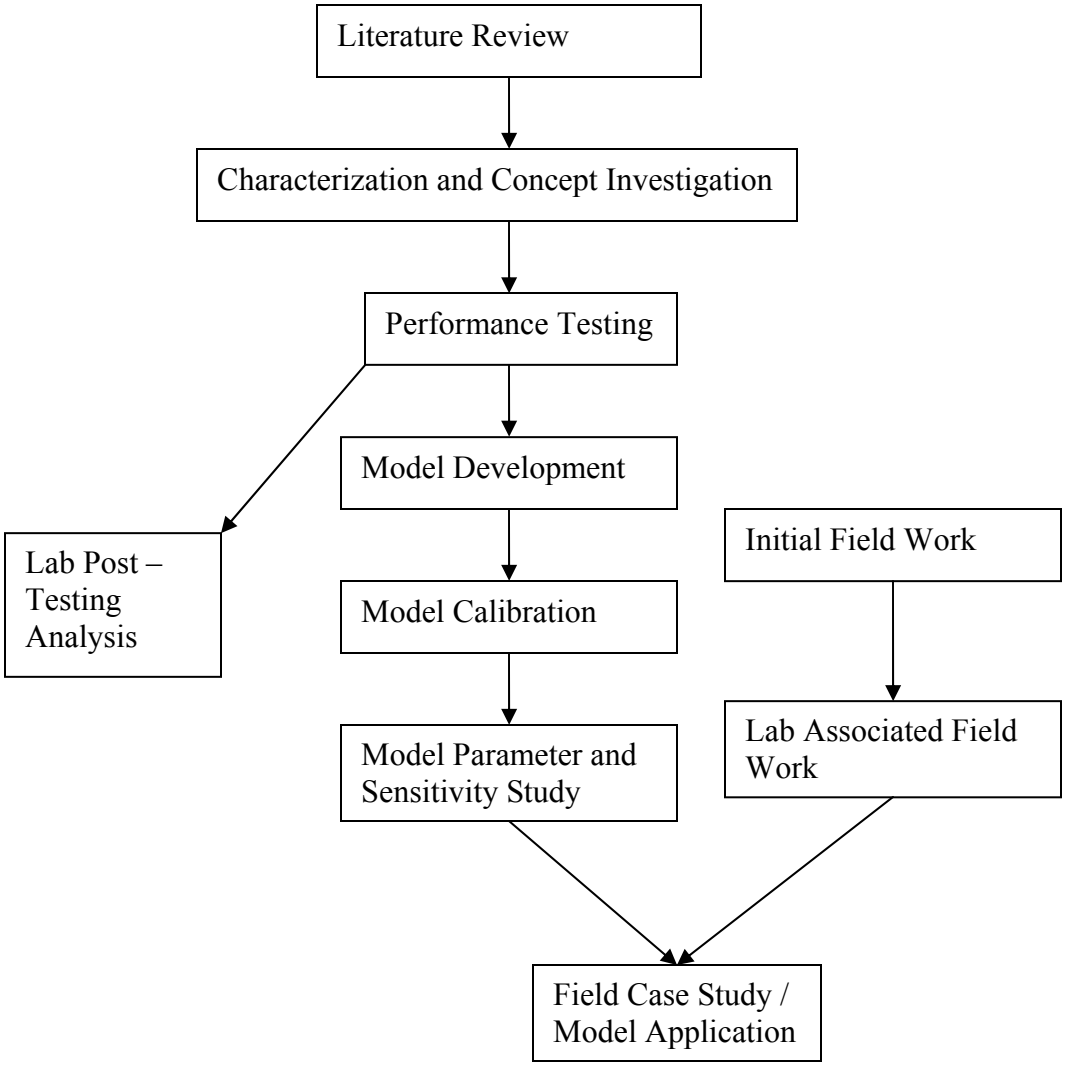

Figure 1.1: Flowchart Detailing Research Program and Model Development

Chapter 1 provides a general introduction, while an in – depth literature review is presented in Chapter 2. The experimental program and materials utilized are enumerated in Chapter 3. Flow – through results are detailed in Chapter 4, followed by micro – analysis of colloidal mobility in Chapter 5, and batch contamination results in Chapter 6. Chapter 7 presents the model development and validation of model results. The field case study is the focus of Chapter 8 and Chapter 9 contains the summary and conclusions. Recommendations for future work are enumerated in Chapter 10.

1.5 Significance of Work

Although the research scope is limited in extent with regards to the type of contamination, it is anticipated that results will be applicable to numerous types of contamination including most radioactive heavy metals and select phases of light and dense NAPLs. An additional potential contribution to the Geoenvironmental field includes the applicability of this remediation to low permeability soils. A decrease in the hydraulic conductivity of a soil typically corresponds to a decrease in the effectiveness of existing remediation measures that rely on removal of contaminants via the aqueous phase. Removal of the sorbed phase of contamination, historically the source of most remediation problems, is another area where this procedure could prove beneficial. Probably the greatest potential contribution however, is the relatively quick remediation times associated with this type of technique over previous remediation measures.

Chapter 2. Literature Review

2.1 History of Problem

In man's never – ceasing search for new and better methods of power production, the ability to transport, contain, and dispose of unwanted by-products tends to take a backseat. With regulations governing these practices comparatively in the infant stage when waste was generated in significant quantities, it is not difficult to understand the magnitude of contamination caused by many years of uncontrolled and unregulated activities. What is difficult, however, is the development of effective remediation procedures to restore contaminated sites back to pre-spill conditions (i.e. brownfield restoration) and the implementation of regulations to reduce and eliminate future contamination. Significant progress has been made both in the area of remediation and regulation, but more needs to be accomplished in order to repair the magnitude of the environmental damage.

Generally, research occurring even as recently as the 1990's considered a two phase system for contaminant analysis … that is the thought that sorbed contaminant is immobile within the soil matrix while dissolved contaminant is the only mobile phase. Increasing knowledge of contaminated sites and movement of contamination has recently discarded this two phase system approach in favor of a more accurate three phase system of immobile sorbed contamination bound to the soil matrix, mobile dissolved contamination in the groundwater, and sorbed contamination bound to mobile colloids. The addition of this third, and previously unconsidered, phase has further complicated an already complex problem.

The various phases of contamination with respect to the three – phase system are schematically illustrated in Figure 2.1.

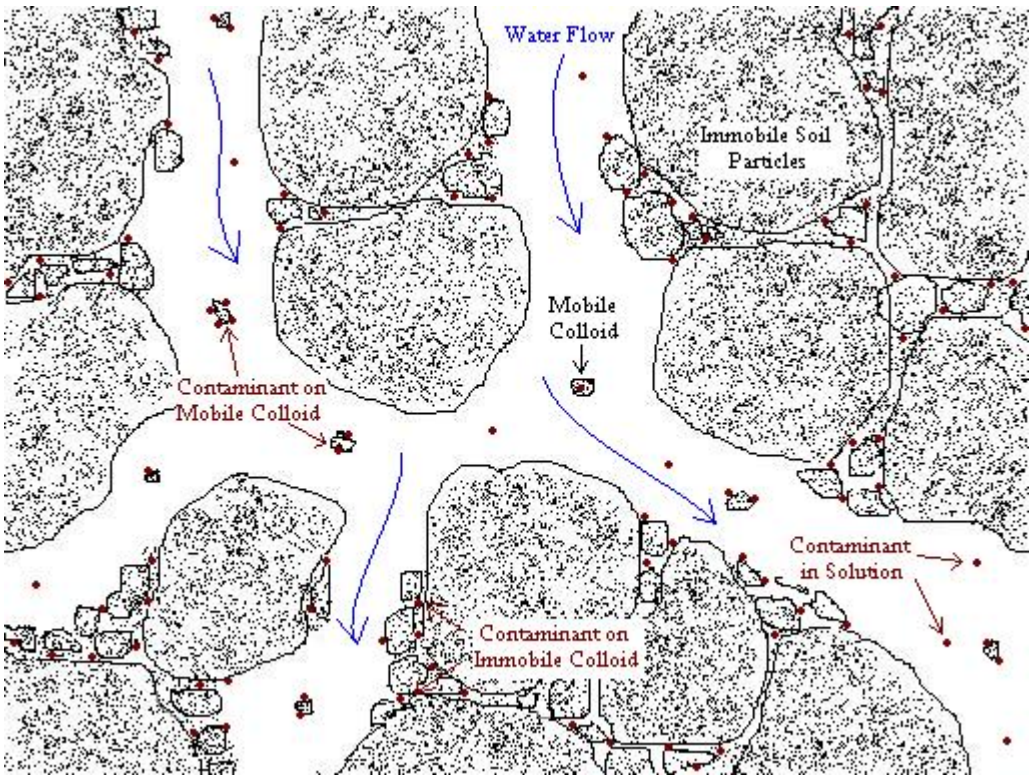

Figure 2.1: Various Phases of Contamination

Sorbed contamination, illustrated by (●), is shown to be attached to both mobile and immobile colloidal particles. Additionally, mobile concentration not associated with colloidal particles is also illustrated with (●). This contamination can be present in either the dissolved phase or as a droplet or precipitate. The dissolved phase is more likely to be the mobile phase with the precipitate or free product being immobile, but it is possible to mobilize precipitate as colloids themselves and free product in the same manner as pore water. While Figure 2.1 illustrates contamination in a three – phase system of dissolved – mobile, sorbed – mobile, and sorbed – immobile; it does not indicate relative concentrations. These relative concentrations affect the system equilibrium, and become one of the major

influences of extended spatial and temporal contamination. As a final note, this system is a saturated one; if saturation was less than 100 percent two additional factors would need to be considered. The first is that the vapor phase would also need to be factored into equilibrium and contaminant concentrations. The second is the incorporation of air – water interfaces, which have a high energy that could assist in colloid mobilization.

2.2 History of Colloids

In a 1990 article from Environmental Science and Technology, Penrose et. al. writes "colloidal materials … are capable of binding and transporting radionuclide contaminants in the subsurface system. It is likely that colloid – mediated mobility of radionuclides and other contaminants will be encountered in many other locations once investigators have become aware of its importance." Prior to this point, the existence of colloids was thought to be divided into two distinct types: harmful and benign. Those colloids, or particles in the sub-micrometer range, deemed harmful in the groundwater setting were mainly viruses and bacteria, while minerals that fell into the size and mobility category to be classified as colloids were considered benign. The realization that these otherwise benign minerals could, in fact, sorb harmful contamination, thus transporting it in the subsurface system, created the need to further consider methods of colloid generation and mobility in the subsurface environment.

2.2.1 Colloid Generation

"Colloids in groundwater originate from two sources: (1) mobilization of existing colloid – sized minerals in the aquifer sediments and (2) *in situ* precipitation of supersaturated mineral phases" (Ryan and Elimelech, 1996). Figure 2.2 illustrates the presence of 4.8 μm mineral colloids on 1 mm sand grains.

Figure 2.2: Picture of Colloids on Sand (from cover of Vadose Zone Journal, May 2004)

The existence of pure minerals or soil particles that fall into the range of colloid – sized material is unquestionable, thus the mobility of colloids is not so focused on the creation of these particles, but rather on the association with contamination, which converts the benign colloid into a potentially harmful one. The significance of the sorbing properties of these colloidal – sized particles is what makes colloid generation such a serious concern with regards to contaminant transport. Particles of this size are often composed of clay minerals, which possess high specific surface areas and cation exchange capacities. Specific surface area is the ratio of the available surface of a particle to the mass of that particle.

Cation exchange capacity is the degree to which a soil can weakly adsorb and exchange cations. The combination of large surface areas, with associated low masses, that can freely sorb and exchange cations is an ideal location for many forms of some contamination. Add to this the hydrophobic nature of many of the contaminants of concern, and it is clear that these contaminants would prefer to sorb to the soil surface, rather than dissolve in the groundwater or volatilize in the air phase.

2.2.2 Colloid Mobility

Although the generation of colloids in the subsurface environment is a forgone conclusion, the mobility of these colloids is more open to discussion. In order to achieve mobility, some form of chemical or physical perturbation is necessary. From a chemical point of view, studies have shown that "the stability of a colloidal suspension is largely affected by the thickness of the diffuse part of the double – layer around particle surface … [with the] stability of suspension approximately related to ionic strength" (Rivto, 2003). This suggests that a decrease in the ionic strength of a flushing solution would increase the thickness of the diffuse double layer for particles and thus increase the mobility of colloids in the subsurface. Conversely, an increase in the ionic strength would compress the diffuse double layer, reducing the repulsive forces, and result in a flocculation of colloidal materials. Although ionic strength variations are the most common chemical perturbation that can affect colloid mobility; others exist, such as changes in pH or surface charge variations. Of particular importance is the fact that these chemical perturbations "commonly occur in contaminant plumes, thereby generating colloids in the midst of contaminants" (Ryan and Elimelech, 1996).

On the other hand, the physical perturbation most commonly associated with colloid mobility is that of flow velocity variations. Increases in flow velocity increase the hydrodynamic shear applied to colloids and often initiate colloidal movement. These flow velocity increases can either be natural, as in the case of rapid infiltration due to rainfall events; or man made, as in the case of various pumping schemes. Either application has the potential to raise the shear force on colloidal particles enough to initiate movement, but it is possible in both cases to increase the flow velocity without actually reaching the shear force necessary to initiate colloid mobilization. Kosakowski (2004) notes that "if colloids have the same charge as the wall material of the fracture, repulsion effects tend to move colloids more to the center of the fracture where water velocities are higher. This causes the average colloid velocities to be larger than the average water velocities." Additional factors that need to be considered with respect to flow velocities and colloid mobility are the length of time of the increased flow, flow directions, delays associated with infiltration or schematic pumping, and air – water interfaces if unsaturated conditions are present. Unusually high fluid velocities may actually initiate movement of particles outside the size range of typical colloids. This movement, while increasing the mass of soil particle, may not affect the mass of contaminant removal, as the contamination may not be associated with the larger mobilized particles.

An additional consideration with colloidal mobility, whether by chemical or physical means, is the effect of plugging or clogging of the soil fabric and the associated reduction in the hydraulic conductivity. This reduction can decrease the rate of colloidal mobility not only by reducing the flow velocities, but also by reducing the number and size of available flow paths through which colloids can travel. Ryan and Elimelech (1996) stress the

importance of this fact and state "clogging by clay dispersion, where mobilized particles are deposited in narrow pore throats, is irreversible without a change in flow direction." The likelihood of plugging or clogging seems to be related to soil mineralogy and aquifer formation, and can vary greatly from site to site.

2.3 Colloid – Facilitated Transport

As the concept of a three – phase system on contamination became more widely recognized and applied, previously unexplained phenomenon suddenly became more clearly understood. The mobility of contamination sorbed to colloidal particles increases the spatial influence of that contamination, not only in the sorbed phase, but also in the dissolved phase. This fact is due to the re-equilibrium of dissolved and sorbed phase contamination at some distance from the initial point of contamination. This distance is where contaminated colloidal particles have reached, but dissolved contamination has not yet arrived. "As the strength of the contaminant – colloid association increases, the time to reach desorption equilibrium increases, resulting in increased distances for colloid – facilitated transport" (Ryan and Elimelech, 1996). So for those contaminants that are strongly bound and hydrophobic in nature, the mobility of colloidal particles to which they are attached can provide a significant transport mechanism to allow migration far from the original source. The kinetics of colloid mobilization is complicated and "the destabilization of suspended colloids in groundwater … does not necessarily mean that they will be rendered immediately immobile" (McCarthy and Zachara, 1989). Therefore it becomes necessary to consider, not only the association of the contaminant with the colloidal particles, but also the colloids with the rest of the subsurface environment.

2.4 Previous Colloid – Facilitated Transport Studies

Numerous studies have been conducted with regards to colloid – facilitated transport of contaminants. While some have considered laboratory column studies (e.g. Saiers and Hornberger, 1996, Grolimund et. al., 1996, Roy and Dzombak, 1997, Gamerdinger and Kaplan, 2001, Chen et. al., 2005, Levin et. al., 2006), others have focused on field conditions (e.g. Penrose et. al., 1990, Ryan et. al., 1998, Kersting et. al., 1999, Nimmo et. al., 2004). Many have considered the role physical and chemical perturbations have played, with factors such as flow rate variations and changes in pH and ionic strength. A few have considered the effects pore structure and preferential flow have on overall mobility. Some have considered colloid dispersion as a function of clay mineralogy, total clay content, and soil moisture content. Whichever focus the research takes; most consider these effects in terms of one or more of three main issues: (1) dispersion or release of in situ colloids, (2) size and stability of the dispersed colloids, and (3) pore size and geometry of the actively conducting pore system. Figure 2.3 illustrates these three processes in a simplified and general manner.

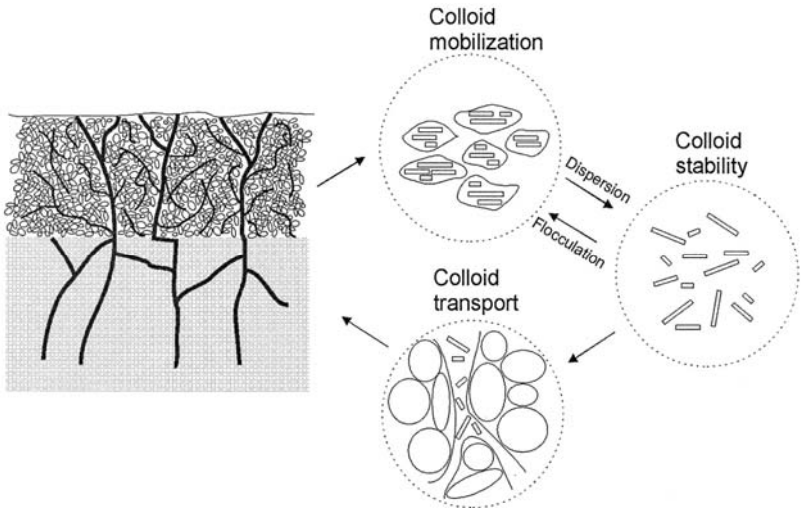

Figure 2.3: Three main processes to consider in colloid – facilitated transport (from de Jonge, et. al., 2004)

2.4.1 Laboratory Studies

Column experiments, on a small or large scale, are the most common testing method for analyzing colloidal transport in the laboratory environment. The type and focus of these experiments, however, are distinctly more varied. On one extreme Roy and Dzombak (1997) utilized both artificial (latex) colloids and an artificial (glass bead) "soil" matrix for testing. At the other end, researchers have employed undisturbed soil columns for testing colloidal transport (Rousseau et. al., 2004). Between these two extremes there has been countless research utilizing a range of disturbed samples of natural soil (Grolimund et. al., 1996, Schelde et. al., 2002, Grolimund and Borkovec, 2005) to natural soil matrices with artificial colloids (Gamerdinger and Kaplan, 2001) or manufactured soil matrices of quartz sand with manufactured kaolinite colloids (Saiers and Hornberger, 1996). One study (Chen et. al., 2005) even separated the natural soil colloids from the rest of the natural sample, before utilizing both in the same test. Experiments considered the introduction of colloids in the influent water (Saiers and Hornberger, 1996, Gamerdinger and Kaplan, 2001, Chen et. al., 2005) as well as the mobilization of intact sample colloids (Schelde et. al., 2002, Rousseau et. al., 2004, Levin et. al., 2006). Variations in contamination, pH, ionic strength, and flow velocities were all considered in diverse combinations. The goal for most of these tests was a better understanding of the nature of colloidal mobilization, transport, and deposition; but with the purpose of minimizing such transport.

2.4.2 Field Site Studies

Unlike the relatively controlled conditions present in the lab, the study of colloidal behavior in the field is a more daunting task, complicated first and foremost by limitations

associated with obtaining access to a contaminated site and procuring permits which allow for site testing and manipulation. Many of the field sites on which research has been conducted are current and/or former government test sites or disposal sites. These include the Los Alamos National Laboratory, Rocky Flats Plant, the Nevada Test Site, Idaho National Engineering and Environmental Laboratory, and Nagra's Grimsel Test Site. All five areas are contaminated with some form of radioactive waste, and a major focus at each is the extent to which this contamination has migrated both within site boundaries as well as off – site.

2.4.2.1 Los Alamos National Laboratory

Concern at the Los Alamos National Laboratory in New Mexico is focused on the treated waste effluent which has been discharged into Mortandad Canyon since 1963. Although water treatment acts to remove the majority of actinides from the waste, traces of plutonium and americium can still be found in the effluent. While contamination is limited to laboratory boundaries, no regulations have been exceeded, and no water is derived from the canyon itself, detectable levels have been found as far as 3390 meters downstream – a drastic increase from the laboratory study that predicted limit of less than a few meters. The benefit of this migration is that "these trace level actinides act as excellent tracers to evaluate the potential for colloidal transport of subsurface groundwater contaminants" (Penrose et. al., 1990).

Results from the study found "that the actinides, plutonium and americium, are associated with colloidal materials in a way that is effectively irreversible" (Penrose et. al., 1990). Additionally, the plutonium, and to some extent the americium, that is bound to the

colloidal particles 25 – 450 nm in size can not be exchanged with the adsorption sites on the immobile soil matrix and thus are transported to distances congruent with colloidal transport rather than subjected to typical retarding forces associated with adsorption exchange. The combination of these two factors leads to the observation that "colloidal materials can be mobile in groundwater systems for great distances and are capable of binding and transporting radionuclide contaminants in subsurface systems" (Penrose et. al., 1990).

2.4.2.2 Rocky Flats Plant

In 1998 Ryan et. al. published a study on the effect of rainfall infiltration on plutonium mobilization at the Rocky Flats Plant. Located near Denver, Colorado, the area of study at the plant was the former storage area for drums containing plutonium – contaminated oils. Due to the depth of the groundwater table relative to the depth of contamination migration, groundwater flow does not present a large concern for migrating contamination. Instead, rainfalls, or similar infiltration events, are the focus of concern. Ryan et. al. simulated rainfall events "by applying water over the upslope side of the pits following [a certain schedule, most simulations of which] approximately represents the rainfall intensity of the 100 – year return event for this area. The rainfall was delivered by a triple-nozzle sprayer that traveled back and forth" (Ryan et.al., 1998). Samples were then collected from different locations and depths and measured for volume, colloid concentration, and plutonium activity.

Results found that plutonium activity decreased with depth, and closely related to the particle concentration reinforcing "the assumption that plutonium transport is dominated by particles" (Ryan et. al., 1998). Contrary to what was expected however, was the apparent

lack of relationship between particle concentrations and infiltration velocities as well as particle size and infiltration velocities. The authors believed these "lack of correlations between particle concentration, particle size, infiltration velocity, and soil type may be caused by the dominance of macropore flow;" (Ryan et. al., 1998) a feature of soils that can not be replicated in recreated samples for laboratory column studies. Because the study focused only on rainfall infiltration, the influence of macropores on groundwater flow was not discussed, and may or may not play as important of a role in colloidal transport for horizontal flow applications. Either way, the role of macropores does not diminish the importance of colloids on plutonium transport in the subsurface environment.

2.4.2.3 Nevada Test Site

As with the previous two studies, plutonium, as well as various other radionuclides, was the contaminant of concern in a 1999 article in *Nature*. The site under consideration is the Nevada Test site, located in the southern portion of the state and subjected to contamination from nuclear storage, production, and testing. This site "provides a unique opportunity for studying the transport of radionuclide contaminants" because of its "large inventory ($>10^8$ Curies) of radioactive material deposited in the subsurface [from] 828 underground nuclear tests conducted by the United States between 1956 and 1992" (Kersting et. al., 1999). Both soil and groundwater samples were collected and tested, with groundwater samples filtered to allow for testing of colloidal particles as well as dissolved species.

Results "found that > 99% of the Eu and Pu isotopes, ~91% of the Co, and 95% of the Cs in the groundwater were associated with the colloidal and particulate fractions" (Kersting

et. al., 1999). To further determine the particle sizes with which radioactivity was most associated, a "comparison of the radioactivity of the colloids collected on different filter sizes and the ultrafiltrate fraction" was conducted and normalized to the unfiltered water. For all isotopes listed above, almost 20% were found to be on the > 1μm fraction, and roughly 40% on each of the 50 nm – 1 μm and 7 nm – 50 nm fractions. Less than 10% of the Co and Cs isotopes and virtually none of the others were found in the ultrafiltrate fraction – that portion that passed the 7 nm filter. A study of the extent of contamination suggests that mobilization is most consistent with migration in colloidal form, not as dissolved species, and is focused on a relatively limited size range (7 nm – 1 μm). One concern the authors mention is that the increased rates due to sample pumping could increase groundwater colloidal concentrations and skew some of the results. They note, however, that this bias would be with respect to mass only and not to the sorption levels of various contaminants. Kersting et. al. concludes by saying that "transport models that only take into account sorption and solubility may therefore underestimate the extent to which this species is able to migrate in groundwater" (1999).

2.4.2.4 Idaho National Engineering and Environmental Laboratory

Radioactive waste buried from 1952 to 1997 at Idaho National Engineering and Environmental Laboratory's (INEEL) Subsurface Disposal Area (SDA) compromises "approximately 215,000 m^3 of low-level and transuranic waste containing about 12.6 million Ci of radioactivity" (Nimmo et.al., 2004). Composed of everything from containerized waste to contaminated asphalt and soil, the complete nature of contamination at the site is not fully known. What is known, however, is that contaminant concentrations that "slightly exceed

the essentially zero background concentrations have been detected in the surficial sediments … [and] are a potential source of contamination to the vadose zone and ultimately to the eastern Snake River Plain aquifer" (Nimmo et. al., 2004). This has prompted concern regarding the potential transport mechanisms for various types on contamination.

A 2004 Vadose Zone Journal article discusses the various "features and processes relevant to the issue of buried waste at the SDA" (Nimmo et. al., 2004). What resulted, with regards to colloids and colloidal transport, was that often "conditions that inhibit solute transport may be favorable for colloidal transport" and that colloidal transport itself "inverts some of the traditional concepts of mobility, as sorbed contaminants on mobile colloids may be transported with ease compared with contaminants that are not sorbed" (Nimmo et. al., 2004). A summary of testing conducted by other individuals at the same site mentions "colloid concentrations ranging from 1.8 to 9.8 mg/L in groundwater at INEEL" and filtration tests resulting in "about 25% of the Pu [being] removed by 0.05-μm filtration, suggesting association with colloids" (Nimmo et. al., 2004). A number of other features, including preferential flow, solute transport, and spatial and temporal geochemical variability are also discussed as contributing factors to contaminant transport; colloid mobility is simply one of many concerns at this, and other, sites. The research shows though that the importance of colloids in contaminant transport can not be denied.

2.4.2.5 Nagra's Grimsel Test Site

Situated in the crystalline rock of the Aar-massif in the Alps of Switzerland, Nagra's Grimsel Test Site is the location of the Colloid and Radionuclide Retardation (CRR) experiment. Although many tests were conducted on the site, Kosakowski (2004) focuses on

two which allow for an evaluation of colloidal and solute tracer tests and the comparison "of experimental results with numerical studies and with the evaluation of the colloid breakthrough with continuous time random theory" (Kosakowski, 2004). Suspensions of bentonite, in concentrations approximating 20 mg/L, are the injected colloidal test element, while uranine serves as the non – sorbing solute tracer. The testing location is a 5-meter length of shear zone situated between injection and extraction boreholes, and extraction at a rate 15 times greater than injection assured complete recovery of the conservative tracers.

Results show both the uranine and colloids to behave in a fashion typical of transport with matrix diffusion. Uranine recovery was over 90%, while total bentonite recovery was 55% and varied based on size. Colloidal concentrations were corrected for the presence of natural background colloidal mobilization by monitoring this background concentration prior to testing and subtracting natural levels from the measured colloidal concentration levels during testing. Table 2 summarizes the colloid recovery as a function of size and is based on information from Kosakowski's 2004 article in the *Journal of Contaminant Hydrology*.

Table 2.1: Colloid recovery as a function of size (from Kosakowski, 2004)

Colloid Size	Percent Recovered
Total Colloids	55% (by mass)
50 – 100 nm	90% (by number)
100 – 150 nm	100% (by number)
150 – 200 nm	100% (by number)
200 – 300 nm	40% (by number)
300 – 500 nm	16% (by number)

Recovery variations are likely due to filtration during transport. "The dependence of the degree of filtration on colloid size suggests that gravitational settling and/or mechanical filtration are the most likely immobilization mechanisms" (Kosakowski, 2004). Despite this filtration, a considerable portion of the colloids (especially in the 50 – 200 nm range) still remain mobilized in the system and, if associated with contamination, can provide a significant source of contamination transport.

2.5 Prior Modeling of Colloidal Behavior

Although a number of different models have been developed in order to try and predict the behavior of colloid generation and mobility (Khilar et. al., 1985, Kaplan et. al., 1993, Grolimund et. al., 1996, Saiers and Hornberger, 1996, Schelde et. al., 2002, Grolimund and Borkovec, 2005), most focus on the desire to inhibit colloidal movement and / or predict colloidal deposition. While the amount and rate at which colloids are deposited in the system are important factors to consider in this research, the focus is more on the amount and rate at which these colloids, and the associated contamination, can be mobilized in order to be removed from the soil system. Additionally, many of the existing models focused on the initial conditions of existing colloidal concentration in the flushing solution – and considered reduction in this concentration rather than an increase due to removal of additional colloidal particles from the soil matrix. Because these conditions are also not representative of the research under consideration, it is necessary to develop a new model that more effectively considers the existing conditions. In order to develop such a model, a number of important points need to be taken into account. These include the effects of physical and chemical perturbations, complexity of the soil matrix, and relevant initial conditions.

2.5.1 The Role of Physical Perturbations on Colloid Mobilization

Without fluid movement, the issue of colloid mobilization would be moot. And yet to date, research is still discussing the relative importance of hydrodynamic shear on the rate of colloidal generation. A number of researchers (Khilar et. al., 1985, Kaplan et. al., 1993, Khilar and Fogler, 1998, Laegdsmand et. al., 1999) support the theory that once sufficient hydrodynamic shear is developed due to adequate fluid flow velocities, colloid mobility is initiated and maintained until fluid velocity drops below the shear threshold. Their research supports the necessity of sufficient flow velocities to the initiation of colloid generation and subsequent mobility as well as a correlation between variations in these flow rates and concentrations of colloids in the effluent. Khilar et. al. (1985) even go so far as to enumerate a method for determining the initial flow rate required in order to initiate erosion. Based on soil parameters such as hydraulic conductivity, porosity, and critical shear stress, a minimum velocity can be calculated which would induce piping (i.e. colloid mobility) in the soil matrix.

In contrast, some researchers (Grolimund et. al., 1996, Jacobsen et. al., 1997, Levin et. al., 2006) have expressed a kinetic limitation to particle release while others (Schelde et. al., 2002) discount the concept almost totally. Levin et. al. (2006), assert that the number of pores contributing to fluid flow plays the critical role in colloid mobilization. Their research focuses on a comparison of fluid velocities and developed shear forces versus what they call the "colloid supply mechanisms" as the controlling function for colloid mobility. Results support supply mechanisms as the dominating function – indicating that colloid mobilization is related to the number of soil pores capable of transporting colloids. When flow is

"constrained to fewer soil pores, the total number of pores capable of transporting colloids is decreased" (Levin et. al., 2006).

Schelde et. al. (2002) state that results from laboratory testing suggested that "the irrigation rate did not affect the total amount of mobilized particles." While the stress associated with the increase in flow rate does not appear to enhance colloid mobility, it is important to note that these higher rates do result in an increase in colloidal detachment as a function of time. This increase is due more to the increase in total flow volume, rather than the increase in flow rate, with the implication that the hydraulic shear, due to the increased velocity created by the influent flow rates is not a contributor to colloidal release. With respect to flow interruptions, testing found that greater lengths of flow interruptions (i.e. 1 or 7 days versus 30 minutes) resulted in significantly higher peak concentrations of colloids in the effluent solution collected when infiltration re-commenced after these interruptions. The reasoning behind these results is based on the diffusion rates of colloids from the various phases in the soil sample, and suggests that the diffusion across these phases is the rate-limiting step for colloidal removal. This data set indicates that hydraulic shear is not a contributing factor to colloidal release rates, and that considering the mass of colloids removed as a function of accumulated outflow is a more accurate basis for comparison of mobilization of colloids from the stationary phase.

2.5.2 The Role of Chemical Perturbation on Colloid Mobilization

In contrast to the divided opinion with respect to physical perturbations, the role of chemical modifications appears to be less controversial – at least in a broad sense. Although many types of chemical perturbations exist, e.g. pH variations, chemical composition of pore

fluid, changes in ionic strength, and modifications of ion charge (i.e. the change from mono to divalent and vice versa); most research admits that ionic strength and charge plays the key role in affecting movement (Saiers and Hornberger, 1996, Grolimund et. al, 1996, Gamerdinger and Kaplan, 2001, Rousseau et. al., 2004, Grolimund and Borkovec, 2005).

Saiers and Hornberger stated that "a major obstacle to understanding facilitated transport is an absence of experimental data coupled with a lack of evaluations of models for describing the phenomenon" (1996). This led to their development of the facilitated transport model (FTM), which is a three-phase transport model based on earlier research by Corapcioglu and Jiang (1993). In a set of articles, Saiers and Hornberger (1996 and 1999) analyzed the transport of cesium on kaolinite particles through sand columns in order to determine the effects colloidal concentration in the pore water and ionic strength of the pore water have on the migration of cesium contamination.

The FTM was based on a set of five governing equations that are both algebraic and partial differentials, and describe mass transfer, sorption – desorption, and advection – dispersion for the solid – water – colloid system under consideration. Results from laboratory testing and model development suggested that "the degree to which the transport of radionuclides (and other trace constituents) in aquifers is facilitated by colloids depends strongly on the chemical composition of groundwater" (Saiers and Hornberger, 1999). The accuracy of the model, while promising, is not outstanding. The main failing in the accuracy of the model is in its ability to "estimate the full complement of model parameters on an independent basis" (Saiers and Hornberger, 1999). The authors feel that this is due to the highly sensitive nature of the model with respect to minute changes in parameter input

values. Thus, they recommend caution when "transferring mass transfer parameters from one set of experiments to another" (Saiers and Hornberger, 1999).

Probably the most direct analysis of the effect of ionic charge variation is presented by Grolimund and Borkovec in their 2006 article in *Environmental Science and Technology*. Laboratory experiments showed alternate flushing not only due to different levels of ionic strength solutions, but also due to different compositions of ionic strength solutions through various soil columns. Ionic strength solution compositions varied from monovalent to divalent cations in order to determine the effect of ionic charge on the release of colloids from a contaminated system. The model is calibrated based on extensive laboratory experiments, and was shown to be valid for colloidal transport within and out of contaminated zones. The major focus of modeling was to "address the question of how colloid facilitated transport can be suppressed" (Grolimund and Borkovec, 2005). The primary scenario under consideration is that of a contaminated zone within an area of high concentrations of monovalent cations which is inundated with a large quantity of lower salinity flushing liquid. This scenario is equivalent to sustained periods of rainfall infiltration to contaminated areas under leachate fields (e.g. waste disposal sites). Modeling results suggest the suppression of colloidal movement by the injection of high levels of divalent ionic strength solution. The complication with this measure is the delicate balance required to suppress colloidal release and not induce ion exchange between the injection fluid ions and contaminated particles, thereby releasing contamination in a dissolved, rather than colloid-sorbed form.

2.5.3 The Role of Sample Matrices and Initial Conditions

One of the main limitations associated with prior models is the lack of appropriate sample matrices and initial conditions with respect to the research under consideration. This is due mainly to a difference in the primary focus of previous modeling studies – i.e. suppression of colloid mobility or determination of colloidal deposition from influent permeant – rather than from inherent errors in the modeling process.

In a 2001 article in the Journal of Contaminant Hydrology, Sun et. al. stated that "detailed yet realistic models for colloid transport in subsurface porous media are needed, [however] to date, most available models for colloid transport … consider only physically homogeneous porous media." Because of this, Sun et. al. developed a two – dimensional model that considers both physical and geochemical heterogeneities and combines colloid transport and fluid flow equations to describe colloidal mobility. Both layered and random physical heterogeneities were investigated, with the main characteristic under consideration that of hydraulic conductivity. The layered approach considered several homogeneous layers that combine to form a heterogeneous system, while the random approach considered a lognormal distribution of values. The geochemical focus was on that of ferric oxyhydroxide coatings, which provide "favorable sites (areas) for colloid deposition because they are positively charged whereas the majority of subsurface colloidal particles are negatively charged" (Sun et. al., 2001). This heterogeneity was described by a patch model, which defines favorable versus unfavorable areas of deposition and considered in both layered and random methods similar to the physical heterogeneities above.

Although no laboratory or field studies accompanied the model development, the authors validated the numerical solution of the code with an earlier – derived analytical

solution, finding the results to be in "very close agreement" (Sun e. al., 2001). Results showed "both physical and geochemical heterogeneities play an important role in colloidal transport" (Sun et. al., 2001). The layered approach for both physical and geochemical variations independently resulted in preferential flow, with combined effects magnifying or minimizing this preferential flow. Random physical differences also resulted in preferential flow, creating irregular distributions in colloidal concentrations within the profile. While random geochemical differences did not significantly affect colloid transport behavior, it is important to note that the mean value does affect colloidal movement.

In 2002 Schelde et. al. published an article discussing the Equivalent – Macropore Model. The model was based on laboratory soil column experiments the authors developed because "filtration theory and modeling of colloid transport kinetics have focused on homogeneous porous media, … yet these theories do not apply well to natural porous media characterized by wide particle-size distributions and complex pore geometry" (Schelde et. al., 2002). Instead of considering glass beads, like many previous experiments, work from this program was performed on undisturbed soil columns of a sandy loam. Figure 2.4 illustrates the general concepts of the model with the macropore inserted within the soil matrix. The walls of the macropore consist of a region of immobile water, which the colloids must diffuse through before reaching the mobile water, which can exit the soil matrix.

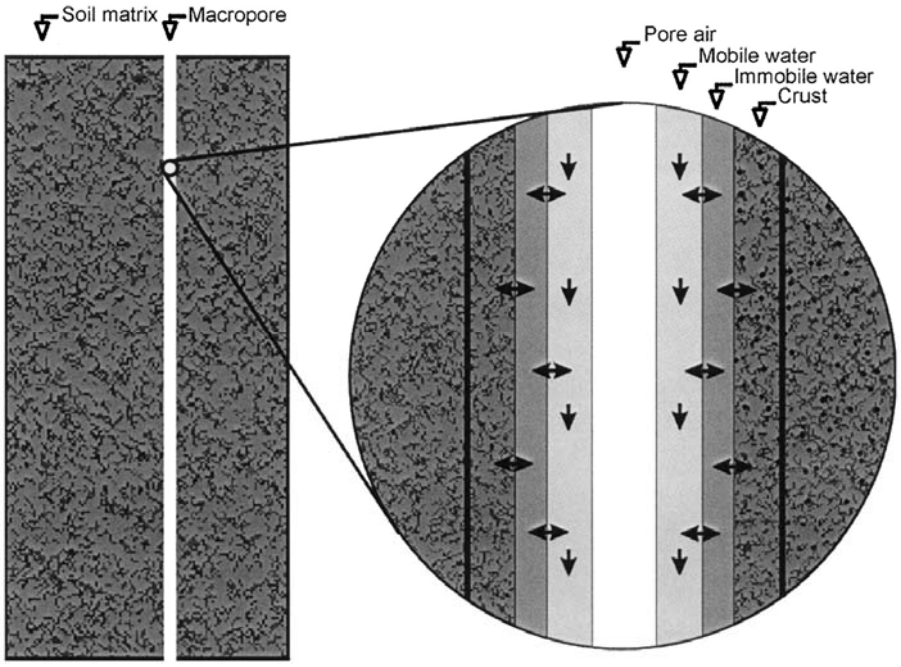

Figure 2.4: Illustration of Equivalent Macro-Pore Model Concept (from Schelde et. al., 2002)

The work focuses on the effect of various flow rates and flow interruptions of the soil solution and the time-dependent nature of the colloidal release process from the soil matrix into the soil solution.

Although natural soil samples are utilized in lieu of glass beads in Chen et. al.'s 2005 work, the colloidal material was first stripped from the soil, the non-colloidal soil was packed into columns, and the colloidal material was then contaminated and flushed through the columns. The goal was to determine the rate of colloidal deposition in addition to the relative affinity for contamination for both the colloidal and remaining soil sediment. The reasoning behind the initial removal of colloidal material from the soil column was to prevent in situ colloid mobilization which would have affected the accuracy of effluent results.

While the theory behind these models and laboratory tests are relevant to the study of colloidal mobility; in the context of enhancing contaminant remediation by the process of

colloidal removal and modeling this practice, the current models are not sufficient. To this end, a model based on the initial conditions of existing contamination, existing colloids within the soil matrix and flushing of various ionic strength solutions at different induced hydraulic gradients will be developed with a concentration on enhancing the colloidal mobility and subsequent removal as a means of contaminant remediation.

2.6 WIDE System

WIDE technology was developed and demonstrated by researchers from North Carolina State University (NCSU) and funded by the US DOE National Energy Technology Laboratory (NETL) for almost eight years (US DOE 2001). WIDE is an in situ remediation system that has been demonstrated to remove DNAPLs, LNAPLs, and radioactive metals in the subsurface environments of fine-grained soils possessing hydraulic conductivities ranging from 10^{-3} to 10^{-8} cm/second.

Field construction is typically closely spaced offset rows of alternating lines which can be used for either extraction or injection. All wells are attached to a header piping system on the surface, which runs to injection or extraction units. This surface piping network is designed to allow connections solely to either injection or extraction units or to both injection and extraction units in an alternating row manner. A concurrent injection and extraction allows for a balancing of liquid volumes, which reduces the potential of introducing volumetric changes and subsequent reduction of hydraulic conductivities. Figure 2.5 illustrates a typical plan view of a complete WIDE system installation layout.

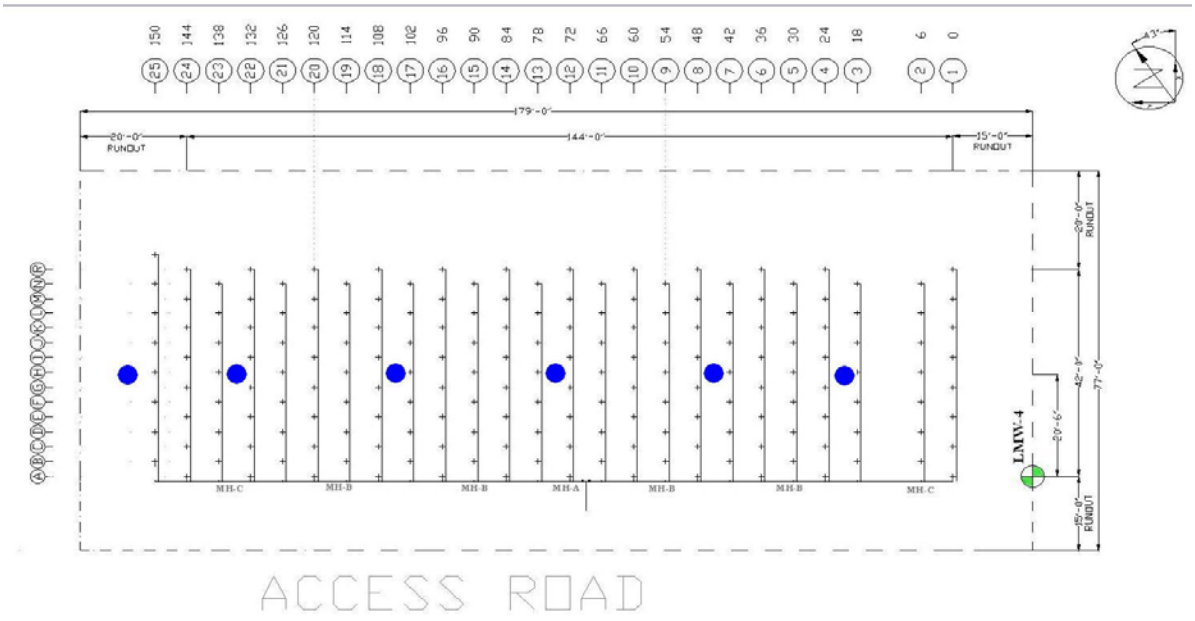

Figure 2.5: Typical WIDE Test Pad Layout

Individual PVWs are noted as plus (+) signs, while solid blue circles indicate installed piezometer locations, which are used in order to monitor subsurface water table fluctuations during testing (Gabr, et. al., 2006). Monitoring wells and other important site features, such as the access road, are placed appropriately. The depth specific targeting option of the WIDE system allows for focus in the low hydraulic conductivity layers that often experience minimal remediation with conventional treatments due to preferential flow in higher permeability layers. These low hydraulic conductivity layers are composed of silt and clay – sized particles, either alone or intermixed with sands and gravels. Clay percentage affects remediation by the reduction in hydraulic conductivity, and clay minerals are also soil particles to which many contaminants are strongly sorbed, the contaminant phase typically most difficult to remove. The high level of contamination associated with this phase suggests that remediation measures that target these lower hydraulic conductivity layers and

clay minerals could conceivably increase removal efficiencies and overall remediation levels. In a low permeability soil system, WIDE also offers the advantage of fracturing the soil, albeit in the vertical direction, by virtue of its installation on close spacing.

The choice of WIDE as the delivery/extraction system was facilitated by the ability of this technology to induce large hydraulic gradients by incorporating concurrent injection – extraction for maximum differences in hydraulic head over a relatively short transport pathway created by the close well spacing of ≈ 1 m (3 feet). Additionally, WIDE has the ability during operation to integrate versatile pumping schedules by varying injection and extraction rates, as well as injection and extraction locations. Large hydraulic gradients are one of the greatest contributing factors to the development of piping, or the process of soil particle movement due to an imbalance of seepage forces acting on the individual particle. Previous research in the area of piping is focused mainly on the negative results piping presents with regards to dam failure (Fenton and Griffiths 1997, Griffiths and Fenton 1998, Foster and Fell 2001, Fell et. al. 2003) and the ability to predict and prevent future occurrences.

2.7 Piping

The factor of safety with regards to piping is defined as the ratio between the critical hydraulic gradient of a soil and the existing hydraulic gradient. When this ratio is less than one, failure is likely to occur. The critical hydraulic gradient (i_{cr}) of a soil is defined by the following equation:

$$i_{cr} = (Gs - 1) / (1 + e) \qquad \text{eqn. (2.1)}$$

where Gs is the specific gravity of the soil, and e is the void ratio of the soil. Utilizing typical values of specific gravity (from 2.5 to 2.9) and void ratio (0.4 to 1.3), a factor of safety analysis is performed on an example system for illustration of the concept utilizing WIDE PVW spacing of 0.91 m (3 feet) on center and a pressure application of 34.5 kPa (5 psi), an applied hydraulic gradient of 3.44 is obtained. For all specific gravity and void ratio combinations the factor of safety against piping was less than one, ranging from 0.2 to 0.4, since the i_{cr} is typically in the range of 0.6 – 1.4.

Piping as a remediation measure is only effective, however, if three conditions are met: 1) the colloidal particles can be dispersed and enter into the flushing fluid and thereby be removed, 2) sufficient contamination is associated with the particles to be removed that removal will result in lower contamination concentration levels in the subsurface environment, and 3) particles to which contamination is not as greatly associated are prevented from migration and subsequent hindering of contamination removal.

As late as 1990's, condition 1 was not thought to be valid. Researchers still considered a two – phase system for contaminant analysis; that is the thought that sorbed contaminant is immobile within the soil matrix, while dissolved contaminant is in the mobile phase. The concept of colloidal mobility dispels this belief and creates the need for a three phase system that should include the mobile colloids in addition to the immobile soil matrix and the mobile water. This three phase system quickly became widely accepted, as shown by Kersting et. al. (1999), when they state "mobile colloids – suspended particles in the submicrometre size range – are known to occur naturally in groundwater." Today, it is not whether or not colloids exist in the environment, but to what extent do they affect contamination mobility. McGechan and Lewis (2002) found that "the presence of colloids

typically enhanced metal transport by 5 – 50 fold over the control treatment with no colloids" and Seaman et. al. (1995) stated "colloids can increase the mobility of strongly sorbing contaminants such as radionuclides, transition metals, and hydrophobic organics." Colloid mobility and contamination continues to emerge as an important research topic, with an entire special section in the May 2004 Vadose Zone Journal dedicated to colloids and colloid – facilitated transport of contaminants in soils. Thus, previous research has confirmed that conditions one and two for piping are sufficiently met. A more extensive analysis of previous research can be found in subsequent chapters.

Condition three will be addressed in this research by analyzing the geotextile filter around the PVWs to ensure filtration of larger particles and variations of injection – extraction rates and locations as necessary in order to maximize colloidal removal while minimizing well blockage. The ability of individual wells to be easily converted from injection to extraction, and vice versa, without complicated adjustments is one of the unique benefits of the WIDE system.

2.8 Cesium Contamination

Cesium contamination is of particular concern due mainly to the "significant human and ecological risks" (Kaplan, et. al., 1999) and the potential for a high bioavailability of contamination in the environment. "The largest single source (of cesium contamination) was fallout from atmospheric nuclear weapons tests in the 1950s and 1960s, which dispersed and deposited cesium-137 world-wide" (www.epa.gov, 2007). Other major sources include nuclear reactors, waste retention ponds at nuclear sites, and hospital and research

laboratories. Release of cesium contamination to the environment from these sources is typically an accidental process – almost none is released on a controlled basis.

The existence of cesium in the environment is in the +1 oxidation state. Three isotopes have half – lives that are long enough to be considered a concern for cesium contamination. These include ^{134}Cs with a half – life of 2.05 years, ^{135}Cs with a half – life of $3 \cdot 10^6$ years, and ^{137}Cs with a half – life of 30.23 years. Cesium typically does not exhibit complexation, and most often exists in the subsurface as the uncomplexed Cs^+ ion. An analysis of cesium complexation in the aqueous state was performed utilizing the Visual Minteq computer program and considering cesium, bromide, chloride, sulfate, and nitrate in equal concentrations. Results, program output of which can be found in Appendix A, showed that over 93% of cesium exists as the Cs^+ ion, almost 5% as $CsSO_4^-$, and the remaining ~2% divided almost equally as the aqueous $CsNO_3$, CsCl, and CsBr. When a competing ion (e.g. calcium) is introduced, the percentage of Cs^+ increases, while the percentage of all other complexes decreases. Results of an EPA study conducted in 1999 concluded that "aqueous complexation is not thought to greatly influence cesium behavior in most groundwater systems" (EPA 402-R-99-004B, 1999).

The most likely phase of cesium contamination is that of the sorbed phase. A majority of soils tend to readily sorb cesium, while some (e.g. illite and vermiculite) "tend to intercalate (fix) cesium between their structural layers" (EPA 402-R-99-004B, 1999). The favoritism of these silicate minerals for cesium has led to the utilization of clay minerals as a means of reducing the bioavailability of cesium in the environment. In 1988 Komarneni and Roy employed phlogopite mica as a sieve for cesium decontamination of not only the environment, but of animals and humans as well. By K-depleting the phlogopite, Komarneni

and Roy were able to adjust the interlayer spacing in the clay mineralogy to favor cesium selectivity and found that "the cesium ions that entered the structure cannot escape from the collapsed interlayers, that is, effectively leading to the fixation of the cesium ions" (Komarneni and Roy, 1988).

Kaplan et. al. (1999) "tested the hypothesis that an addition of naturally occurring phyllosilicate minerals to wetlands would sequester ^{137}Cs and, thereby, reduce its bioavailability" (Kaplan et. al., 1999). Results of the laboratory work confirmed that available cesium concentrations decreased with an increase in the level of mineral amendments. Results from the field deployment of the concept were presented in 2002 and support the laboratory assessment. Kaplan et. al. found that ^{137}Cs "levels in water were reduced 35- to 40-fold, activity concentrations in aquatic plants were reduced 4- to 5-fold, and concentrations in fish were reduced 2- to 3-fold. Equally important, the technique did not destroy the sensitive wetland environment and full-scale deployment costs were estimated to be six times less than the baseline technology, 'muck and truck' methods" (Kaplan et. al., 2002).

Both the research by Komarneni and Roy (1988) and Kaplan et. al. (1999 and 2002), utilized clay minerals as a means of reducing aqueous cesium contamination. This reduction did not lower the level of cesium in the environment, however, but simply reduced the bioavailability level. The immobilization of cesium, when attached to the clay minerals, presents itself as a solution to bioavailability, but still poses a viable threat to the overall site contamination level. The cesium itself is still present in the environment, and as this research shows, the association of cesium with mica minerals is such that any cesium removal will occur only with the removal of the mica as well.

2.9 Summary of Review

The incorporation of both a physical and chemical focus in this research is designed to maximize benefits associated with each. Justification for the chemical focus was based on prior research by Gamerdinger and Kaplan (2001) and Blume et. al. (2002). Both studies expressed the importance ionic strength plays in colloid mobilization and deposition, with Blume stating "changes in ionic strength may modify the balance between the forces at the particle – grain interface and result in particle detachment." Although increases in ionic strength tend to inhibit colloid mobilization, research has proven that initial flushes at high ionic strength followed by inundation of a low ionic strength solution can actually enhance colloid mobilization. Thus, the application of pulses of varying ionic strength will initially be applied in testing, followed by flushes of a low ionic strength solution. These variations in ionic strength would occur in the first pore volume of injected fluid only. Subsequent pore volumes of injected liquid would possess an ionic strength equivalent to that of tap water (approximately 0.0025 M).

It is expected, for early pore volumes, the higher the initial ionic strength of the injected water, the lower the colloidal removal efficiency. This is due to the fact that increases in ionic strength compress the diffuse – double layer and tend to inhibit colloid mobilization. As the number of pore volumes increases, however, the greater the variation from the higher initial pulse ionic strength to the current low ionic strength has shown in previous studies to enhance the mobilization of colloidal particles. Thus, the greatest colloidal removal efficiency is expected in subsequent pore volumes following the initial highest ionic strength injections. It will be necessary to determine whether or not the delay in increased removal efficiency due to the higher ionic strength pulse is sufficiently balanced

with the magnitude of the increase in removal efficiency. It may be that a more moderate ionic strength injection will result in greater removal efficiencies without as great of a delay associated with a large number of injected pore volumes.

The basis for the physical focus was obtained from an analysis of conditions that cause the development of piping. Based on the critical hydraulic gradient of a soil, and the factor of safety associated with piping, conditions that are conducive to failure can be calculated. Once these failure conditions for the soil are calculated, it is possible to determine if such conditions can be developed in a given field situation. Prior research by numerous individuals (Penrose et. al., 1990, Saiers and Hornberger, 1996 & 1999, Ryan et. al., 1998, Kersting et. al., 1999, Grolimund and Borkovec, 2005, Chen et. al., 2005) has shown the relationship between contamination and the colloid – sized particles, as well as the ability of these mobilized particles to transport the associated contaminant over significant distances. Current research will focus on the variation of induced hydraulic gradients on the effectiveness of colloidal mobilization. Considerations in addition to the mobilization effectiveness include the ability of WIDE to create and maintain rates and pressures required to induce necessary hydraulic gradients and the effectiveness of the geotextile surrounding the PVWs as a filtration mechanism for the prevention of excess particle migration.

Chapter 3. Experimental Program

3.1 Program Overview

The experimental program will consist of laboratory work, modeling, and a field case study. The chapter will begin with a brief synopsis of the work performed, followed by a more in depth description of materials and methods utilized in the laboratory portion of testing.

3.1.1 Laboratory Work

Laboratory work will include flow – through testing, contamination testing in batch mode, and post testing analysis. Flow through testing will be conducted using flexible wall permeameters that have been modified to include larger tubing. This design modification was necessary in order to prevent clogging of the tubing due to colloidal removal. Sample setup will consist of a porous stone and filter paper at the inflow, and the geosynthetic used on the PVWs at the outflow. The use of the porous stone and filter paper will prevent the introduction of additional small particles to the sample, while the geosynthetic at the outflow allows for filtration testing collected to predict effectiveness of the PVWs in the field. The effluent fluid will be measured gravimetrically according to EPA Method 160.1 – Residue Filterable (EPA, 1983). Testing will consider a natural soil sample as well as a number of manufactured soil samples consisting of sand with either 10% or 15% of kaolinite or bentonite, respectfully. All portions of testing will be conducted at three ionic strength

variations (existing tap water of ~ 0.0025 M, and 0.1 M and 1.0 M NaCl) and hydraulic gradient variations induced by three influent pressures (1, 2.5, and 5 psi).

Performance testing will incorporate contamination and be conducted in batch mode. Cesium, in the form of CsBr, will be used for this stage of testing. The choice of cesium was based, not only on the fact that it is the contamination of concern at the field site, but also because "despite its high solubility, Cs^+, like K^+, can be selectively adsorbed and strongly bound to zeolites and certain 2:1 phyllosilicate clays" (Seaman et. al., 2001).

Post testing analysis includes mass balance checks for individual testing, grain – size distribution testing, and microscopic analysis of removed colloidal particles. Mass balance determinations will be conducted by comparing the initial mass of each sample with its final mass plus the mass of fines removed. Mass balance is performed in order to determine if any losses occur during testing. Grain – size distribution testing, including sieve and hydrometer analysis, will be performed on 3 – 5 samples along the course of testing. This analysis will assist in confirming that the difference in grain – size distribution from pre to post testing is confined to the loss of fines only. Additionally, some samples will be sectioned into three distinct parts, with grain – size distribution performed on each, which will allow for the determination of colloid removal as a function of sample location.

3.1.2 Modeling

Modeling will be applied to link laboratory testing with existing field situations in order to determine the viability of testing at specific field sites. The model proposed in this thesis would consist of a three – phase system, including water, soil, and colloids. It will have initial conditions of existing deposited colloids and existing contamination. Consideration will be given not only to the release and deposition of colloids from soil, but

also to the sorption and desorption of contamination from colloids and the soil matrix. Additionally, chemical and spatial variability of the soil and flushing solution, including ionic strength variations, will be incorporated. Calibration of the model will be based on laboratory results. A sensitivity study will be performed to determine the required accuracy of model input parameters, and a parameter study will occur to qualify the relative importance of individual input parameters. In this manner it will be possible to determine not only which variables are the most important to the accuracy of modeling results, but also to what degree the accuracy of the input affects the output results. Once this portion of the model is complete, it will be used in a case study of an existing field site.

3.1.3 Field Case Study

The field site being used is at Battelle Laboratories in Columbus, Ohio. The site is the location of abandoned filter beds and is contaminated with radioactive cesium at concentrations well above regulatory limits (negotiated to be 15 pCi/g). The WIDE system was employed at the site as a possible remediation measure for the existing contamination. An 18.3 – meter by 36.6 – meter (60 ft x 120 ft) test pad was established with approximately 2200 PVWs installed to 3.7 – 4.6 meter (12 – 15 ft) depth at 0.6 meter (2 ft) spacing. The site was run in injection only mode on small scale testing plots but funding was discontinued. Prior to pad installation, laboratory testing was conducted in order to determine various physical properties of the soil profile. Application of the model to this site will utilize the existing WIDE layout for well spacing, hydraulic conductivity information, and hydraulic gradient limitations. The combination of lab and field work will provide input parameters to allow a case study of anticipated results based on model output.

3.2 Test Soil

The soil tested for this research program consisted of one natural soil obtained from the field test site, and a number synthetic "manufactured" soils composed of sand and one of two types of clay: kaolinite or bentonite, in various proportions. Characterization performed on the samples included specific gravity, grain size distribution, and Atterberg limits (where applicable). All tests were performed adhering to appropriate ASTM standards: ASTM D 854 – 02 for specific gravity, ASTM D 422 – 63 for grain size distribution, and ASTM D 4318 – 00 for Atterberg limits.

3.2.1 Natural Soil

The material used in the testing program was a natural soil obtained from the top meter of soil at the Abandoned Filter Beds at Battelle Laboratories West Jefferson North Site, roughly ten miles west of Columbus, Ohio. This site is a part of the US Department of Energy's Columbus Closure Projects. Battelle is remediating the Abandoned Filter Beds as a part of their NRC D&D plan to terminate the NRC Material License SNM – 7. The Abandoned Filter Bed area has been extensively characterized for radioactive constituents, with cesium – 137 being the only radioactive constituent found above free release levels. The area had previously been remediated by excavating the leach field tiles and sand from the area and replacing with fill. However, residual amounts of cesium were entrained on the soil fines, and within the soil pores, during the re-grading effort. The Cesium contamination ranges from slightly over 15 pCi/g to 200 pCi/g in an area that is approximately 35 meters long by 20 meters wide by 2.5 meters deep. The contamination is mostly immobile as verified by monitoring wells and periodic sampling.

Results from Atterberg testing indicated that the soil was a CL (low plasticity clay) according to USCS standards, with a liquid limit of 37.6 and a plastic limit of 25.8 (giving a plasticity index of 11.8). The specific gravity of the soil was 2.63 and the organic carbon content ranged from 0.93 – 1.76%. Figure 3.1 illustrates the grain size distribution curve of the natural soil sample, which indicates that approximately 28% of the soil by mass is less than 2 μm in diameter.

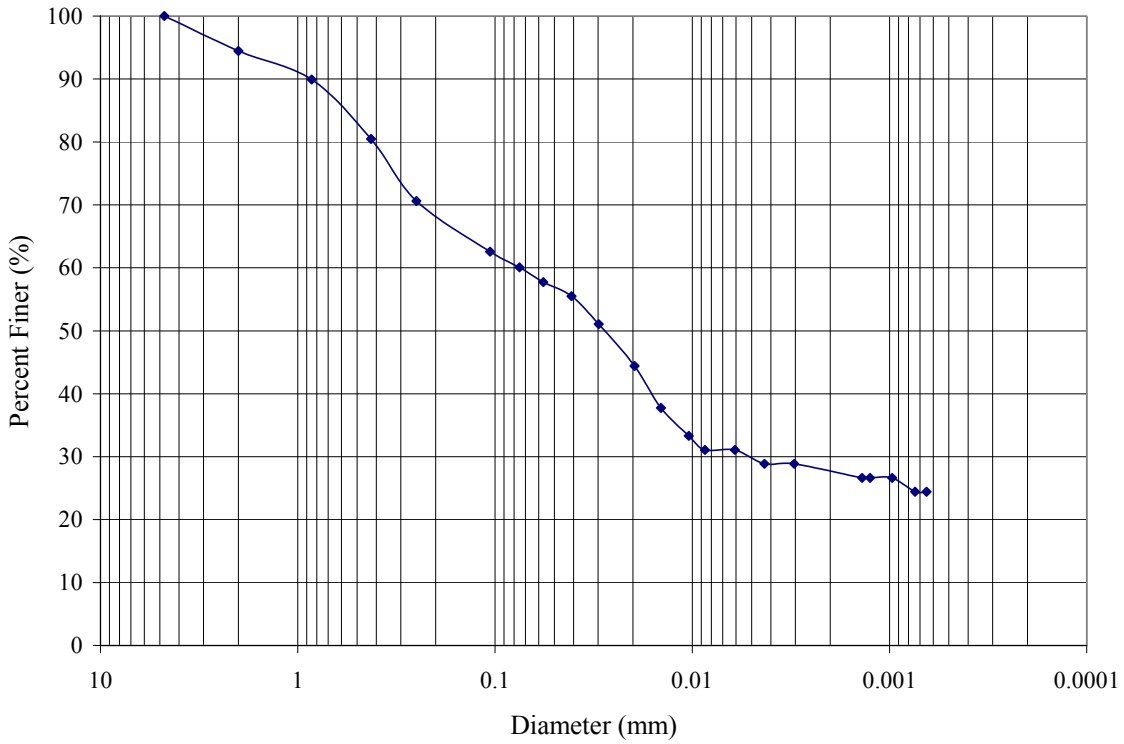

Figure 3.1: Grain – Size Distribution Curve for Natural Soil Sample

Soil Survey Data from Madison County Ohio indicate the soil is a Medway silt loam (Mk). A copy of the soil survey map, with the area under consideration delineated, can be found in Appendix B. The survey indicates engineering index properties of a Medway soil are USCS classifications of ML, CL, or ML – CL, liquid limits between 20 – 40, and

plasticity indices between 3 – 15. These properties match well with those obtained from physical characterization testing performed in this study (and mentioned previously), providing a level of confirmation to the Medway soil series determination.

Figure 3.2 depicts a set of photos of the natural soil.

a) complete natural soil (10x)

b) silt and clay on sand (60x)

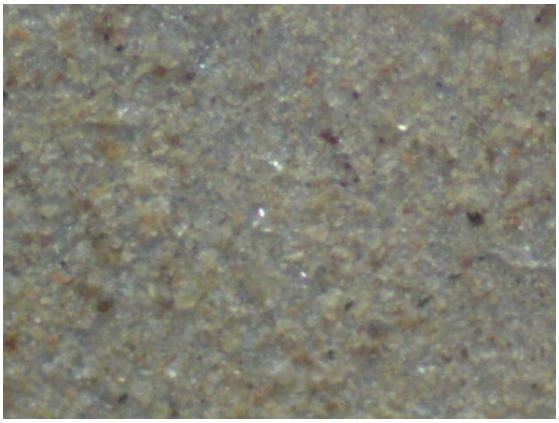

c) Natural fines (200x)

d) clay on silt (from above – 200x)

Figure 3.2: Pictures of Natural Soil Under Light Microscope

Light microscope pictures were taken of different portions and under various magnifications as noted in the figure sub – headings. Picture (a) is the entire natural soil magnified ten times, while (c) is 200x magnification. Figure 3.2 (b) is magnified 60 times

with the focus on a single sand grain occupying most of the frame and a smaller silt particle showing clear in the top right. This silt particle and the smaller clay particles are more clearly visible in (d), which is a 200x magnification focused on the silt grain from (b).

In addition to traditional engineering laboratory testing, the natural soil sample also underwent a number of standard soil science tests including soil fractionation, specific surface area analysis, cation exchange capacity analysis, and X-ray diffraction analysis in order to obtain a more complete characterization of the sample.

3.2.1.1 Soil Fractionation

Before undergoing soil mineralogy testing, the soil sample was subjected to a number of pretreatments in order to remove any rock fragments larger that 2-mm, correct for soil moisture content, and remove any carbonates and organic matter that may have been present (which enhances dispersion of the soil sample). Complete details of the procedure utilized can be found in Appendix C.

Soil fractionation results, on a mass basis, can be found in Table 3.1.

Table 3.1: Percent Fractionation of Soil Sample (by mass)

Soil Type	Percent (by mass)
Sand (2 mm – 50 μm)	31.6%
Silt (50 μm – 2 μm)	30.9%
Coarse Clay (2 μm – 0.2 μm)	16.4%
Fine Clay (< 0.2 μm)	21.1%

This fractionation shows a relatively equal percentage by mass of soil particles in the sand, silt, and clay fractions respectively. The slightly higher concentration of clay particles (37.5%) confirms the clay designation obtained from engineering properties and the USCS classification. Fractionation results help separate different minerals in addition to being useful from an engineering standpoint in the determination of the effectiveness of various remediation measures under consideration. Fractionation plays a large role in the hydraulic conductivity of a soil, and thus influences the time factors associated with many remediation measures. Fractionation can also help determine a rough estimate of a required removal mass when considering dispersion and piping for the removal of fines as a remediation measure for reducing free release levels of radioactive cesium in the subsurface environment.

3.2.1.2 Specific Surface Area Determination

Both external and total specific surface area analyses were performed on the soil samples to provide detailed mineralogical interaction of the fine particles. Procedural details are presented in Appendix C.

Like fractionation, specific surface area can not directly contribute to the mineralogical determination of soil samples, but can, to some extent, confirm results obtained from X-ray diffraction analysis. Table 3.2 lists external and total specific surface area results for each of the soil types tested.

Table 3.2: Specific Surface Area by Soil Type from Natural Sample

Soil Type	External SSA (m^2/g)	Total SSA (m^2/g)
Sand	1.32	--*
Silt	3.52	--*
Coarse Clay	21.32	59.10
Fine Clay	94.48	208.70

* Testing not performed

For samples where duplicate testing occurred, presented results are the mean of tests performed. Total SSA was not performed on sand and silt samples due to the fact that internal surface area is unlikely to be present in the minerals from which these fractions are composed. The large differences between total and external SSA for both the coarse and fine clay fractions suggests the presence of different 2:1 clay minerals with available interlayer space. The relatively low values for the coarse clay may imply the presence of mica-like minerals, where the higher values for the fine clay hint at a composition of vermiculites or smectites. XRD analysis will provide a more definitive determination of mineralogical composition.

3.2.1.3 Cation Exchange Capacity Determination

Cation Exchange Capacity (CEC) determination was performed on the coarse and fine clay portions of the soil sample, as well as the silt portion. Due to the mineralogical composition of the sand portion, the CEC values were expected to be relatively low, and thus testing was not performed. The method utilized, as described by Sumner and Miller, 1996, is

presented in Appendix C. Table 3.3 lists the Cation Exchange Capacity and standard deviations for the various fractions of the natural soil sample.

Table 3.3: Cation Exchange Capacity Determination by Soil Type for Natural Sample

Soil Type	CEC (cmol/kg)	Standard deviation
Silt	6.60	0.585
Coarse Clay	20.73	0.398
Fine Clay	48.49	2.060

As expected, CEC values of the clay portions of the soil were significantly greater than that of the silt portion, with the fine clay fraction possessing the highest overall cation exchange capacity. The relatively low CEC value in the silt portion suggests the possible presence of quartz and larger – sized clay minerals (i.e. phyllosilicates), although in fairly low amounts. The majority of the silt fraction, by mass, is most likely quartz or other minerals (e.g. feldspars) and is an unlikely contributor to contamination retention. CEC values imply the presence of smectite or vermiculite minerals in both the coarse and fine clay fractions. With a value of approximately 20 cmol/kg, the CEC of the coarse clay fraction is in the moderate range for clay minerals. The fine clay CEC value of roughly 50 is more in the mid-range, but still somewhat low when considering many secondary clay minerals boast CEC values in the low hundreds. Still, the existence of even moderate levels of CEC can impart significant complications when considering contamination remediation.

Cation exchange capacity is a result of isomorphic substitution during mineral formation, and thus is considered a constant charge for the soil. Because of the permanent

nature of this charge, it is usually unaffected by typical pH variations, ionic strength variations, or other changes commonly occurring in the natural environment. Thus, this constant charge is an important component affecting the retention of various organic and inorganic contaminants. As with specific surface area, CEC values can not directly classify mineralogical composition, but can serve as general guidelines in conjunction with X-ray diffraction analysis results.

3.2.1.4 X-ray Diffraction Analysis

Sample mounts for X-ray Diffraction (XRD) analysis were performed differently depending on if it was the coarse or fine-grained portion of the soil sample. For coarse-grained portions (i.e. sand and silt) random powder mount samples were prepared, while for the fine-grained portions (i.e. coarse and fine clay) a paste or slurry method will be employed to make oriented mounts. Complete sample preparation, testing, and test interpretation are presented in Appendix C.

X-ray diffraction analysis results were interpreted utilizing Whittig and Allardice's "Phyllosilicate Equivalent Plane Spacing" found in Methods of Soil Analysis and the JCPDS Mineral Powder Diffraction File. Output results for all soil types can be found in Appendix D. The main component for both the sand and silt fractions of the sample was determined to be quartz. This was a rather unsurprising result considering the typical composition of sand, visual inspection of the sample, and the low SSA values obtained for both fractions. The effect of the quartz mineral in the sand and silt fraction with regards to remediation of the site assists in confirming the belief that the cesium contamination is focused in the fines fraction of the soil. Cesium binds typically by means of cation exchange, and quartz is not a mineral

typically known for a high CEC value. These factors in combination with the low calculated CEC values suggest the amount of cesium associated with the sand and silt fractions of this soil is expected to be low to negligible.

From XRD analysis, the coarse clay fraction appears to be composed of mica, kaolinite, and a hydroxy – interlayered vermiculite. The latter was indicated by the shift in the 1.4 nm peak that occurs with heating. These minerals are types that can be expected to be found in the area and conform to SSA and CEC determination results. The presence of mica in the soil sample will provide an interesting addition to remediation analysis. Previous studies have shown that the presence of mica creates an adsorption hysteresis with cesium, that is the rate at which adsorption occurs is much greater than the rate at which desorption occurs. The reason for this slow rate of desorption is the fact that the ditrigonal cavity on the octahedral layers of mica minerals are the perfect size for a cesium ion. Once the ion is fit into place in this layer, even high concentrations of other ions are not sufficient to displace it. This suggests that typical pump and treat, or any flushing measure, would not be an effective remediation treatment. However, the mobilization and subsequent removal of these mica particles by dispersion and piping could remove the contaminated cesium and provide a more effective remediation measure.

The fine clay fraction of the soil contains vermiculite, smectite, kaolinite, and mica, in order of relative abundance. Again, these minerals are reasonable ones for the sample location, as well as for the measured SSA and CEC. As with the coarse clay fraction, the presence of a mica mineral will provide the same remediation challenge discussed above. Additionally, the smectite and vermiculite, with a high CEC value, would also be a contributing factor to the sorption of cesium in the fines fraction of the soil. The vermiculite

is probably the most important in terms of remediation, in that it is very abundant and possesses a high charge.

3.2.2 Manufactured Soil

Manufactured soils were composed of commercially available homogeneous sand and either kaolinite or bentonite. The manufactured soils were sand with either 10% or 15% by mass of one of the two types of clay. Samples were combined and thoroughly mixed in a dry state in batches large enough to perform all necessary testing. Relevant engineering testing was performed on each of the homogeneous soils independently.

3.2.2.1 Sand

The sand used in testing was a double washed playground sand with a grain size distribution as shown in Figure 3.3. With a uniformity coefficient of 2.18 and a coefficient of curvature of 0.97, the sand is considered poorly graded (SP) according to USCS. The average particle diameter (D_{50}) is 0.42 mm, and the specific gravity is 2.65 g/cm^3. Because of the fairly spherical shape of the grains, and the chemical composition (typically quartz), sands usually exhibit a relatively low surface activity, i.e. a low tendency to react with contaminants. However, it is possible that the highly hydrophobic nature of the contaminant will overcome the low activity and result in sorption on sand, though typically on a limited basis. A photo of the sand magnified sixty times is illustrated in Figure 3.4.

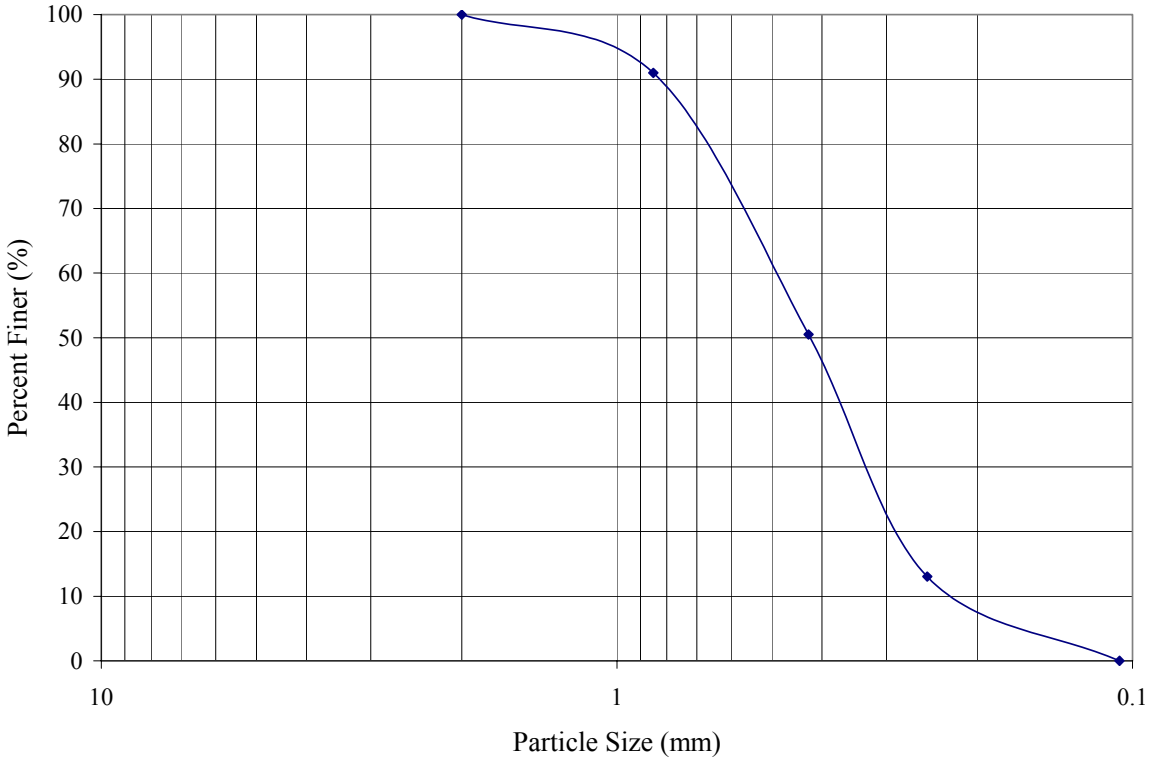

Figure 3.3: Grain Size Distribution Curve for Sand

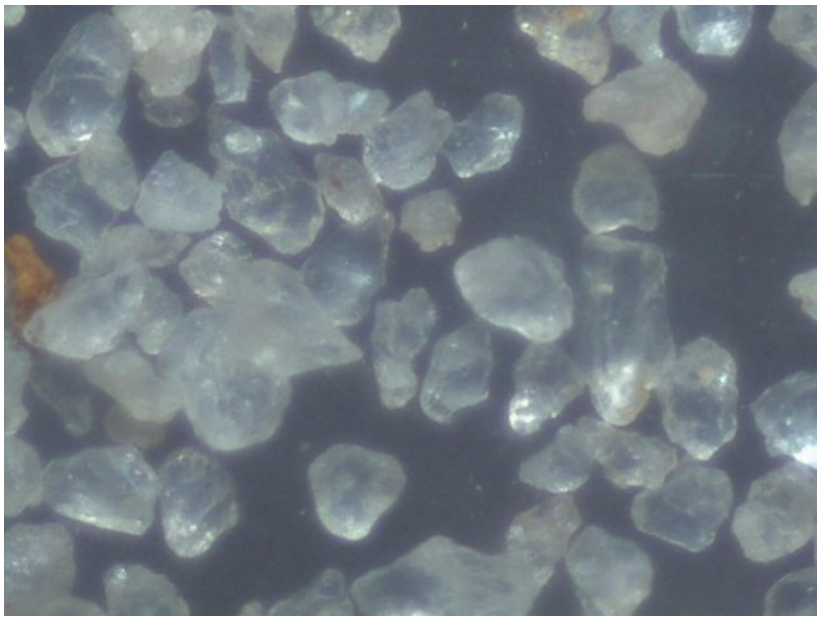

Figure 3.4: Manufactured Sand Used in Testing (60x magnification)

3.2.2.2 Kaolinite

A 1:1 clay mineral, kaolinite is composed of a silica tetrahedral layer bonded with an aluminum octahedral layer. The specific gravity of kaolinite is 2.65, which is on the low end of the range of values for most clay minerals. The test kaolinite has a liquid limit of 49% and a plastic limit of 24%, which yields a plasticity index of 25% and a USCS classification of a low plasticity clay (CL). Seventy – five percent of the particles are less than 0.002 mm in diameter from the grain size distribution curve. Figure 3.5 illustrates a 200x and an 800x magnification of the kaolinite used in testing.

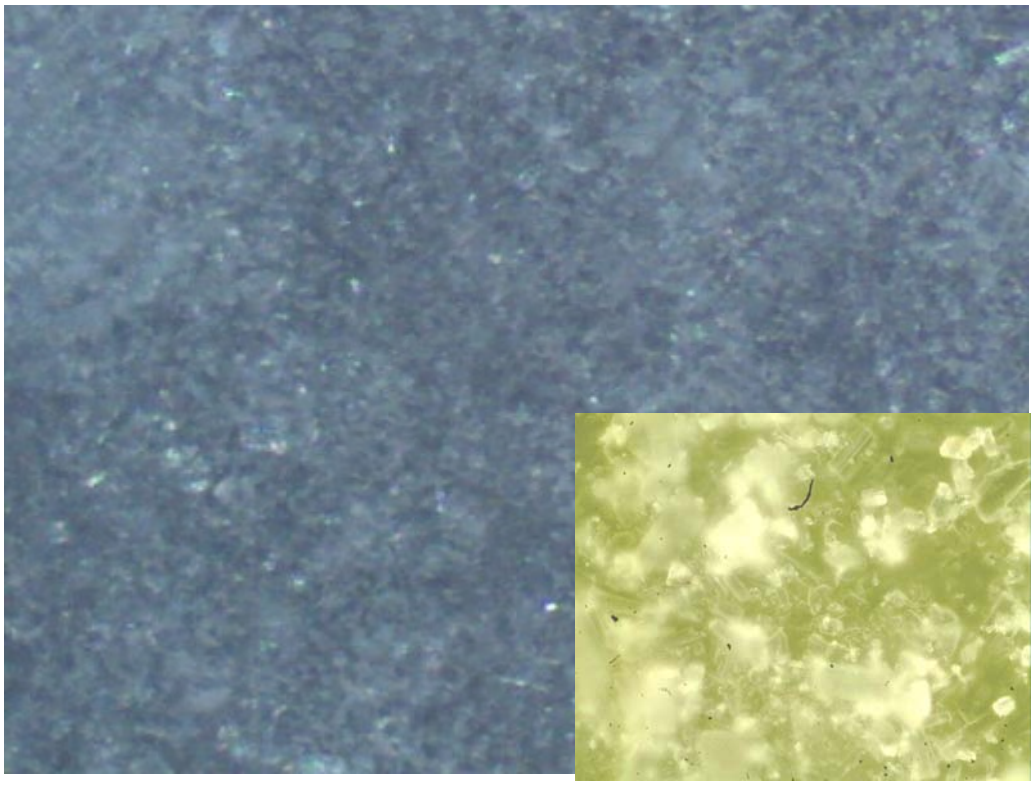

Figure 3.5: Kaolinite magnified 200x (inset magnified 800x)

Very little interlayer space is present due to the hydrogen bonding between layers, and thus kaolinite has almost no shrink – swell potential and a relatively low SSA compared

to many other clay minerals (Sparks, 1995). This low SSA in combination with the lack of isomorphic substitution results in a low cation exchange capacity of between 2 – 15 cmol/kg (Sparks, 1995). In addition, kaolinite has an activity of 0.33, low when considering some clays have activities as high as 7. Therefore, kaolinite can be considered to be a much less active sorbent than some other clays, such as bentonite.

3.2.2.3 Bentonite

In contrast to kaolinite, bentonite is composed of smectite, a 2:1 clay mineral composed of a single aluminum octahedral layer sandwiched between two silica tetrahedral layers. Bentonite is a rock type rich the clay mineral smectite, which exhibit virtually unlimited expansion in water and possess some of the greatest SSA values when compared to other soils (Sparks, 1995). Average CEC values for smectites range from 70 – 120 cmol/kg (Sparks, 1995), and activities range from 1 – 7. The combination of these characteristics supports the belief that bentonite will be a highly active sorbent of contaminants. The test bentonite has a specific gravity of 2.80, a USCS classification of CH, and is pictured in Figure 3.6.

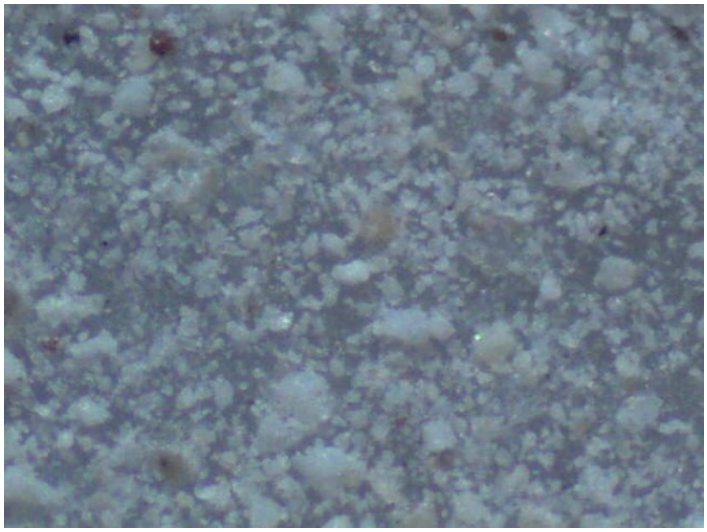

Figure 3.6: Bentonite magnified 200x

3.3 Test Contaminant

At the Battelle Laboratories Site in Columbus, Ohio, the contaminated area of concern is a retired filter bed area composed of tills that were compacted on site and are characterized by a high clay content and low hydraulic conductivity. The radioactive cesium contamination is chemically bound, on a molecular scale, to the micaceous/clay minerals of the soil and is present at levels as high as 93 pCi/g. Desired remediation levels are concentrations on the soil of less than 15 pCi/g and preferably less than 3 pCi/g. Proposed remediation efforts included the development of chemical solutions to desorb the cesium and extract it within the flushing liquids, but required heating the soil to 90 ºC (194 ºF). Portions of the advanced laboratory testing will include contaminated soils in order to confirm the association of contamination with the colloidal portion this research seeks to extract.

The contaminant used in research testing is cesium, and was chosen based on the fact that it is the contamination of concern at the field site. Additionally, cesium is often strongly

bound to the soil matrix, especially to the micas and vermiculites typically found in the clay portions.

The form of cesium utilized in laboratory testing is a non-radioactive cesium compound of cesium bromide (CsBr). Since the radioactivity itself does not affect the binding capabilities of cesium, it was decided to take additional precautions and simply utilize a non-radioactive form of Cs. The pairing of Cs^+ with Br^- as opposed to Cl^- was chosen in order to allow for the presence of a non-reactive tracer in testing, since for ionic strength testing, Cl^- will be present due to the addition of NaCl. An analysis of possible complexations, utilizing Visual Minteq, shows that over 98.5% of cesium occurs as a Cs^+ ion, with the remaining percentage almost equally divided between aqueous CsBr and CsCl. The addition of sodium to the analysis does not significantly change the cesium speciation, or relative concentrations (see program output runs in Appendix A).

3.4 Testing Program

The laboratory testing program includes flow – through, performance testing and post testing analysis. Flow – through testing is conducted using flexible wall permeameters that are modified to include larger tubing and pictured in Figure 3.7. This design modification is necessary in order to prevent clogging of the tubing with colloidal removal.

Figure 3.7: Flow – Through Test Set Up for Three Separate Samples

Sample setup consists of a porous stone and filter paper at the inflow, and a geosynthetic (commonly used on the PVWs) at the outflow. The use of the porous stone and filter paper prevents the introduction of additional small particles to the sample, while the geosynthetic at the outflow allows for filtration testing in order to predict effectiveness of the PVWs in the field. Collection of the effluent fluid is measured according to EPA Method 160.1 in order to determine colloidal mass concentrations.

3.4.1 Flow - Through Testing

Physical variations consider different induced hydraulic gradients. Variations in influent pressure head of 6.9, 17.2, and 34.5 kPa (1, 2.5, and 5 psi) are employed to induce hydraulic gradients in the samples of approximately 6, 14.5, and 29, respectively. Operating WIDE in an extraction – only mode field situation with a close well spacing of 62 cm (2

feet), these gradients translate into vacuum pressures of 5.8, 14.4, and 28.6 inches of mercury. Typical values of vacuum pressures in the field are between 16 – 20 in Hg, but values as high as 25 in Hg have been obtained and maintained over extended periods. Field vacuum pressures are limited by the size of the air extraction system, number and depth of the PVWs installed, depth of sheathing on the PVWs, and the effectiveness of the PVW seal in the top meter (2 – 3 feet) of installation.

Chemical variations consist of utilizing three ionic strength magnitudes (existing tap water of ~0.0025 M, 0.1 M of NaCl, and 1.0 M of NaCl). The lowest, 0.0025 M, corresponds to the existing ionic strength of the laboratory tap water. The other two, 0.1 M and 1.0 M, were mixed utilizing USP/FCC grade sodium chloride into deionized water. Ionic strength variations are implemented in a pulsed manner consisting of a single pore volume pulse of a solution possessing the specified ionic strength followed by subsequent flushing with tap water for the remaining test pore volumes. Salinity concentrations are measured in the effluent using the conductivity function of a Wissenschaftlich – Technische Werkstätten Multi 340i. These concentrations can be correlated to the ionic strength of the effluent solution using the calibration curve presented in Figure 3.8.

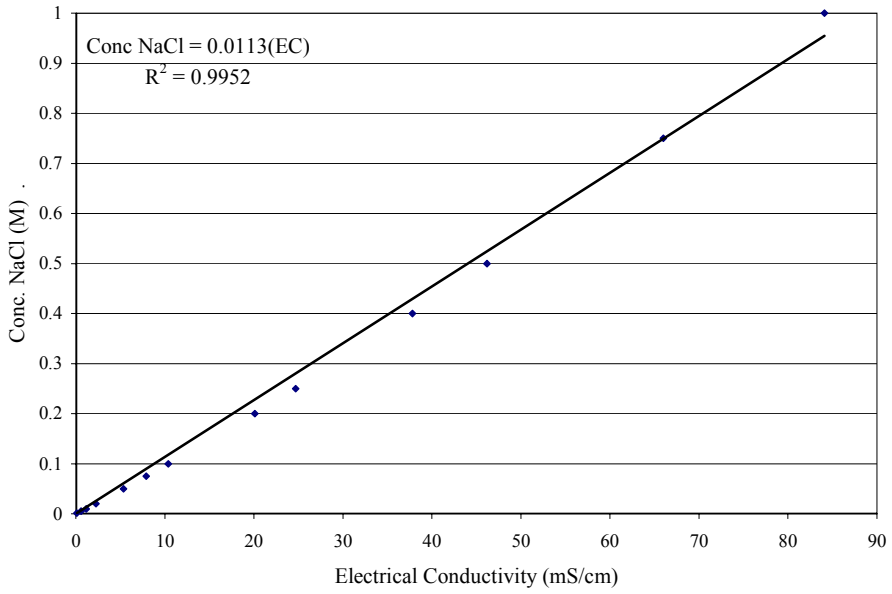

Figure 3.8: Ionic Strength Calibration Curve

As shown in Figure 3.8, a linear relationship between electrical conductivity and ionic strength can be expressed by equation 3.1, which has an $R^2 = 0.9952$.

$$\text{Ionic Strength} = 0.0113 \cdot (\text{Electrical Conductivity}) \qquad \text{eqn. 3.1}$$

3.4.2 Cesium – Contaminated Soils

Performance testing incorporating contamination is conducted in batch mode. Cesium, in the form of CsBr, is used for this stage of testing. Tests are conducted in 15 mL disposable centrifuge tubes. Prior to the commencement of batch testing, it was necessary to establish a soil solution ratio (SSR) that would be the most ideal for this testing program. SSR is defined as the ratio of the number of parts of soil (grams) to the number of parts of water (grams) in a suspension. To promote uniformity, it was desirable to use the same SSR

for all four soil types. However, because of the differences in the sorption capacities of the soils, a balance was needed in order to maximize results from all soil tests. To this end, ratios of 1:2, 1:4, 1:5, 1:10, 1:20, 1:25, 1:100 and 1:200 were initially tested. The three lowest ratios (1:2, 1:4, and 1:5) exhibited complications with the kaolinite. The solutions contained such a high amount of soil that adequate mixing was not possible. On the opposite end of the spectrum, the amount of sand in the ratios of 1:20 and higher was not sufficient to result in sorption of even 0.5 % of the contaminant in a 24 hour period. The remaining SSR of 1:10 was sufficient for sand and kaolinite, allowing the sand to sorb roughly 1 % of the contaminant, while also allowing thorough mixing of the kaolinite samples. The natural soil was not an issue in the determination of a SSR because the amount of sand prevented any mixing issues from arising, while the presence of silt and clay, as well as organic matter, resulted in sufficient sorption at any ratio.

The bentonite was a concern for all SSR due to the expanding nature / water adsorption of the clay. All mixtures turned into "gel" materials – and it was surmised that this semi – solid state created a lack in adequate mixing for the samples.

Since lower SSR values did not prove additionally beneficial, it was determined to stay with the 1:10 ratio. Overall 36 tests were performed. Twelve of each of three soils underwent sorption testing. For desorption, each soil underwent low, medium, and high ionic strength testing at each of 3, 18, and 42 hour test periods. One soil at each ionic strength for each time period was tested in duplicate; with each ionic strength – time period testing combination having a QA/QC test sample.

3.4.2.1 Sample Preparation

Cesium bromide, as a salt, is dissolved in water at approximately 10 mg/L (significantly below the solubility of 550 mg/L) to form soluble cesium concentrations of approximately 7 mg/L The solution is made in a single large batch and then utilized in all test samples, blanks, and controls, in order to assure consistent "contamination" concentrations. Sorption and desorption equilibration is conducted in a New Brunswick Incubator Shaker at 200 rpm and a constant temperature of 20 °C. Sorption is conducted for 24 hours, while desorption occurred in 3, 18, and 42 hour increments.

Upon completion of sorption, samples are centrifuged at 25,000 rpm for 10 minutes to separate soil from solution. At this point it was discovered that the bentonite "gel" did not settle out at this centrifugal force, which is the highest the 15 mL containers could withstand without leakage. Both higher centrifuging speeds (including different bottles) and lower SSRs were tested, but results showing significant separation of solid and liquid were not obtained. For this reason bentonite was ultimately not included in the Cesium batch the testing program.

Once samples are separated by centrifugation, the supernatant is filtered through a 0.2 μm polycarbonate filter using the Millipore units and vacuum application. This filtered solution is placed in labeled vials, where a couple of drops of 5M HCl are added for preservation and the samples are refrigerated and stored until testing.

The contaminated soil is then introduced to 10 mL of either the low, medium, or high ionic strength solution. Samples are sonicated until no large lumps remained, shaken, and weighed. The weight is used to determine the amount of entrained solution present in each sample vial. Samples were placed back into the incubator shaker for desorption testing.

Once samples underwent the predetermined desorption period, they are subjected to the same procedure for centrifugation, filtration, and preservation as the sorbed samples. Additionally samples are diluted to concentrations of either 0.005 M (for adsorption and low ionic strength samples) or 0.1 M (for medium and high ionic strength samples) concentration of NaCl. The salt addition to the adsorption and low ionic strength samples is necessary to prevent ionization and cesium concentration measurements in the atomic absorption spectroscopy machine. Medium samples are acceptable as is, but high (1.0 M) samples needed to have a reduction in salt concentration to prevent excessive salt build – up on the equipment. The adjustment to 0.1 M allowed for a single set of calibration standards to be valid for both sets of testing.

3.4.2.2 Atomic Absorption Spectrometry Analysis

Once salt additions and dilutions are complete, samples are used for atomic absorption spectrometry (AAS) testing. The Perkin Elmer 3100 AAS machine was calibrated to read cesium (wavelength of 852.1 nm) at concentrations between 0 – 4 mg/L. Because of the nature of cesium, the readings were fairly noisy, necessitating multiple readings for each sample. Each reading consisted of a set of three tests with the average results and relative standard deviations reported. Most samples (>95%) underwent duplicate testing. Additionally, as the calibration curve would shift during testing – re-calibration roughly every ten samples is needed. Calibration curves are established before and after every subset of 12 and values are averaged for each subset. An example calibration curve is presented in Figure 3.9.

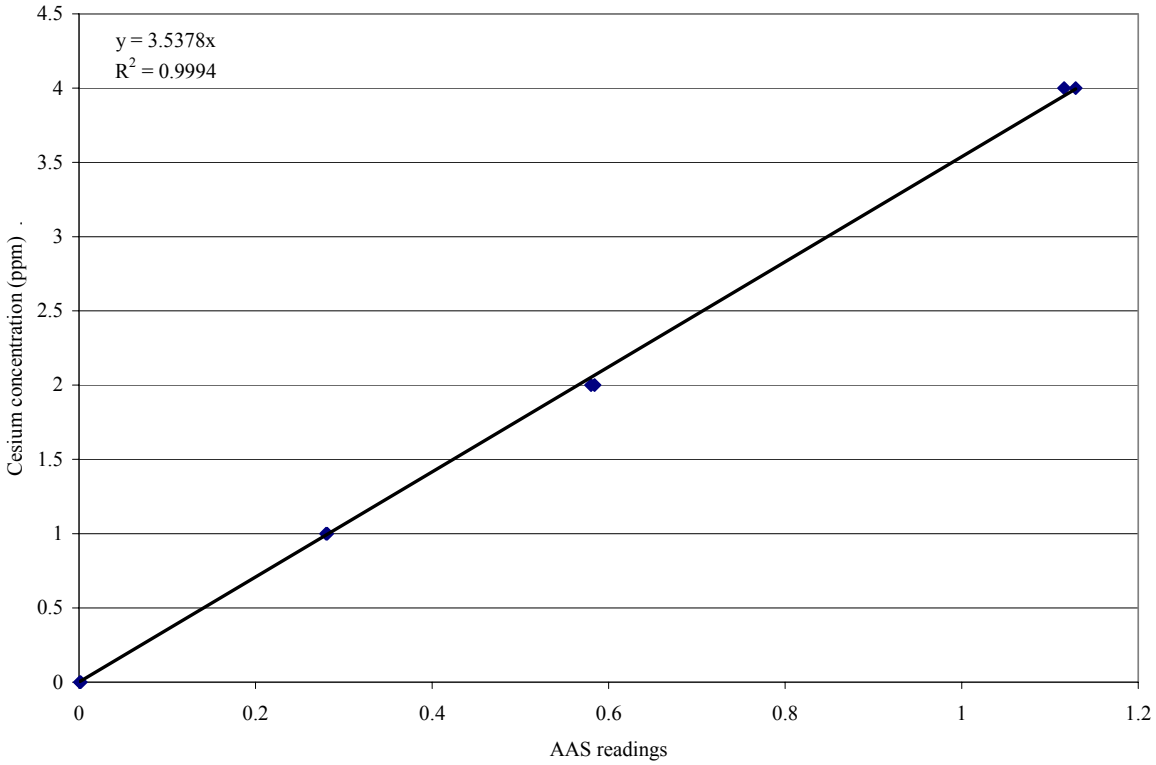

Figure 3.9: Example Calibration Curve for AAS work

All curves exhibited a linear relationship and possessed R^2 values of greater than 0.997. In addition to different correlation slopes; results are adjusted to account for dilution factors and "contaminant" concentrations inherent in the entrained solution.

3.4.3 Post Testing Analysis

Post testing analysis includes mass balance checks and grain – size distribution testing. Mass balance determinations are conducted by comparing the initial mass of each sample with its final mass plus the mass of fines removed. Mass balance is performed in order to determine if any losses occur during testing. Grain – size distribution testing,

including sieve and hydrometer analysis, are performed on 3 – 5 samples along the course of testing. This analysis will assist in confirming that the difference in grain – size distribution from pre to post testing is confined to the loss of fines only. Additionally, some samples will be sectioned into three distinct parts, with grain – size distribution performed on each, which will allow for the determination of colloid removal as a function of sample location.

3.4.4 Summary of Laboratory Tests

In addition to physical and mineralogical characterization of the test soils, laboratory testing includes flow – through and batch testing on soil contaminated with CsBr. Flow – through tests is performed on five different soils, one natural sample and four manufactured samples consisting of sand and either kaolinite or bentonite at 10 or 15% by mass. Testing is conducted at three different ionic strengths, as well as three different induced hydraulic gradients. Performance testing is conducted in batch mode with cesium contamination. Testing is conducted on three individual soil types – natural, kaolinite, and sand – and under all three ionic strength test levels. Post – testing analysis is conducted for the confirmation of mass balance, as well as for the determination of properties of the removed mass and / or contamination.

Quality assurance / quality control measures are undertaken at all stages of testing. Flow – through work includes 50 tests, while 36 batch tests are conducted in the performance work. A summary of the laboratory testing program, including the number of tests and various considerations for each stage, can be found in Table 3.4.

Table 3.4: Laboratory Testing Program Summary

Lab Testing Stage	Various Considerations	Total Number of Tests
Flow – through	• Soil types (5 w/ QA/QC) • Ionic strength (3) • Hydraulic Gradients (3)	50
Performance (batch)	• Soil types (3 w/ QA/QC) • Contamination (1) • Ionic strength (3) • Sorption (1) • Desorption (3)	36

Chapter 4. Flow – Through Column Results

4.1 Summary of Flow – Through Testing Layout

The purpose of flow- through testing in the laboratory was to determine the effects of chemical and physical perturbations on the rate of colloidal mobility within different soil samples. Three ionic strength variations in combination with three different hydraulic gradients were performed on five soil types. Results of testing showed the potential of initiating and maintaining clay dispersion and piping. Figure 4.1 depicts effluent solution from all five soils at both the initial pore volume (left) and final pore volume (right).

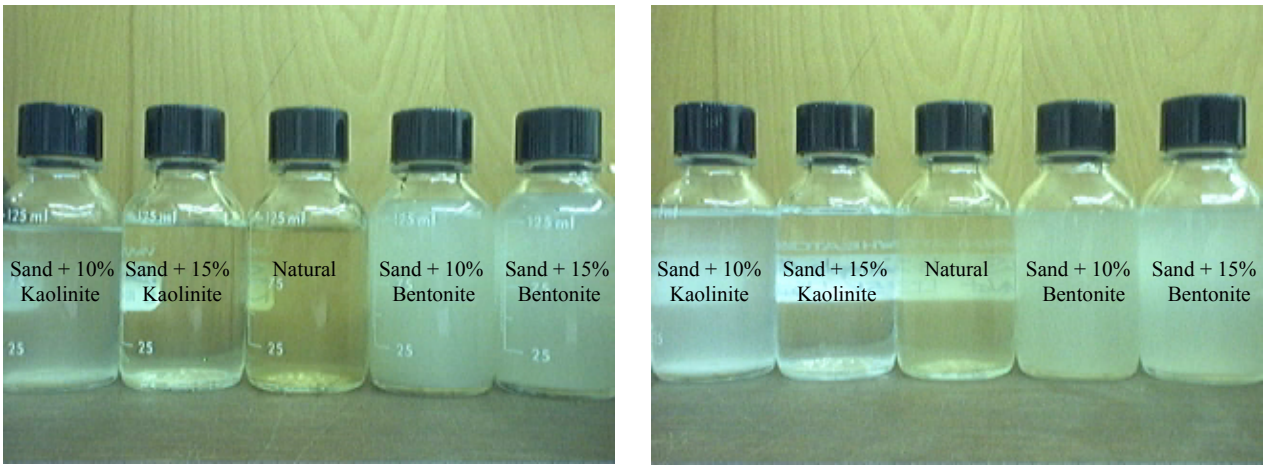

Figure 4.1: Visual Comparison of Colloidal Concentration at start (left) and end (right) of low (0.0025 M) ionic strength low (6) hydraulic gradient test for all soil types

Roughly 100 pore volumes were flushed through the samples for each of the forty – five tests performed. The visual comparison in Figure 4.1 illustrates the continual colloidal removal, even after significant pore volume flushes. It should be noted that even the slightly cloudy

nature of these samples correlates to approximately 200 – 500 mg/L colloidal concentration. As physical and chemical variations were induced, water ranging from the slightly cloudy effluent pictured above to distinctly cloudy samples with colloidal concentrations above the 1000 mg/L range was obtained. Although these higher concentrations were achieved, the more modest results were more likely to be maintained over an extend period of time.

Permeability as a function of cumulative pore volume was monitored at certain points throughout ten of the tests. These were the moderate and high hydraulic gradient (i = 14.5 and i = 29, respectively) tests with 0.1 M ionic strength. Results, for the most part, show an initial increase followed by a subsequent decrease in the permeability of the samples (see Appendix E). Exceptions to this trend include the natural soil samples, at both hydraulic gradients, which experienced a steady increase in permeability for the tests performed, and the sand with 10% bentonite at the moderate hydraulic gradient (i = 14.5) which showed a decrease only as a function of cumulative pore volume. Values presented are averages of multiple (3 to 5) tests for each point. With the exception of the sand and 10% bentonite (at i = 14.5), all tests showed permeability variations of less than an order of magnitude, and a majority of variations were less than a half of an order of magnitude. Sample standard deviations were roughly two – tenths an order of magnitude, suggesting that permeability variations were not caused by sample testing and did vary as a function of cumulative pore volume.

For the majority of testing, with the exception of those listed above, it appears as though the removal of colloids initially results in an increase in permeability. This conforms to the expected results in that a removal of soil volume leads to an increase in soil voids, and thus an increase in the volume available for liquid movement; and is especially true if no

micro-pore plugging occurs within the sample. The subsequent decreases in permeability could be a result of particle trapping or possible clogging of smaller – diameter pores within the samples. When considering the natural soil, the permeability for both hydraulic gradients shows a continuous increase as a function of pore volume. This would suggest a continuous removal of soil particles with any significant reduction in pore diameter or pore clogging. When the removal rates of these samples are considered in comparison to the other soils, total mass removed at the culmination of testing is two to three times greater than those soils which experience the initial increase and then decrease in permeability values.

The effects of different physical and chemical variations – either individually or in combination – are presented in this chapter.

4.2 Physical Variations – Effect of Hydraulic Gradient

The three hydraulic gradients used in testing are approximately 6, 14.5, and 29. Values are approximate due to slight variations in sample height in comparison to regulated applied inflow pressures of 6.9, 17.2, and 34.5 kPa (1, 2.5, and 5 psi respectively). All values correspond to hydraulic gradients that can be achieved in the field, the highest of which would most likely require concurrent injection and extraction through the WIDE system; while the lower two could be accomplished by any of the three operating methods: injection only, extraction only, or concurrent injection and extraction. Laboratory testing was conducted in a manner similar to injection only – i.e. pressure was applied to the inflow portion of the sample, while the effluent was open to the atmosphere. Results of the natural soil are presented in Figure 4.2. This graph plots the cumulative mass removed divided by the total mass of the sample (percent of total mass removed) as a function of cumulative pore

volumes for each of the three different hydraulic gradients at the lowest (0.0025 M) ionic strength.

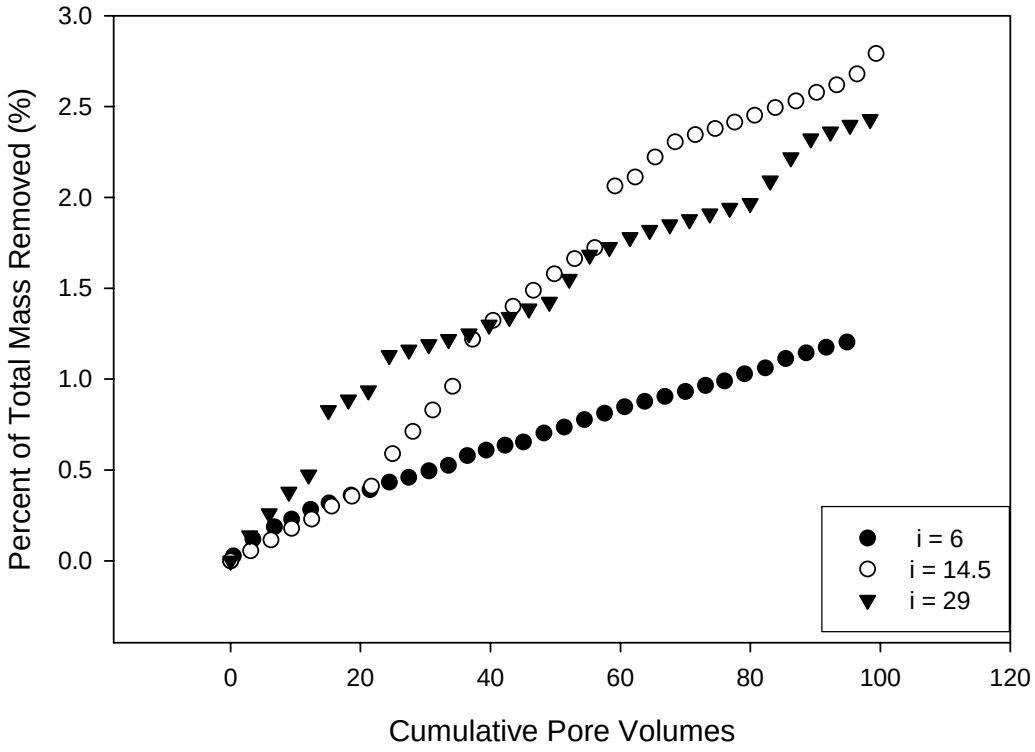

Figure 4.2: Colloidal Removal as a Function of Pore Volume for Natural Soil

From Figure 4.2, it is possible to see the differences in colloidal removal as a function of hydraulic gradient. Initially, all three hydraulic gradients resulted in similar removal rates for the first 5 – 10 pore volumes. As the number of pore volumes increased, the rate of removal for the lowest hydraulic gradient remained fairly stable – with a steady linear increase in the amount of colloids removed. On the other hand, the higher hydraulic gradients showed comparable increases in colloid removal. The highest hydraulic gradient began to diverge upward in fewer pore volumes than the middle gradient, but both trends diverged upward from the lowest gradient. Similar to testing under i = 6, the i = 14.5 test

results show a steady rise, albeit slightly less linear, for the entire testing period. In contrast, the highest gradient has a more abrupt increase, and actually falls below the middle gradient at higher pore volumes. It is hypothesized that the cause of this reduction in colloid removal is likely due to trapping of some of the colloids within the pore channels. Initially high levels of colloid concentration in mobile solution can cause constriction, and ultimate blockage, of major flow channels through a soil. Even if pores are not totally blocked, a reduction in diameter can decrease the ability to transport colloidal material out of the soil sample (Khilar et. al., 1985, Mohan et. al., 1993, Mohan and Fogler, 1997). It is thought that the highest hydraulic gradient possesses sufficient shear force to mobilize an excess of colloidal particles. The intermittent jumps in colloid concentration could be due to "breakthroughs" in constricted channels, which then allow resumed higher flow concentrations briefly, before reverting back to lower concentrations caused by pore constrictions. Data in Figures 4.3 and 4.4 support this theory, showing comparable results for both the sand and 10% kaolinite and the sand and 15% bentonite, respectively.

As shown in Figure 4.3, the sand and 10% kaolinite also experienced similar rate removals for the first 5 – 10 pore volumes; which is analogous to the natural soil. Subsequently, the lowest (6) hydraulic gradient maintained a steady linear increase, while the higher gradients increased at a more modest rate. Similar to observations made for the natural soil, the sand and kaolinite test soil appeared to experience partial plugging and a reduction in colloid removal, however even the middle gradient (i = 14.5) resulted in this occurrence – suggesting, logically, that soil type is a consideration when determining required shear forces for mobilization. The impact of soil type will be discussed in more detail later in this chapter.

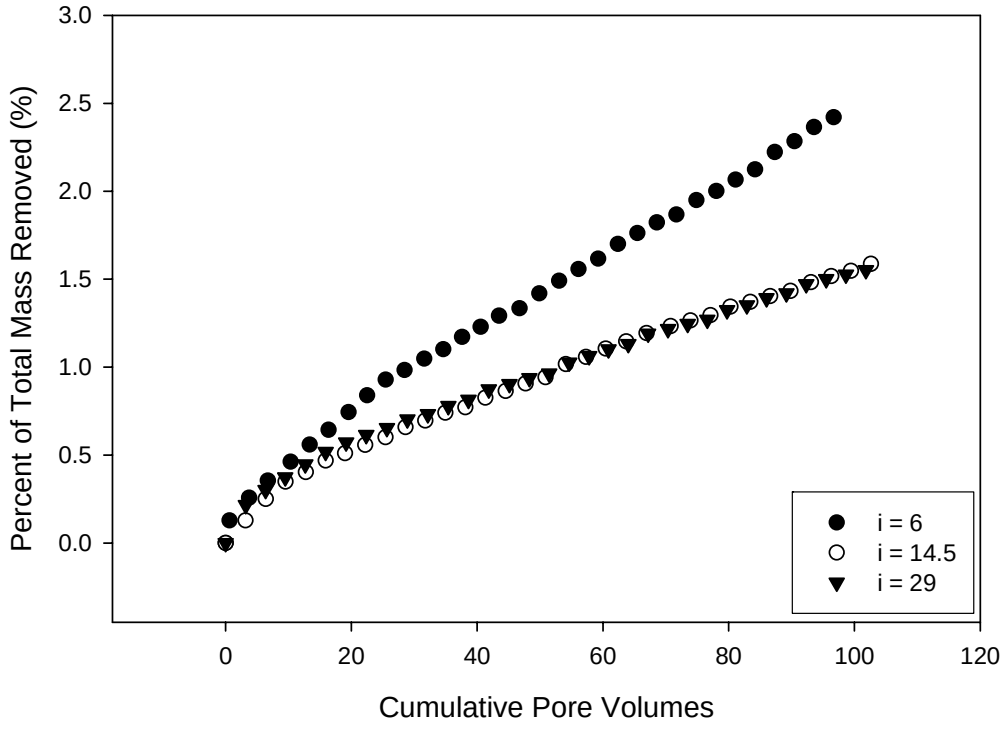

Figure 4.3: Colloidal Removal as a Function of Pore Volume for Sand + 10% Kaolinite

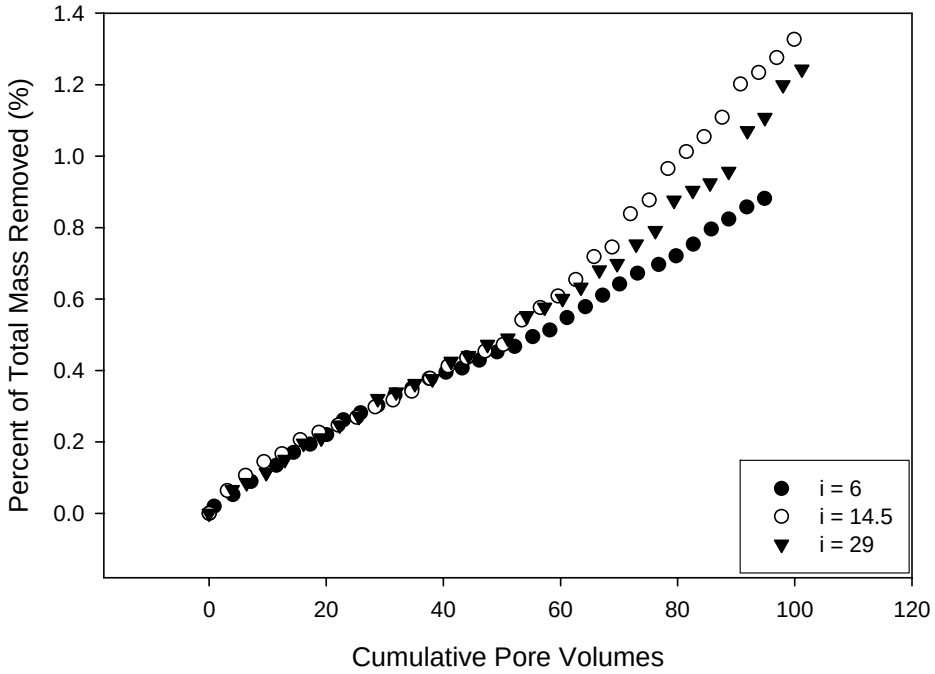

Figure 4.4: Colloidal Removal as a Function of Pore Volume for Sand + 15% Bentonite

In contrast to data in Figures 4.2 and 4.3; the sand and 15% bentonite mixture yielded consistent removal rates for all hydraulic gradients for almost 50 pore volumes, before diverging slightly based on hydraulic gradient in a manner parallel to that of the natural soil (Figure 4.4). One of the important items to note, however, is the different scale of this removal rate to that of the previous two. Overall mass removed from this soil is less than half (on a percentage basis) of that from the previous two soils – another soil type effect that will be discussed later.

4.3 Chemical Variations – Effect of Ionic Strength

Three different ionic strength values are employed in testing. Higher levels of ionic strength do not indicate continuous flushing of the solution, but rather a single pore volume pulse of the higher (e.g. 0.1 M or 1.0 M) solution followed by a subsequent flush of low ionic strength (0.0025 M) liquid. Although continuous influx of higher ionic strength solutions have been shown to reduce colloid mobility and transport (Aurell and Wistrom, 2000, Rivto et. al., 2003, Grolimund and Borkovec, 2006), pulses of high ionic strength, followed by flushes of a low ionic strength solution can actually enhance colloidal removal. Results from testing the natural soil are presented in Figures 4.5 and 4.6. Both figures are plotted as the ratio of mass of colloids removed over total mass of sample versus cumulative pore volume for the low (6) and medium (14.5) hydraulic gradients, respectively (i = 29 will be discussed later).

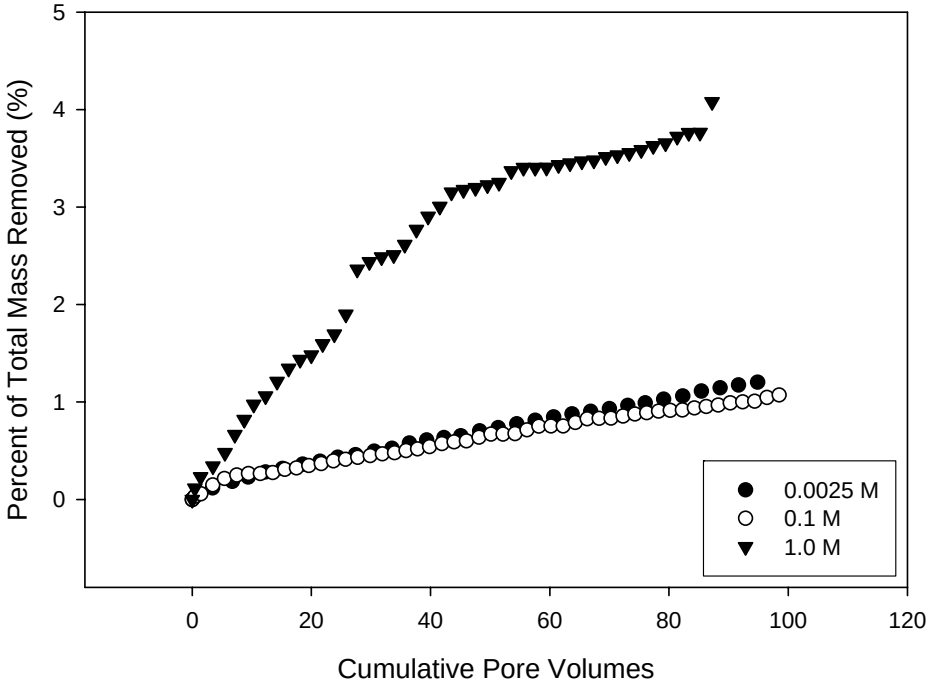

Figure 4.5: Variations in Colloid Removal as a Function of Ionic Strength for Natural Soil at Low (6) Hydraulic Gradient

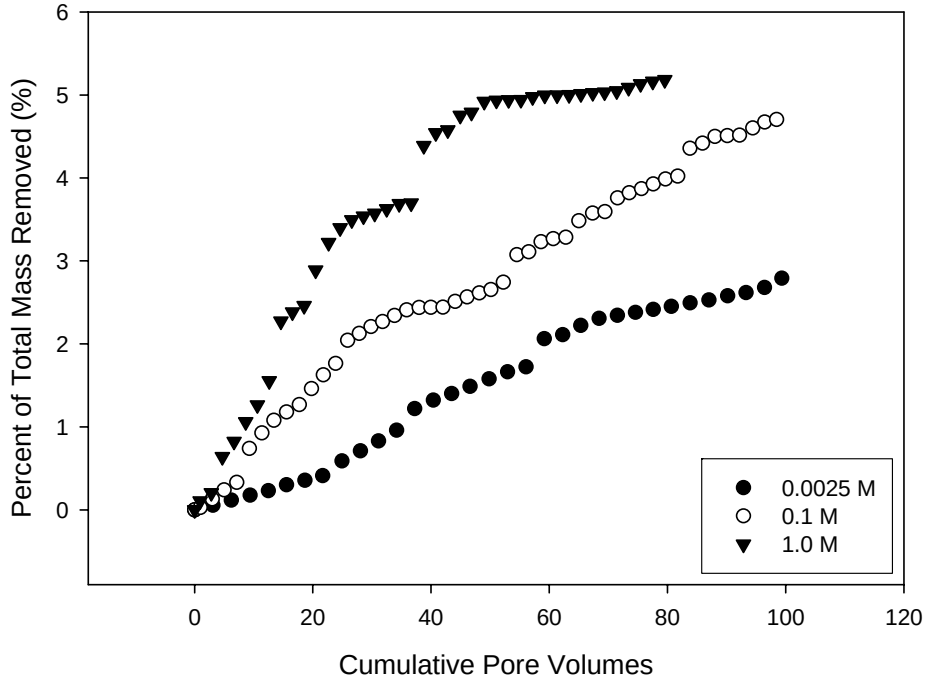

Figure 4.6: Variations in Colloid Removal as a Function of Ionic Strength for Natural Soil at Medium (14.5) Hydraulic Gradient

For both the low and medium hydraulic gradients, the highest ionic strength pulse (1.0 M) resulted in the greatest percent of mass removed. These higher values, however, show a tendency to level off, suggesting that expedient, rather than gradual, colloid mobility results in trapping and a narrowing of the pore channels and a reduction in the overall efficiency of the system. Results from the medium (0.1 M) ionic strength pulses are more tempered. For the low (i = 6) hydraulic gradient; differences in the medium ionic strength and low ionic strength are effectively negligible.

A more drastic difference is apparent in the experimental data using the medium (i = 14.5) hydraulic gradient comparison. Here, at the conclusion of the test, the percent of total mass removed from a 0.1 M pulse is 4.8% as compared to 2.8% obtained from the low background ionic strength test. It is possible that at the low hydraulic gradient (i = 6), the more moderate chemical adjustment (0.1 M ionic strength) is not sufficient to dominate the relatively low physical shear force application, while either a higher chemical (1.0 M solution) or physical (14.5 hydraulic gradient) application allows for increased removal efficiencies. This is confirmed, to an extent, when looking at the ionic strength effect at the highest (i = 29) hydraulic gradient for the natural soil; which is graphed in Figure 4.7.

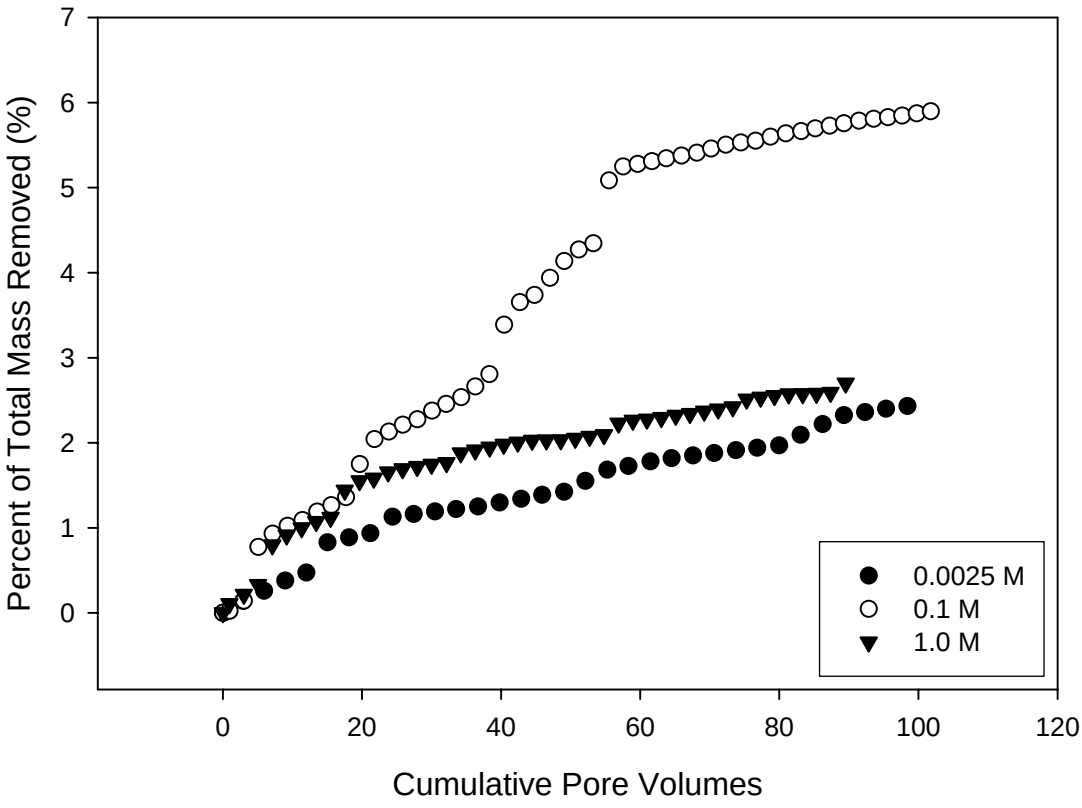

Figure 4.7: Variations in Colloid Removal as a Function of Ionic Strength for Natural Soil at High (i = 29) Hydraulic Gradient

As shown in Figure 4.7, it is possible to see the more drastic difference in overall colloidal removal from the low to medium ionic strength variations. In this case, the highest ionic strength does not result in the greatest removal efficiency. It is hypothesized that particle trapping, a greater concern in the higher hydraulic gradients (as shown in the previous section), is responsible for the trend reduction. A combination of both high hydraulic gradient and high ionic strength is even more likely to contribute to partial plugging and pore constriction complications it seems, as aggressive and expedient particle mobilization does not allow for the gradual removal of colloids from the system. These

results illustrate the importance of considering both chemical and physical variations on the maximization of colloidal removal.

Effects of ionic strength variations can also be seen in the manufactured soil testing results. Data from the sand and 15% kaolinite is plotted in Figure 4.8 in the same manner as previous figures.

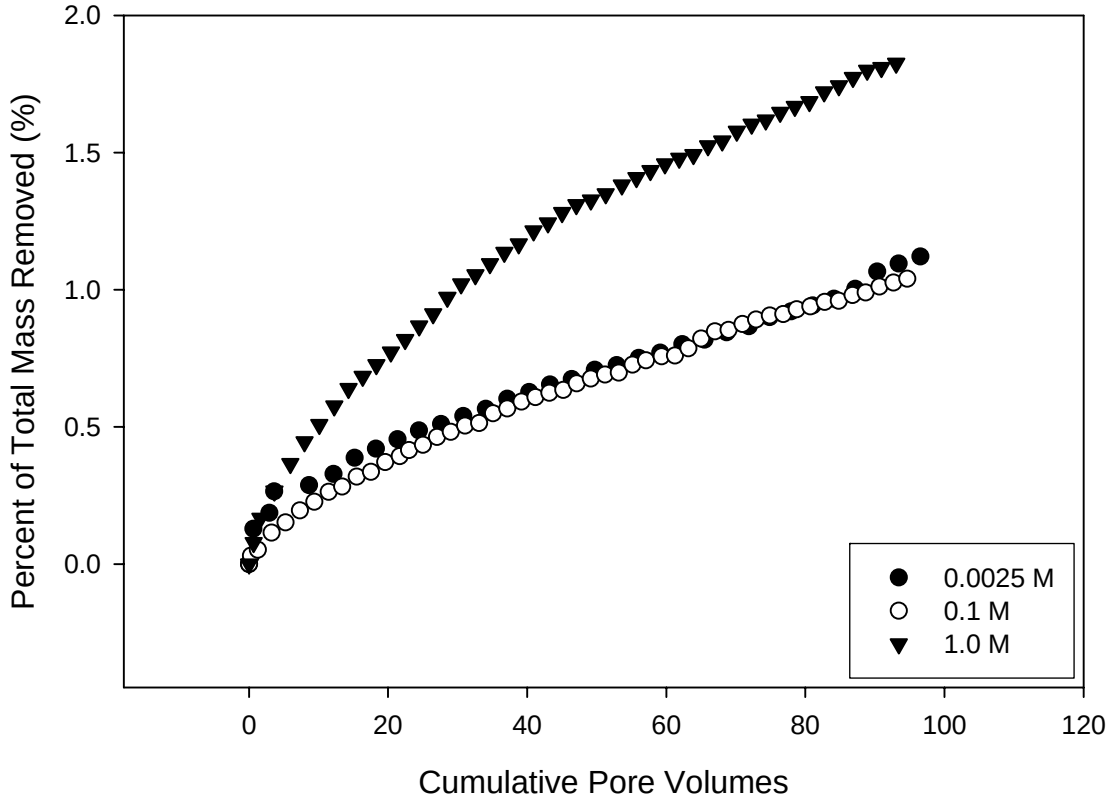

Figure 4.8: Variations in Colloid Removal as a Function of Ionic Strength for Sand + 15% Kaolinite at Low (i = 6) Hydraulic Gradient

Similarities between these results and that of the natural soil, at the same hydraulic gradients (Figure 4.5), are noteworthy. Both show sizeable differences (here almost double

on a percent mass basis) between the high ionic strength and the two lower ones, while the medium and low ionic strengths diverge only slightly from one another.

Comparisons can also be made between the natural soil and the sand and 10% bentonite at higher hydraulic gradients. Graphed in Figure 4.9 are the results from the sand + 10% bentonite test for various ionic strengths under medium (i = 14) hydraulic gradient conditions.

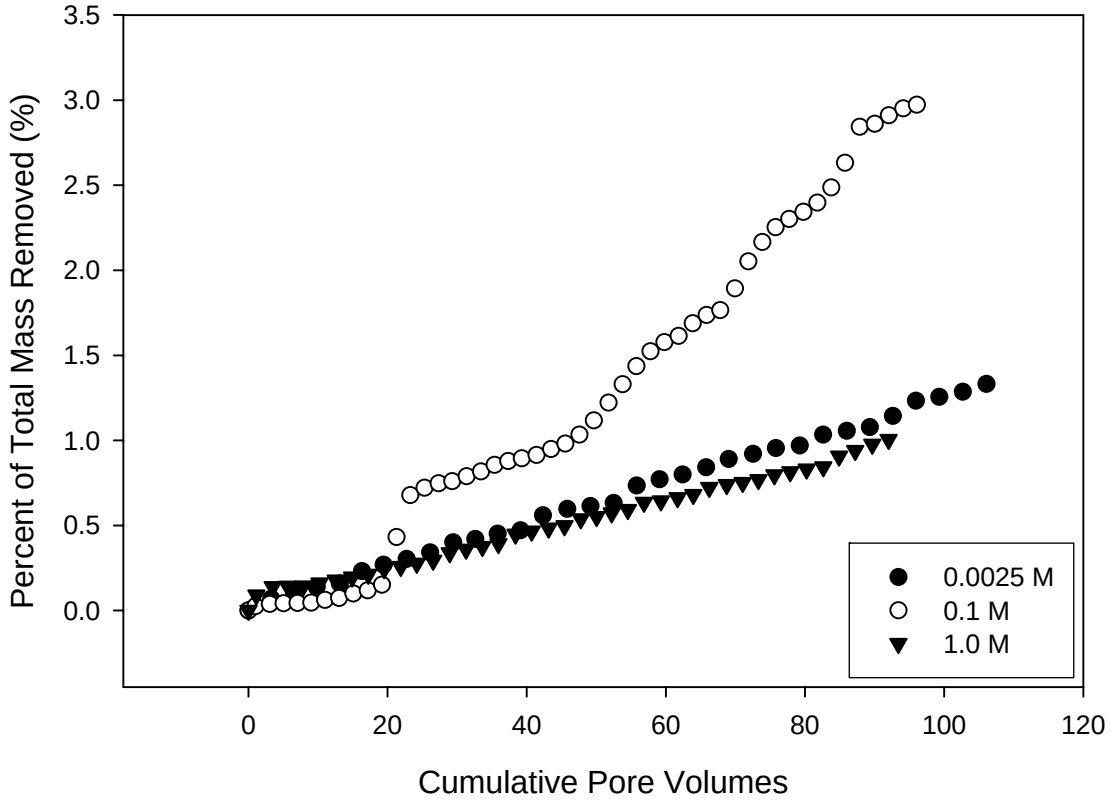

Figure 4.9: Variations in Colloid Removal as a Function of Ionic Strength for Sand + 10% Bentonite at Medium (i = 14.5) Hydraulic Gradient

The data exhibits the characteristic difference between the low (0.0025 M) and medium (0.1 M) ionic strength variations present in the medium and high hydraulic gradient

results of the natural soil. Additionally, the high ionic strength (1.0 M) displays suppression of colloidal removal – most likely from pore constriction and particle trapping due to higher concentrations of colloids in solution. Although different from the medium (i = 14) hydraulic gradient results of the natural soil, it mirrors the higher (i = 29) hydraulic gradient for the natural soil – a difference that may be attributable to soil type variations and physical or chemical perturbations required to facilitate mobilization.

4.4 Effect of Soil Type

Five different natural or synthetic soil materials, including a natural soil, sand and 10 % kaolinite, sand and 15% kaolinite, sand and 10% bentonite, and sand and 15% bentonite were used during testing. Samples were subjected to all ionic strength and hydraulic gradient combinations, with each test sample undergoing approximately 100 pore volume flushes.

When considering a comparison of soil materials – a brief review of critical soil properties is beneficial to the explanation of results. For the manufactured soils, typical ranges for general properties were utilized; while it was necessary to measure natural soil values, since published data was not available. Table 4.1 summarizes these results, and is followed by a brief discussion of the importance of each.

Table 4.1: Summary Table of Relevant Soil Properties

Property	Natural	Kaolinite	Bentonite
Clay Fraction (%)	37.5	10 or 15	10 or 15
Total SSA (m^2/g)	131.43*	15	800
CEC (cmol/kg)	32.26*	2 – 15	70 – 120
Activity	0.31	0.33	1 – 7

*SSA and CEC based on values for coarse and fine clay weighted with respect to percent of clay type by mass (contributions from silt and sand neglected)

Clay fraction is the proportion of clay particles (by size) in each sample. Since the manufactured samples varied on clay percentage, both the 10 and 15% values are included to give a total of 5 soil samples. Because of their greater SSA and CEC, clay particles are the greatest contributors (compared to sand and silt) to contaminant binding in the subsurface, with larger percentages indicating a greater affinity to bind contamination. The two main factors controlling affinity for contamination are the specific surface area (SSA) and the cation exchange capacity (CEC). Specific surface area is the ratio of the surface area of a particle to the mass of that particle. Larger SSA values indicate a greater availability of binding sites for contamination. Cation exchange capacity is a measure of the soil's ability to accommodate positively charged ions on its negatively charged surface. The higher the CEC, the greater the attraction of contamination to the clay minerals. Activity is the ratio of the plasticity index divided by the clay fraction of the soil. Soils with an activity of less than 0.75 are considered inactive, ones that fall in the range of 0.75 – 1.25 are normal, while those with values greater than 1.25 are considered active clays.

These properties form the basis for the soil comparison between kaolinite, bentonite, and the natural soil. Based on the data from Table 4.1, it is expected that the natural soil is more likely to behave like a bentonite, since many of the relevant soil properties of the natural soil more closely match those of bentonite than those of kaolinite. The main differences between the natural and bentonite samples, are the soil activity (natural sample is more closely aligned with that of kaolinite), and the clay content (natural sample is more than double that of any other sample).

Complications arise with considering all data due to the difficulty in determining which effects are from the soil type, and which are from the ionic strength and hydraulic

gradient variations. Accordingly, the comparison to discern the significance of soil type would be from the low ionic strength (0.0025M) and low hydraulic gradient (i = 6). This will serve as a benchmark for the different soil tests. Further analysis of the effects of chemical and physical perturbations on the various soil types will be discussed in the following section. Figure 4.10 plots the results for all soil types at the "benchmark levels".

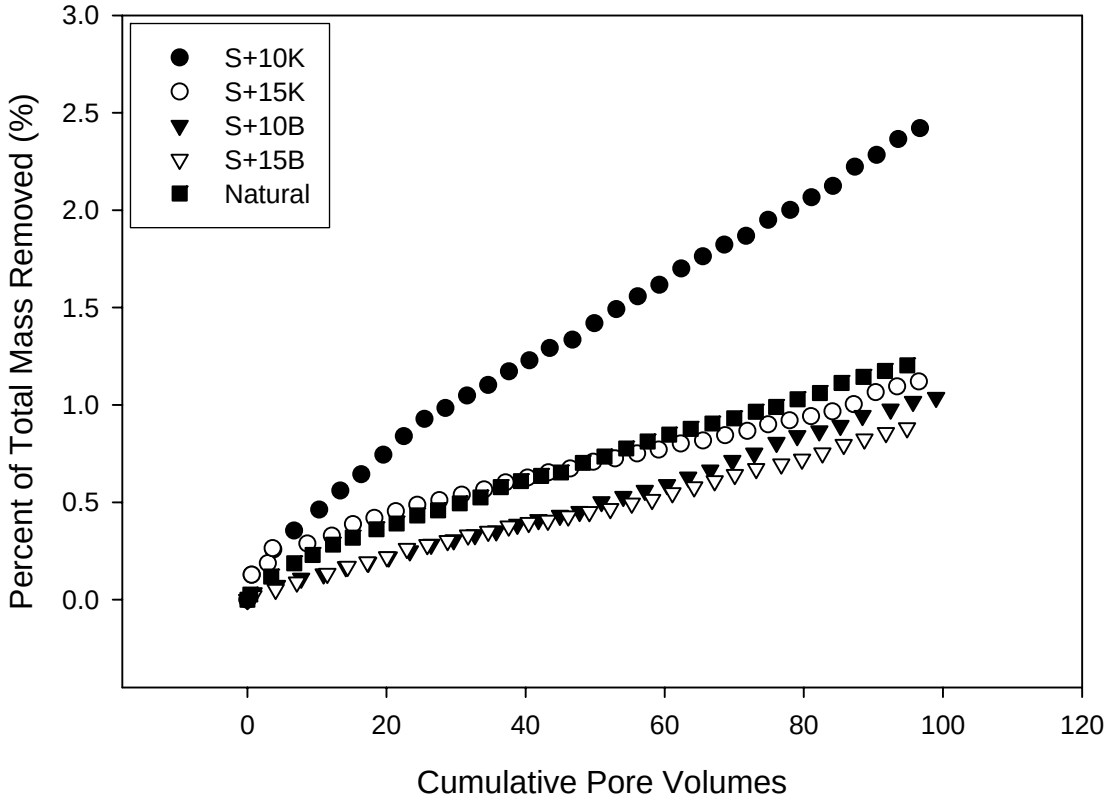

Figure 4.10: Variations in Colloidal Removal for All Soils at 0.0025M and Low (i = 6) Hydraulic Gradient

The most noticeable feature of this plot is the difference in the sand and 10% kaolinite versus other soils tested. The low reactivity (i.e. affinity of colloids for soil matrix and each other) and clay percentage allows this soil to yield the highest colloidal removal.

But then, the addition of 5% more kaolinite reduces the efficiency by almost half. It is hypothesized that this reduction is due to the reduction in permeability, the decrease in pore diameter, and the increase in overall clay content caused by the 5% kaolinite addition.

In contrast to this 1:1 kaolinite mineral, the 2:1 bentonite, as well as the natural soil, all exhibit roughly similar results. The two bentonite samples even overlap for the first 50 pore volumes, before diverging slightly at the end. This divergence is within the statistical variations seen in QA/QC testing on similar soil types. The natural soil performed as anticipated with comparison to the manufactured soils. The trend for the natural soil, for the most part, followed that of the bentonite; but did deviate slightly. With regards to clay content; it appears to have a greater effect on soils with a lower CEC and SSA, than those of a higher CEC and SSA. Whether or not this trend holds consistent with the application of chemical and physical variations will be determined in the following section.

4.5 Combined Effects of Physical, Chemical, and Soil Variations

Probably an accurate way to consider the effectiveness of colloidal mobilization is to take into consideration not simply one of the parameters, such as hydraulic gradient, ionic strength of flushing solution, or soil type; but rather to consider all in unison. The difficulty with this approach, however, is the complication associated not only with the variations themselves, but also with the interaction between combinations of these variations. Where a combination of both a moderate ionic strength increase with a mid – level hydraulic gradient can prove beneficial, the same ionic strength with a higher gradient, or same gradient with a higher ionic strength, can induce in excessive mobilization and result in pore constriction, clogging, and ultimately an overall reduction in the potential removal rates.

In order to obtain an accurate assessment of what is occurring; it is critical to take into account larger quantities of data than can be seen on a single plot. To accomplish this goal, a series of graphs are presented in tandem (see Appendix F) – with the goal of crystallizing a bigger picture in the discussion that follows. All of the information is plotted as a percent of total mass removed versus cumulative pore volumes. Data is presented for all five soil types in a single graph with the same hydraulic gradient and constant ionic strength. Scales for both the x and y axes are consistent throughout the graphs, which facilitates visual comparisons. Graphs for a single ionic strength are on the same page, while the same hydraulic gradient can be found at the same location on each page.

Based on the data presented in Appendix F, the following observations can be stated:

1. The greatest colloidal mobility rates for kaolinite were realized at either low ionic strengths or low hydraulic gradients. Colloidal removal results were higher for mixtures with the 10% kaolinite than for those with 15% kaolinite content. Hydraulic gradient increases tested resulted in decreased colloidal removal efficiencies for 1:1 clay mineral colloids.
2. The greatest colloidal mobility rates for the bentonite were realized at moderate ionic strengths and moderate to high hydraulic gradients. Again, colloidal removal was higher with the lower (10%) clay content over the higher (15%) clay content. Hydraulic gradient increases tested resulted either in continuous increases (10% bentonite) or initial increases then decreases (15% bentonite and natural soil) in colloidal removal efficiencies for 2:1 clay mineral colloids.

3. The greatest colloidal mobility rates for the natural soil were realized at moderate to high ionic strengths and moderate to high hydraulic gradients – although not at both high ionic strength and hydraulic gradient.
4. Ionic strength effects for the kaolinite were suppressed with increases in hydraulic gradient – although overall trends within each sample were consistent for all ionic strengths and hydraulic gradients.
5. Ionic strength effects for the bentonite and natural soil were more effective at moderate levels over elevated levels for virtually all hydraulic gradients (natural low gradient is the exception).

4.6 Ionic Strength Normalization with Respect to Soil Type

One of the most interesting features of the effect of ionic strength on different soil types is that this effect can be normalized when certain soil and solution properties are taken into consideration. First, it is necessary to convert the ionic strength of the flushing solution to a total amount of cations (in cmols). Next the total CEC of the soil is calculated in cmols. The ratio of these concentrations (cmol cations / cmol in soil) is determined, and corrected based on the soil activity. The resulting values are presented in Table 4.2 for each of the five soils and three ionic strength conditions.

Table 4.2: Ionic Strength Normalization Parameters for All Samples

Ionic Strength Level	Sand + 10% Kaolinite	Sand + 15% Kaolinite	Sand + 10% Bentonite	Sand + 15% Bentonite	Natural
Low	0.025	0.016	0.008	0.006	0.003
Medium	0.775	0.546	0.478	0.254	0.076
High	8.61	5.47	4.72	2.38	0.842

If the normalized ionic strength parameters are compared to the colloidal removal efficiencies, the following conclusions can be drawn:

1. Soils that have normalized ionic strength parameters of less than 0.05 do not experience any discernable benefit from the flushing solution ionic strength level with regards to improved colloidal removal rates.
2. Soils that have normalized ionic strength parameters of greater than roughly 0.9 experience suppression in the colloidal removal levels.
3. Soils that possess normalized ionic strength parameters between approximately 0.05 and 0.9 manifest the greatest benefit from flushing solution ionic strength levels. This leads to the most improved colloidal removal levels.

Figure 4.11 illustrates the three previous points by plotting the ionic strength normalization parameter versus the total mass removed for each of the five soils tested. The shaded portion of the graph delineates the range at which ionic strength application is optimized. Removal rates are based on a moderate hydraulic gradient (i = 14.5) for all soils. Focus is on the trend for the individual soil, not comparison between soil types. The trends for all soils show the highest removal levels when the ionic strength normalization parameter is in the range of 0.05 – 0.9. Below this range is the control for ionic strength effects. Above this range soils experience suppression in the colloidal removal levels, apparently due to increased dispersion and colloid trapping.

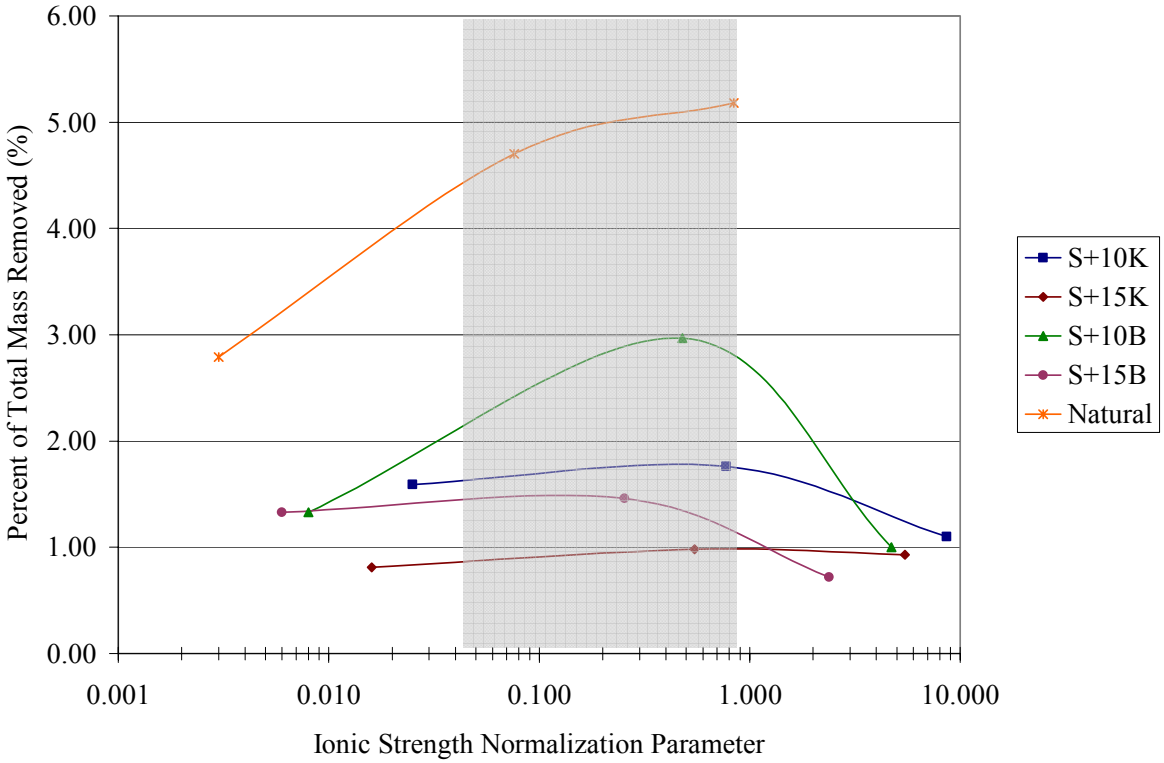

Figure 4.11: Trends of Percent of Total Mass Removed as a Function of Ionic Strength Normalization Parameter for All Soil Types (shaded area indicates optimized ionic strength application level)

4.7 Quality Assurance / Quality Control for Flow – Through Testing

Precautions were taken during all stages of testing in order to ensure the highest quality of testing results. With regards to the repeatability of testing for flow – through samples, and thus the reliability of results, five tests were conducted in duplicate to determine the consistency of results. Figure 4.12 presents three of these duplicate sets of tests. One is for the sand and 10% kaolinite at the lowest hydraulic gradient, one for sand and 15% bentonite at the middle hydraulic gradient, and the third for the natural soil at the highest

hydraulic gradient. All are for the low ionic strength concentration. Solid points indicate one set of data, while the duplicates are open points of the same shape for each of the tests.

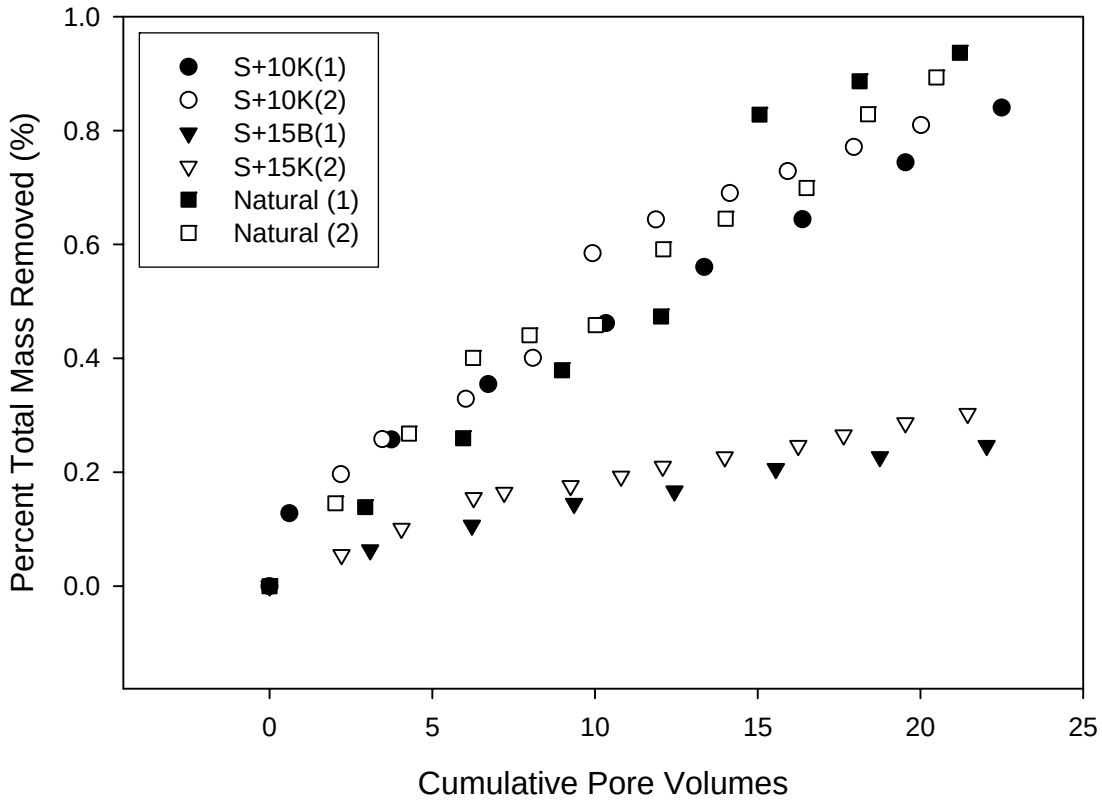

Figure 4.12: Quality Assurance / Quality Control Comparison for Multiple Soil Types and Multiple Hydraulic Gradient Variations

Duplicate testing was conducted for approximately 25 pore volumes. Although this is less than the typical testing of almost 100 pore volumes; most testing reached a steady trend (consistent removal rate) by the 25 pore volume mark and thus it was deemed unnecessary to continue past this point for duplication purposes. Tests showed reliable results – with duplication matching to within 0.05% of the total mass removed at the culmination of testing. Within testing, variations were slightly higher, but this was mainly due to fluctuations in

colloidal concentration with pore volume not overlapping across sample testing. The more general trends for each duplication were much better aligned than individual pore volume analysis; as well as being a more representative comparison for reliability.

Chapter 5. Micro – Analysis of Colloid Mobility

As mentioned previously, the three questions to consider when analyzing colloid mobility are 1) can the colloidal particles be dispersed, enter the flushing solution, and remain suspended long enough to be removed from the subsurface? 2) is sufficient contamination associated with the colloidal particles that their removal equates to a reduction in contamination levels? and 3) can larger particles, ones without associated contamination, be prevented from migration and removal?

This chapter will focus on the validity of concerns 1 and 3 from above; that is the mobility of the smaller colloidal particles and the rigidity (in terms of movement) of the larger soil particles. The association of contamination will be addressed in batch performance testing in Chapter 6.

Two approaches can be used when looking at mobilized versus stationary particles. One is to consider what is removed; the second is to consider what remains. Testing was conducted in both manners, with mass balance calculations performed in order to determine the overall accuracy of results. Table 5.1 summarizes mass balance results from the low ionic strength, low hydraulic gradient tests for each of the soil types tested considering overall mass differences, as well as percent of total sample difference.

Table 5.1: Summary of Mass Balance Results

Test Sample	Mass Difference (grams)	Percent Difference (%)
Natural	1.76	0.31
Sand + 10% Kaolinite	0.51	0.07
Sand + 15% Kaolinite	1.38	0.17
Sand + 10% Bentonite	1.43	0.17
Sand + 15% Bentonite	1.64	0.20

Mass balance data shows that less than 2 grams of each sample were unaccounted for in testing, correlating to a percent difference on average of less than 0.2%. These low magnitudes signify a high degree of confidence in the accuracy of mass removal measurements, grain size distribution and hydrometer analyses, and percent removal calculations presented herein.

5.1 Post Testing Grain Size Analysis

At the conclusion of testing, select soil columns underwent grain size distribution analysis. Both sieve and hydrometer testing were performed, not only on complete samples, but also on various portions (top, middle, and bottom) of select samples. Figure 5.1 plots the grain size distribution curve for a natural soil sample before and after testing.

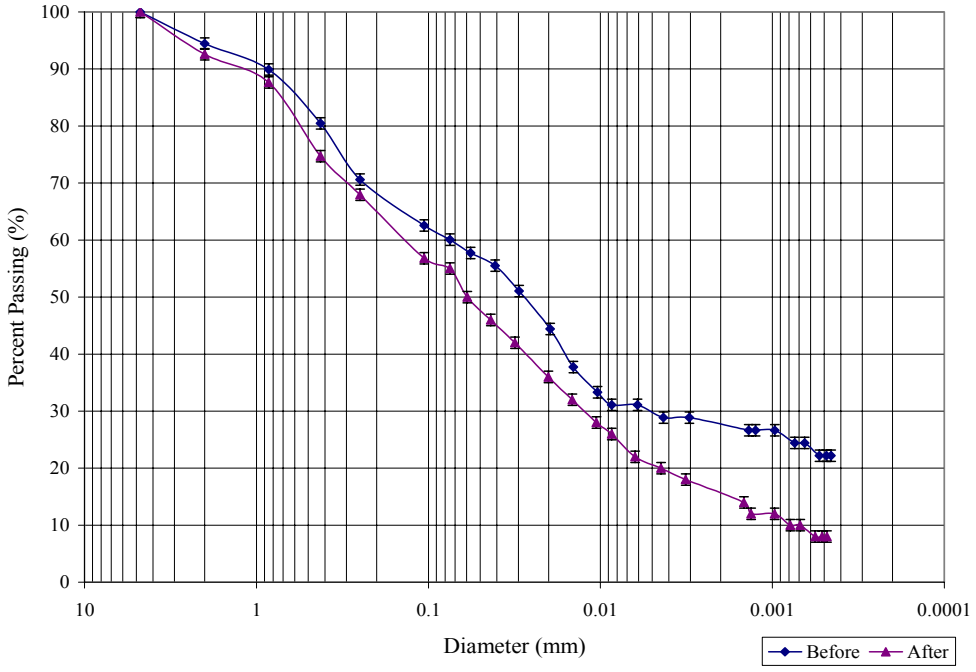

Figure 5.1: Grain Size Distribution Curve for Natural Soil Before and After Testing

The curves are averages of multiple tests, with the average as the plotted value and error bars indicating measured variations. From this graph one can see that the grain size distribution of the natural soil, after testing, plots consistently lower than that obtained prior to testing. In the larger particle diameter range, these differences become negligible when considering the testing range (as indicated by error bars). Where the difference is the most pronounced is in the region of particle diameters less than approximately 0.01 mm.

Results from the other samples are comparable to that of the natural sample, and are presented in Figure 5.2

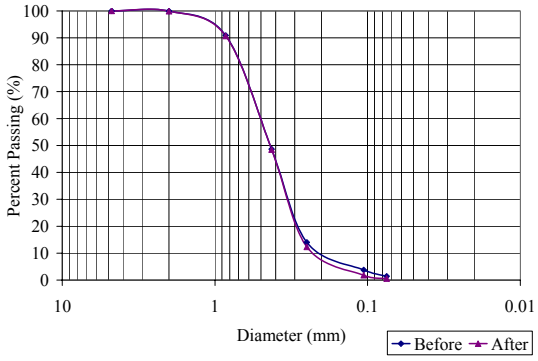

a) Sand and 10% Kaolinite

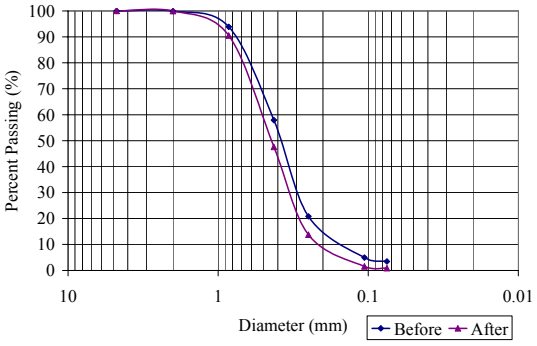

b) Sand and 10% Bentonite

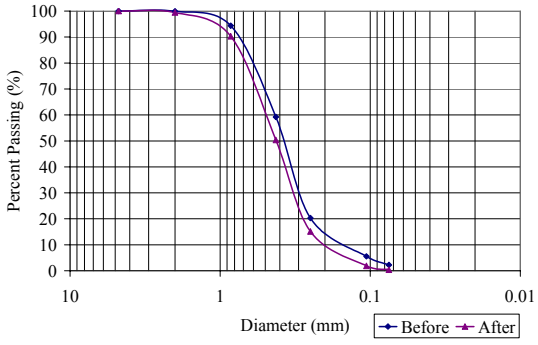

c) Sand and 15% Kaolinite

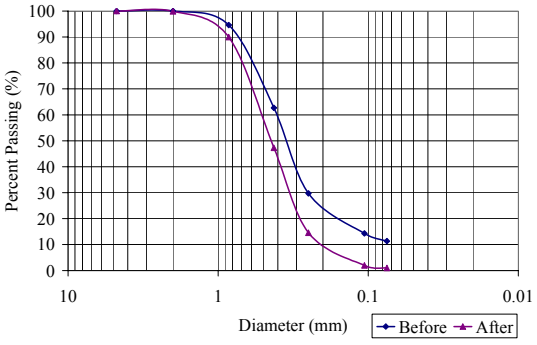

d) Sand and 15% Bentonite

Figure 5.2: Grain Size Distribution Curves for Sand / Clay Mixtures (see figures for various combinations) Before and After Testing

As with the natural soil, the most pronounced regions of difference in grain size distribution is in the range smaller than 0.1 mm, indicating that the finer particles were preferentially removed while the particles larger than 0.1 mm in diameter remained.

To assess how the distribution of particles within the sample changes due to testing, a sample of natural soil was divided into three section – entrance, middle, and exit – and grain size distribution was conducted on each of the individual sections. Results of this sectioned sample are presented in Figure 5.3.

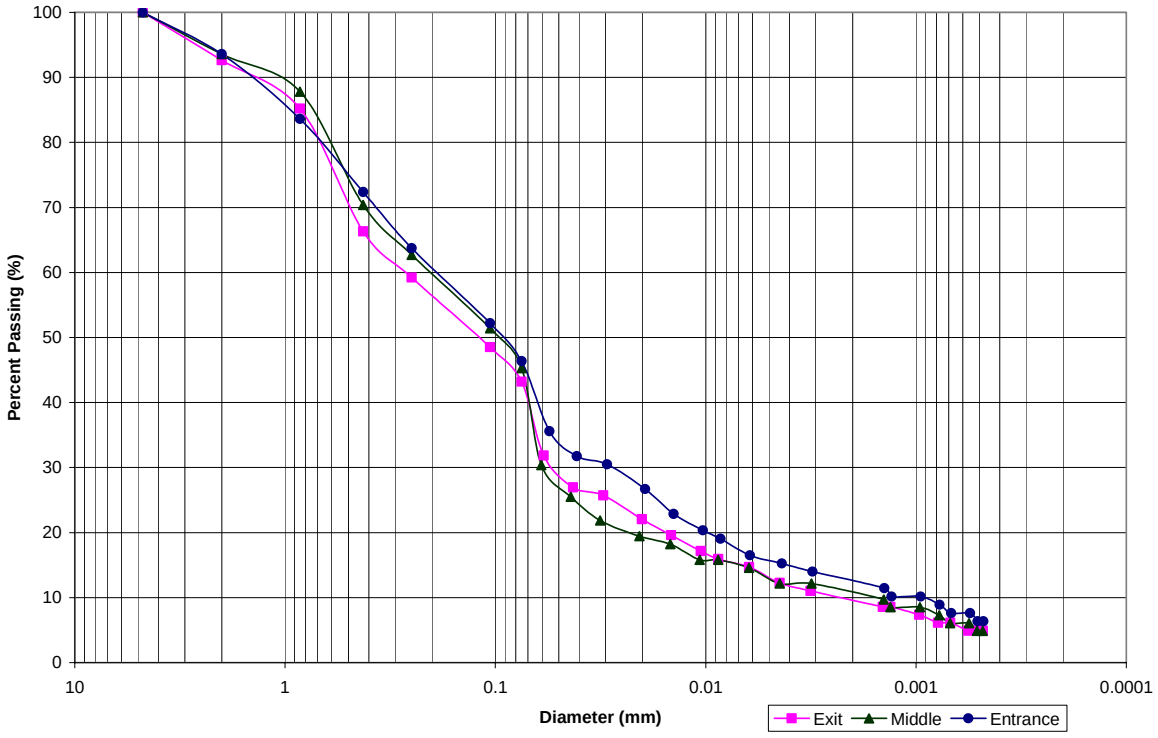

Figure 5.3: Grain Size Distribution Curves from Sectioned Natural Soil After Testing

Although some variation is present when considering each of the three sections, for the most part the grain size distributions are within 10%, or less, passing for each section. This may indicate two points. One, clay particles are being dispersed and mobilized in a

consistent manner throughout the sample. Any preferential flow is established early on and remains unchanged, and colloid removal is not limited to any particular area within the profile. Secondly, larger particles are not subjected to sufficient forces to induce their mobilization and transport. This is important because mobilization of these larger particles is more likely to lead to a reduction in pore diameters, increased clogging, and an overall reduction in permeability and colloidal removal efficiency. The even distribution of these larger soil particles confirms the integrity of the immobile soil matrix.

5.2 Removed Portion of Test Soils

In contrast to the consideration presented previously, it is also possible to take into account that portion of the sample that has exited in the flushing solution. To determine the properties of the colloidal effluent, samples were placed under a microscope and qualitatively and quantitatively analyzed. Qualitative analysis included visual comparisons to particles known to be in the colloidal range for each sample. Quantitative examination included particle measurements with statistical data applied to ensure reliability of results.

5.2.1 Qualitative Analysis of Removed Portion

Qualitative analysis was performed on samples from each of the five test soils under consideration; with results compared to one of three soil types. One is the natural soil, while the other two are the manufactured kaolinite or bentonite respectively. Since test samples were combinations of sand and different percentages of the clays, it is possible to consider only the three soil types. For both clays, the basis of comparison were the clay minerals

themselves, while for the natural soil it was the portion that passes the #270 sieve (or that portion < 53 μm). Comparisons were conducted using a Nikon microscope with a MiniVID Microscope camera attachment. The microscope itself possessed magnifications of 5, 10, 20, and 40; while the camera contained a 20x magnification. Combined this allowed for magnifications of 100x, 200x, 400x, and 800x. Subsequent figures will present the "control" picture, or the colloidal portion that did not undergo testing, with the colloidal picture (i.e. the colloidal portion actually removed during testing) in a side – by – side comparison. Evaluations will be conducted on samples from all hydraulic gradients tested, as well as the different ionic strengths tested. It is important to note for all photos, particle concentration is not indicative of colloidal concentration from effluent.

5.2.1.1 Natural Soil Analysis

Figure 5.4 (a,b,c,d) presents the three different hydraulic gradients tested (low = 6, medium = 14.5, and high = 29) in comparison to the control sample for the natural soil. From these results it is possible to see the general similarities between all four photographs. The major difference is visible when considering the greatest hydraulic gradient (Figure 5.4 d). This figure shows a greater number of larger particles sizes than that of the low and medium hydraulic gradients. However, even these larger particle sizes do not appear visually to exceed the distribution presented in the control figure – indicating the particles for the most part are still smaller than 53 μm in diameter.

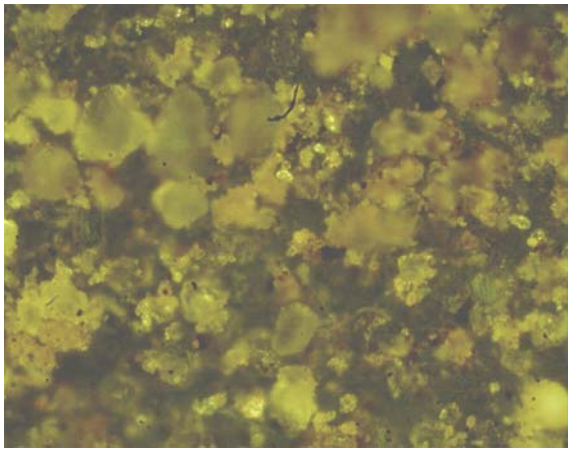

a) Control Natural Soil

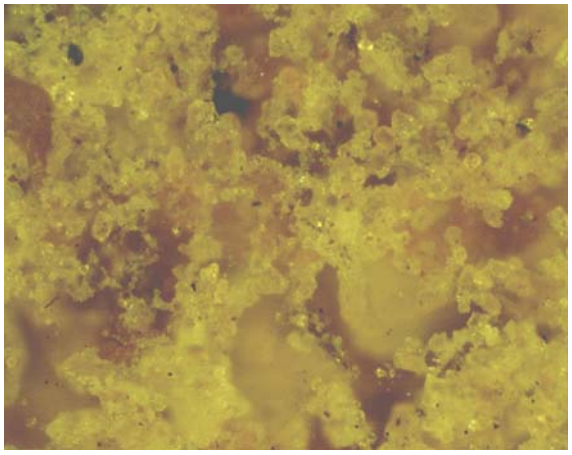

b) Natural Colloids: Low Hydraulic Grad.

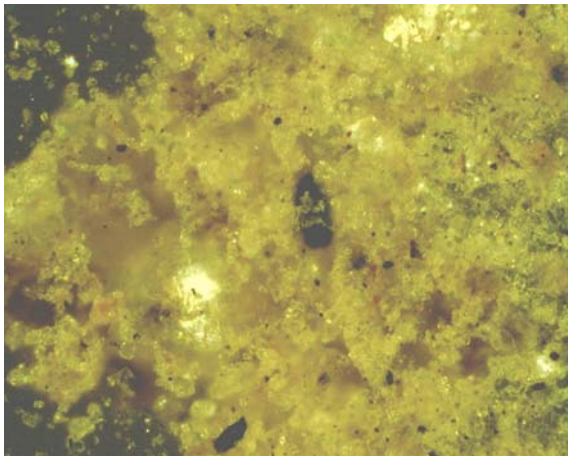

c) Natural Colloids: Med. Hydraulic Grad.

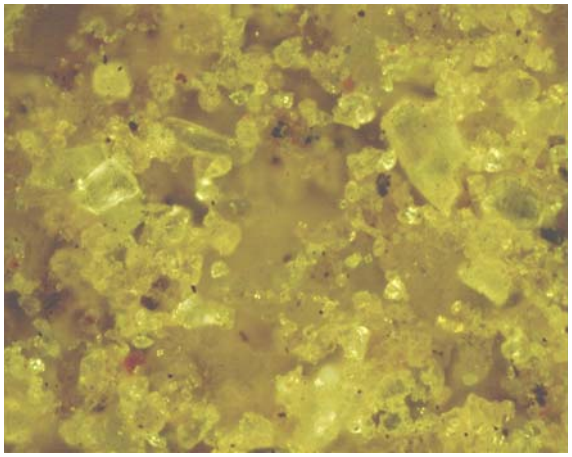

d) Natural Colloids: High Hydraulic Grad.

Figure 5.4: Microscope Photos of Natural Soil under 400x magnification (gives photo length of 500 µm) for All Hydraulic Gradient Variations under 0.0025 M Ionic Strength

Ionic strength comparisons under the high hydraulic gradient can be observed in Figure 5.5(a,b,c,d). Again samples are presented in comparison to the control colloids.

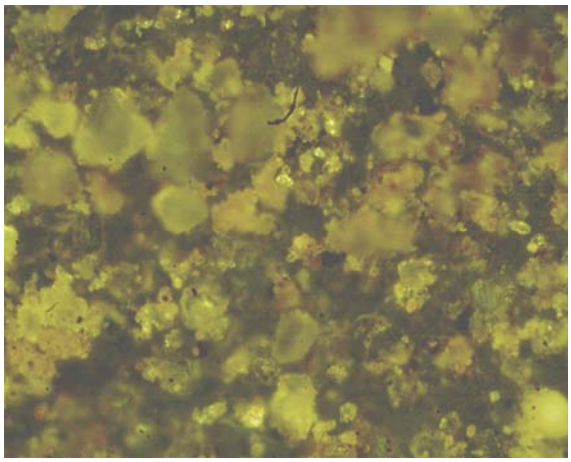

a) Control Natural Soil

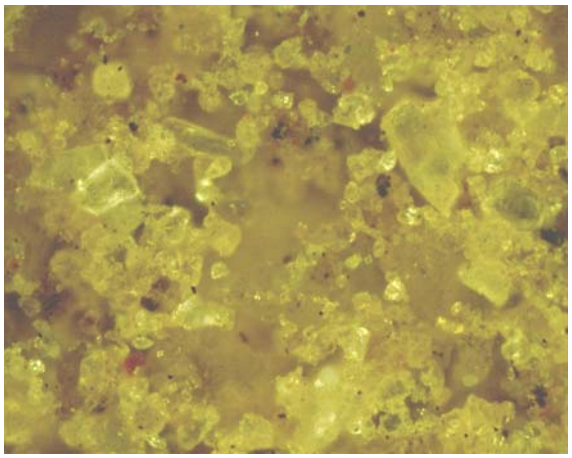

b) Natural Colloids: Low Ionic Strength

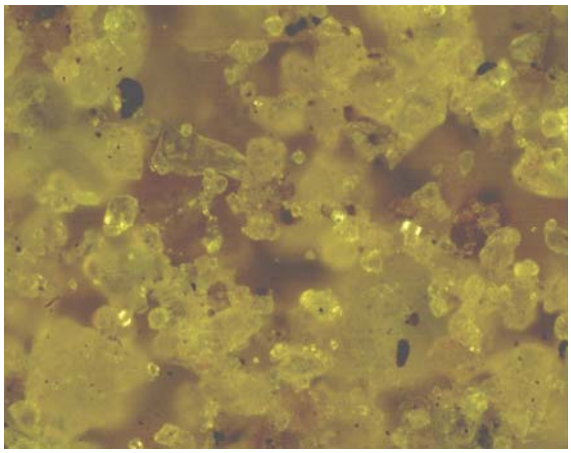

c) Natural Colloids: Med. Ionic Strength

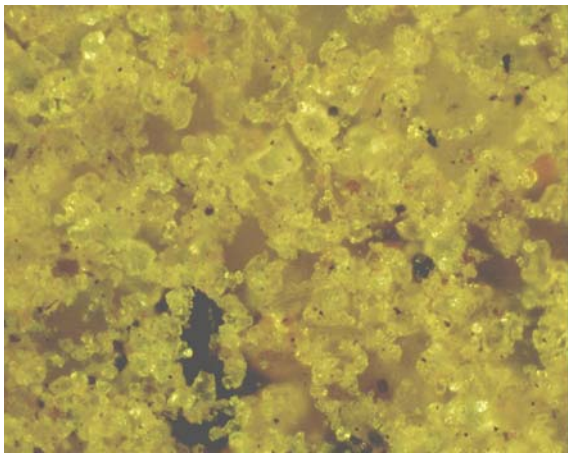

d) Natural Colloids: High Ionic Strength

Figure 5.5: Microscope Photos of Natural Soil under 400x magnification (gives photo length of 500 µm) for All Ionic Strength Variations under High Hydraulic Gradient

Similarities across the photos are apparent. All three ionic strengths illustrate the greater distribution of particle sizes present due to the high hydraulic gradient. Differences across the ionic strength variations show a lack of larger particle sizes in the highest ionic strength. With this photo showing both the greatest ionic strength, as well as the larger hydraulic gradient, particle trapping can be a reasonable justification for these lower values.

5.2.1.2 Kaolinite Analysis

For the manufactured soils, not only will hydraulic gradient and ionic strength variations be under consideration, but variations in the clay fraction (relative percent) of the soil will be taken into account. Samples were constructed utilizing either 10 or 15% of clay by mass with the remaining portion composed of sand. Results are compared to the "control" of the "pure" clay mineral prior to clay / sand mixing. Figure 5.6 (a – h) depicts results from the sand and both the 10% and 15% kaolinite tests under constant ionic strength and different hydraulic gradients

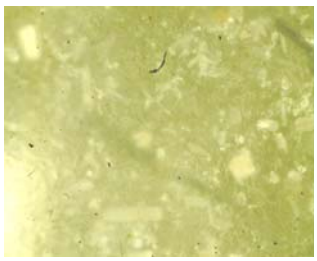

a) Control Kaolinite

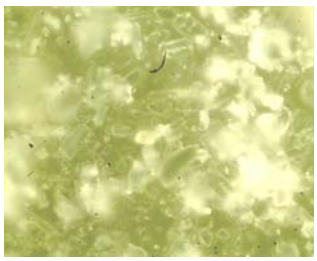

b) Control Kaolinite (800x)

c) Sand + 10% Kaol. Low Hydr. Grad.

d) Sand + 15% Kaol. Low Hydr. Grad.

e) Sand + 10% Kaol. Medium Hydr. Grad.

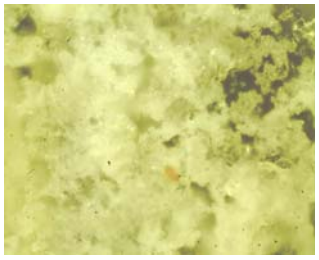

f) Sand + 15% Kaol. Medium Hydr. Grad.

g) Sand + 10% Kaol. High Hydr. Grad.

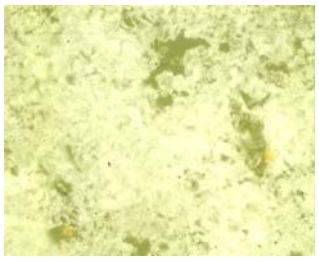

h) Sand + 15% Kaol. High Hydr. Grad.

Figure 5.6: Microscope Photos of Kaolinite under 400x magnification which gives photo length of 500 µm (note b has 800x or length of 250 µm) for All Hydraulic Gradient Variations under 0.0025M Ionic Strength

It should be mentioned that picture quality is the cause for a majority of the initial visible variations between the samples. Particle density within the photos is also a major contributor to the overall effect of photo dissimilarities. If one discounts these anomalies though, the relative size and shape of the particles in each photo are comparable. Particle diameters within these tests show smaller distributions than those of the natural soil. This is probably due to the fact that the colloidal particle size range for the kaolinite encompasses a smaller range than that of the natural soil. This can be observed by comparing Figure 5.4 a) with Figure 5.6 a) and b). Looking at the natural soil one can see a greater assortment of particle sizes than in the kaolinite sample, which is expected if one considers the difference in the grain – size distribution of the natural soil versus that of the kaolinite / sand mixtures (as presented and discussed in Chapter 3).

5.2.1.3 Bentonite Analysis

Variations in hydraulic gradient for the bentonite samples are illustrated in Figure 5.7 (a – g). As with the previous samples, these are compared to the control for both the 10 and 15% bentonite soils at the lowest ionic strength.

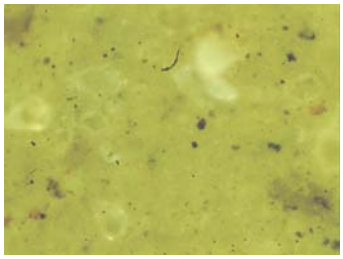

a) Control Bentonite

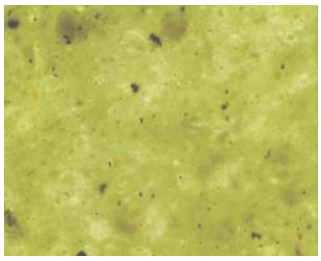

b) Sand + 10% Bent. Low Hydr. Grad.

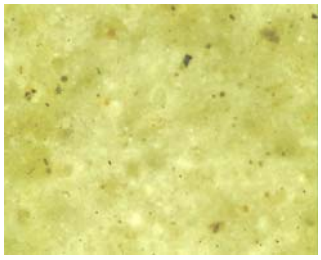

c) Sand + 15% Bent. Low Hydr. Grad.

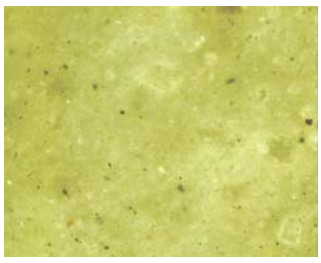

d) Sand + 10% Bent. Medium Hydr. Grad.

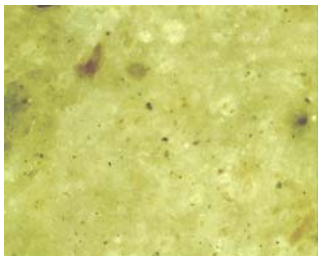

e) Sand + 15% Bent. Medium Hydr. Grad.

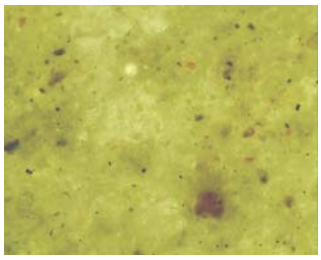

f) Sand + 10% Bent. High Hydr. Grad.

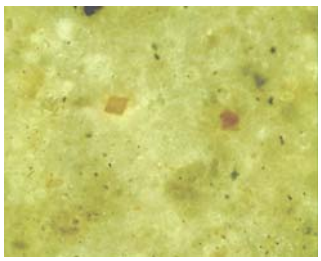

g) Sand + 15% Bent. High Hydr. Grad.

Figure 5.7: Microscope Photos of Bentonite under 400x magnification (gives photo length of 500 µm) for All Hydraulic Gradient Variations under 0.0025 M Ionic Strength

Bentonite samples do not exhibit defined particle shapes more readily apparent in both the kaolinite and natural soil samples. It is possible to see a few larger and more distinct particles in each of the figures, but overall the picture is cloudy. Unfortunately, greater magnification resulted in an indistinct picture which was even less beneficial from the standpoint of visual comparisons. Therefore it is necessary to utilize the reduced magnification for visual assessments. Considering all pictures in unison, one can see distinct similarities between every picture. Colors and patterns are similar, and match well with the control bentonite sample. In contrast, colors and patterns do not match with the sand sample shown in Chapter 3; this can serve as a further confirmation that the effluent colloids are bentonite rather than the sand mixture. This fact is also confirmed with the lack of visibility of large distinctly shaped particles obscuring almost 50% of the frame – a condition that would indicate the presence of even the smallest sand grains (smallest diameter approximately 0.25 mm). The single dissimilarity to note would be the presence of several "larger" (20 – 30 μm) particles in the highest hydraulic gradient photos (Figure 5.6 f and g) that are not present in the lower hydraulic gradient samples. These particles are noticeable in the control photo as well, indicating that the highest hydraulic gradient mobilizes a wider assortment of particle diameters within the colloidal range than the lower hydraulic gradients. Although this mobilization increases the overall mass removed, it is more likely to decrease the pore size diameter and increase the likelihood of particle trapping.

5.2.2 Quantitative Analysis of Removed Particles

In addition to basic visual analysis, a quantitative analysis of removed particles was performed on the natural soil samples. Only the natural soil was chosen due to visual

limitations with the other soils. Separate particle shapes were difficult to discern and reliably measure for both the kaolinite and bentonite, while the natural soil possessed clearer particle distinction that allowed for an analysis and comparison of results.

Comparisons were performed among the different hydraulic gradient variations, as well as the various ionic strength tests. Results were compared to both the control sample, as well as to either the other hydraulic gradients or ionic strengths used in testing. Comparisons between hydraulic gradient and ionic strength are limited in relevance, and thus will not be discussed.

Analysis was performed utilizing the Scope Photo program included with the MiniVID microscope camera. This program allows lines and shapes to be drawn on photos and provides basic dimensions of these drawings in tabular format. For particle diameter, circles were constructed using the two point method and the radius was converted to a diameter of particle in micrometers. Figure 5.8 illustrates an example of this analysis in the form of a screen capture of the program.

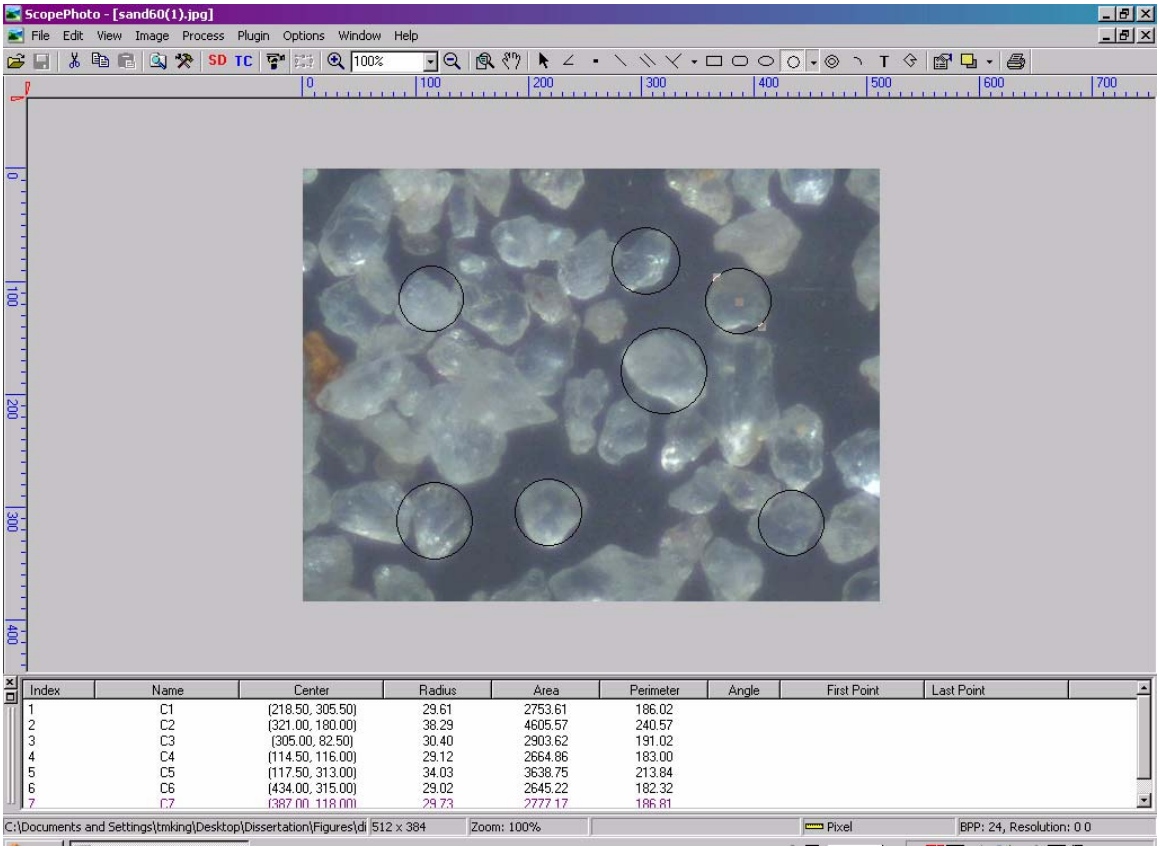

Figure 5.8: Screen Capture of Scope Photo Particle Diameter Analysis

The black circles on the photo are those drawn with the aid of the program, and a summary table visible below lists pertinent information such as radius, area, perimeter, etc. The soil pictured is the sand magnified 60 times. These types of measurements can be performed either on photos already taken, or during observation under the microscope, with no lasting photo of the measured areas obtained. Data was obtained in both manners to increase the area of analysis – rather than simply limiting it to a single photographed area of less than a quarter of a millimeter squared.

Table 5.2 summarizes results for six natural soil samples. Tests are labeled by the hydraulic gradient and ionic strength, or simply as the control sample.

Table 5.2: Particle Diameter Analysis for Natural Soil Samples

Sample Name	Mean Particle Diameter (μm)	Median Particle Diameter (μm)	Standard Deviation	Variance
Control	46.3	44.4	8.49	72.08
Low i, 0.0025M	19.6	20.4	3.96	15.69
Med i, 0.0025M	27.5	26.6	8.29	68.65
High i, 0.0025M	41.8	41.6	6.15	37.88
High i, 0.1 M	29.6	28.7	6.48	42.05
High i, 1.0 M	18.5	17.8	4.01	16.12

Particles under consideration for analysis were the largest particles in any given view during the duration of testing. Mean particles diameter is an indication of the average of the diameter of the largest particles present, not mid-range, smallest, or general representation of all visible particles. Largest particles were chosen in order to more accurately measure diameters, as well as to allow for a comparison of mobilization ranges for the various physical and chemical perturbations performed. Larger standard deviations and variance values simply indicate a greater range in the diameters of the mobilized particles, rather than an inaccuracy of results. It must be noted here that it is not possible to distinguish between individual particles and strongly bound aggregates of smaller particles.

It is expected then, that the greater the hydraulic gradient, the larger the average particle diameter. This is shown to be true when looking at the second through fourth rows of Table 5.2. Average particle diameter increases from 19.6 μm for the lowest hydraulic gradient (i = 6) to over 40 μm for the highest hydraulic gradient (i = 29). All tests showed smaller mean particle diameters and lower standard deviations and variances than the control sample. The significance in the smaller average particle diameter is the confirmation that only fine particles (according to USCS classification) are being removed from the subsurface. Standard deviation and variance are greatest for the middle hydraulic gradient (i = 14.5) signifying the greatest range in particle diameters occurred in this test.

When comparing ionic strength, it is interesting to note that the average particle diameter decreases with increasing ionic strength. Initially this could be looked upon as being caused by either a suppression of clay dispersion, or by the partial blockage of the exiting flow paths. Bearing in mind that these comparisons are conducted for the greatest hydraulic gradient tested (i = 29), a condition that lends itself to the mobilization of a higher number, as well as an increased size range of particles, it is hypothesized that these decreases are caused by partial clogging, which leads to a reduction in pore diameter and thus a decline in the range of particles that can be transported out of the system. A secondary justification for partial clogging over flocculation is the presence of a greater number of smaller diameter particles rather than larger diameter particles. Flocculation increases binding between particles – leading to a larger overall colloidal particle diameter, rather than a smaller one.

5.3 Analysis of Geotextile Clogging

Although permeability tests showed no significant difference for the flow of fluid through the geotextile as a function of testing time (i.e. number of pore volumes flushed), a more visible means of analysis was deemed beneficial to assess the clogging potential of the geotextile utilized as the filter around the PVWs. In the case of laboratory testing, this filter was employed at the exit to the flow – through samples; and pictures were taken comparing geotextile that had not undergone testing with that of geotextile after roughly 1000 pore volume flushes of colloidal solution had passed. Figure 5.9 (a – f) illustrates both the before and after photos of the geotextile at three separate magnifications. This particular after sample was subjected to the natural soil – with the darker coloring and reduced light reflection capabilities; these soil particles are more readily visible against the lighter grey –

colored geotextile. Photos are backlit to allow light to filter through the geotextile. This allows for a more direct comparison of clogging in the before and after over the traditional top-lit microscope pictures.

One interesting note is the presence of non – geotextile particles in the 200x magnified before photo [Figure 5.9 (e)]. Although not severe, it does show that particle capture can occur simply by handling or storing the geotextile in an everyday manner. The difference between these "before" particles and the "after" ones are much more pronounced. Even in the 10x magnification it is possible to see the high levels of textile blockage. The clear portions of Figure 5.9 (b) look almost like starbursts – a visible pattern has emerged within the textile. Since the geotextile itself has no discernable pattern (being non-woven) it is possible that this pattern indicates the development of preferential flow paths within the textile itself (as partial clogging takes place). Closer magnifications (60x and 200x) are too detailed to illustrate the pattern, but do show pictures of individual or groups of particles bound within the matrix of the geotextile itself. Overall fluid and colloidal flow through the textile were not reduced with this level of blockage.

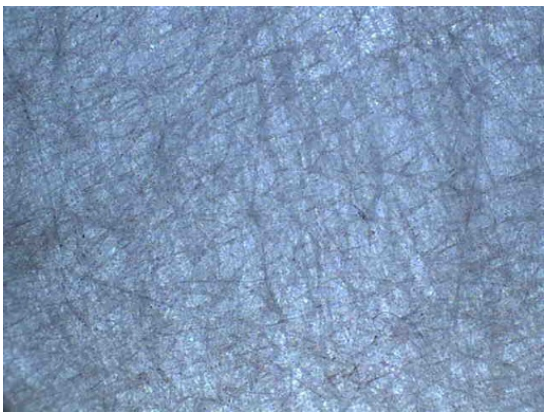

a) Before at 10x (picture length = 2.1 cm)

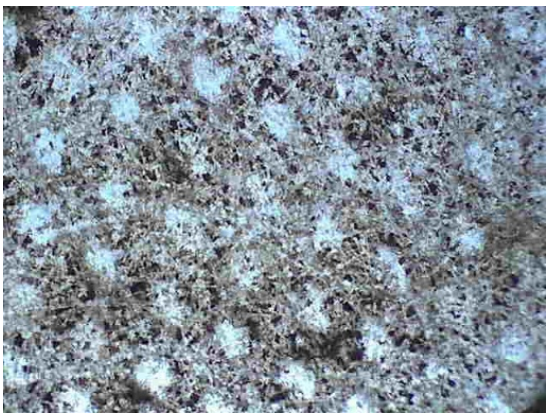

b) After at 10x (picture length = 2.1 cm)

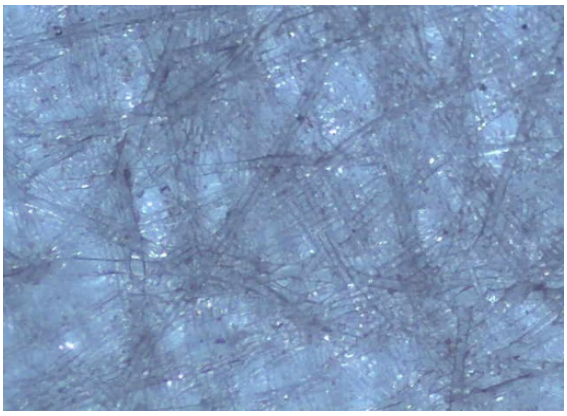

c) Before at 60x (picture length = 2.8 mm)

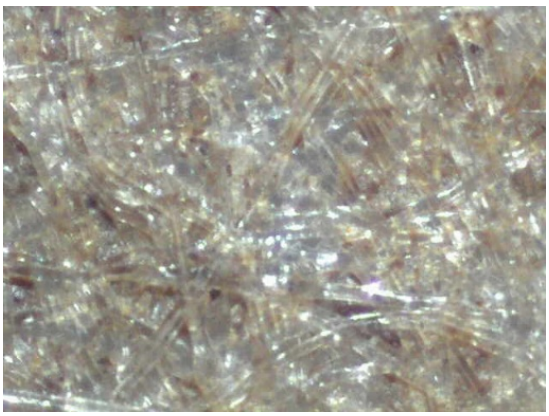

d) After at 60x (picture length = 2.8 mm)

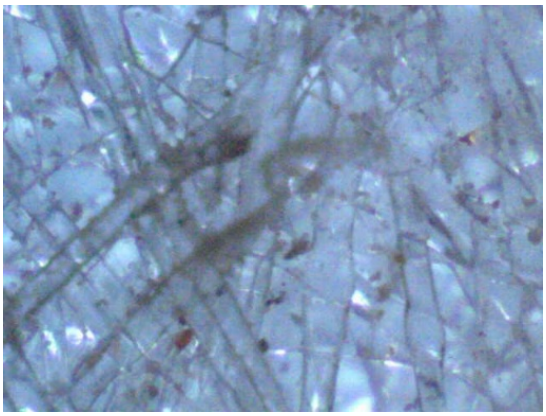

e) Before at 200x (picture length = 1 mm)

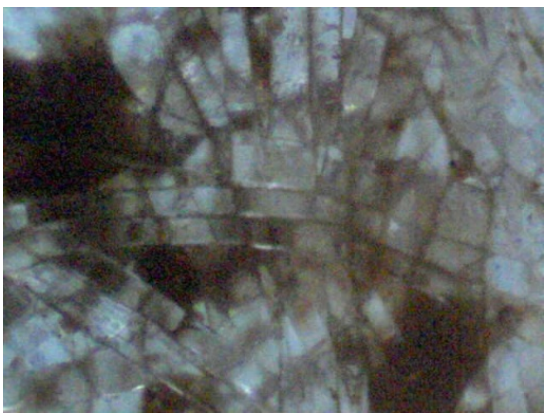

f) After at 200x (picture length = 1 mm)

Figure 5.9: Comparison of Geotextile Before and After Testing

5.4 Summary of Testing Validation

Consideration of both the removed and remaining portions of the various soil samples tested confirms the assumptions inherent in the non-contaminant testing program. Analysis of the soil portion remaining after flow – through testing indicates the immobile nature of the larger particles. This supports the assumption that those particles of a greater diameter, to which contamination is unlikely to attach, remain in the soil profile. Examination of the effluent particles, performed both qualitatively and quantitatively, reveals the mobilized soil falls into the USCS fines classification range. Further study shows that although various physical and chemical perturbations affect the overall range and average diameter of these particles, all applied perturbations resulted in clay dispersion and piping for fines removal.

Analysis of the geotextile with respect to clogging determined that although moderate levels of clogging were shown to occur, these levels did not result in a discernable decrease in the rate of fluid and / or colloidal flow through the geotextile. A possible reduction in the amount of clogging could be accomplished by the incorporation of reverse flow, but due to the lack of significant permeability reduction coupled with the design of the laboratory system, this concept was not tested.

Chapter 6. Contaminant Laboratory Results

The intent of contaminant testing is to prove the validity of the second hypothesis associated with colloidal mobility as a means of in situ cesium extraction from the subsurface. This condition assumes that there is sufficient cesium (Cs) associated with the colloidal particles that their removal equates to a reduction in Cs levels. Batch testing was conducted on the test soils to determine desorption levels at three different time periods. In order to quantify desorption amounts, it was necessary to contaminate soil samples and conduct sorption testing. This testing allowed for the initial Cs levels on the soil to be determined. The relative fraction of desorbed contamination could then be calculated. Results for three of the soils are presented below. Testing was performed on the natural sample, sand, and kaolinite. Bentonite was to be included in testing, but due to complications discussed in Chapter 3, it was ultimately not tested in this research phase.

6.1 Natural Soil Contaminant Testing Results

Due to the high SSA and CEC values for the natural soil, it was expected that cesium contamination would exhibit high levels of sorption, and relatively low levels of desorption for all times considered. Table 6.1 summarizes the sorption results presented by test type and ionic strength used. It is important to note that although these samples are labeled by different test distinctions, all sorption tests were performed identically and results should be fairly comparable. Testing labels were maintained in order to more accurately account for actual sorption levels, rather than considering average levels as representative of all tests.

Table 6.1: Sorption Results for Natural Soil

Desorption Ionic Strength	Sorbed Concentration (mg Cs / g soil)		
	3 hour desorption	18 hour desorption	42 hour desorption
Low (0.0025 M)	0.068 0.068 *	0.069	0.069
Medium (0.1 M)	0.068	0.069 0.069 *	0.069
High (1.0 M)	0.068	0.069	0.069 0.069 *

* Double numbers indicate sample duplicates / all values averages of duplicate runs

One sample with each ionic strength was tested in duplicate for each of the desorbed times used. All samples underwent duplicate analyses with the Atomic Absorption Spectroscopy (AAS) instrument. Each AAS measurement test included a total of three values, of which the average and relative standard deviation were reported. Relative standard deviation values for sorption testing results of the natural soil were in the range of 1.68 – 8.94 %. The standard deviation among results is 0.0005, with a variance of $2.42 \cdot 10^{-7}$ and a coefficient of variation of only 0.7%. This indicates that soil samples were statistically similar, testing was consistent, and results are reliable. Even with these close results, individual sorption values were utilized as the basis for desorption testing analysis.

Results of desorption testing are shown in Figure 6.1. This graph plots the desorbed mass as a fraction of the total sorbed mass versus time for each of the three ionic strength desorption tests.

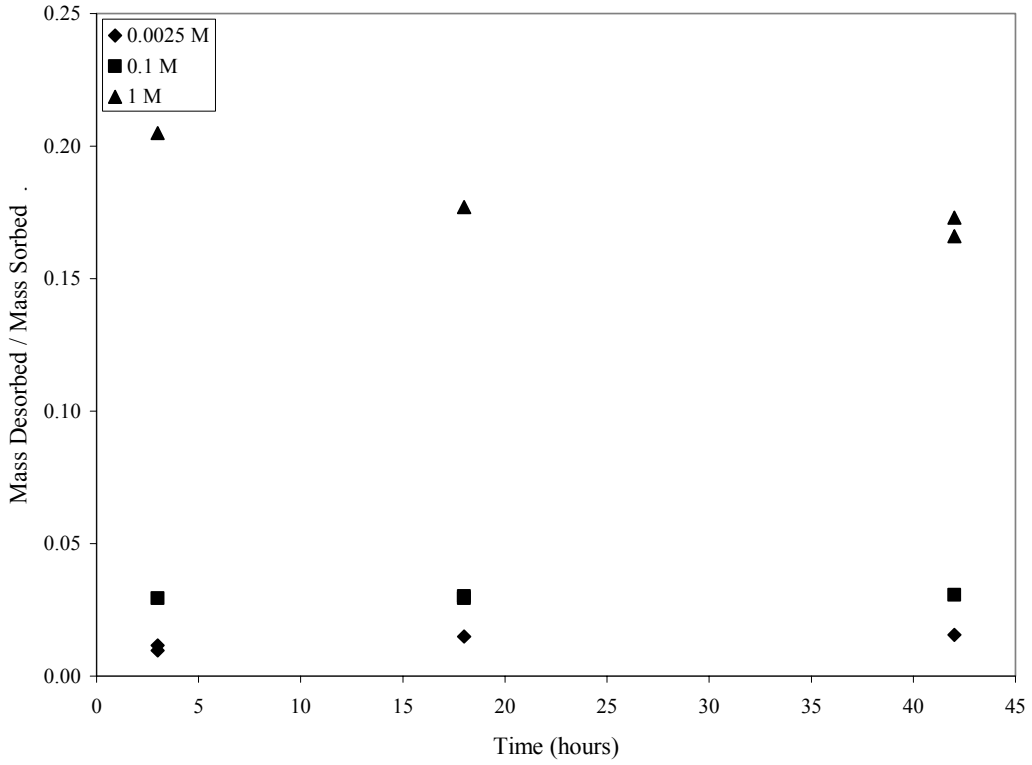

Figure 6.1: Desorption Testing for Natural Soil

Results confirm the low desorption levels for the natural soil. With the exception of the high (1.0 M) ionic strength test; desorption levels were less than 5% of initial sorbed concentrations. Even the high ionic strength – the test most likely to result in increased levels of desorption – showed ≤ 20% for every test point. Time (beyond 3 hours) played almost no influence on desorption levels. Increased desorption times, especially in the high ionic strength samples, led to decreased levels of desorption. This indicates the possibility of a re-equilibration of the Cs salt between the sorbate and sorptive phases.

6.2 Kaolinite Contaminant Testing Results

Although kaolinite is also a clay mineral, the lower CEC and SSA values, in comparison to the natural soil, tend to suggest reduced sorption levels. Desorption is expected to be moderate – on the low side because of the clay classification, but not extremely low due to the mineralogy of the clay. Kaolinite does not possess either the hydroxyl – interlayered vermiculites or the chlorite mineralogy of the natural soil, both of which dominate cesium sorption. Table 6.2 summarizes sorption results for the kaolinite samples. Data is presented in a similar manner to the natural soil data.

Table 6.2: Sorption Results for Kaolinite

Desorption Ionic Strength	Sorbed Concentration (mg Cs / g soil)		
	3 hour desorption	18 hour desorption	42 hour desorption
Low (0.0025 M)	0.012	0.006	0.008 0.008 *
Medium (0.1 M)	0.006 0.002 *	0.004	0.005
High (1.0 M)	0.006	0.008 0.003 *	0.006

* Double numbers indicate sample duplicates / all values averages of duplicate runs

Different samples from the natural soil were tested in duplicate. Unlike the natural soil, with a high consistency in results, kaolinite exhibited a wider range of sorption values – which made it all the more important to use actual sorption results instead of generalized averages as a basis for desorption testing. Statistical analysis of results produced an average sorbed concentration of 0.006; with a standard deviation of 0.002, sample variance of $6.0 \cdot 10^{-6}$, and a coefficient of variation of over 39%. In contrast, the relative standard deviations for testing were between 0.11 and 1.73%, indicating that repeat testing evoked consistent

results; although overall result variations were higher than desirable. The concentrations were over an order of magnitude less than that of the natural soil.

Desorbed results for the kaolinite are presented in Figure 6.2. One data point is not included in this graph because of an inaccuracy (negative value for desorption) of the results. The figure plots the relative desorption as a function of time for all three ionic strength tests.

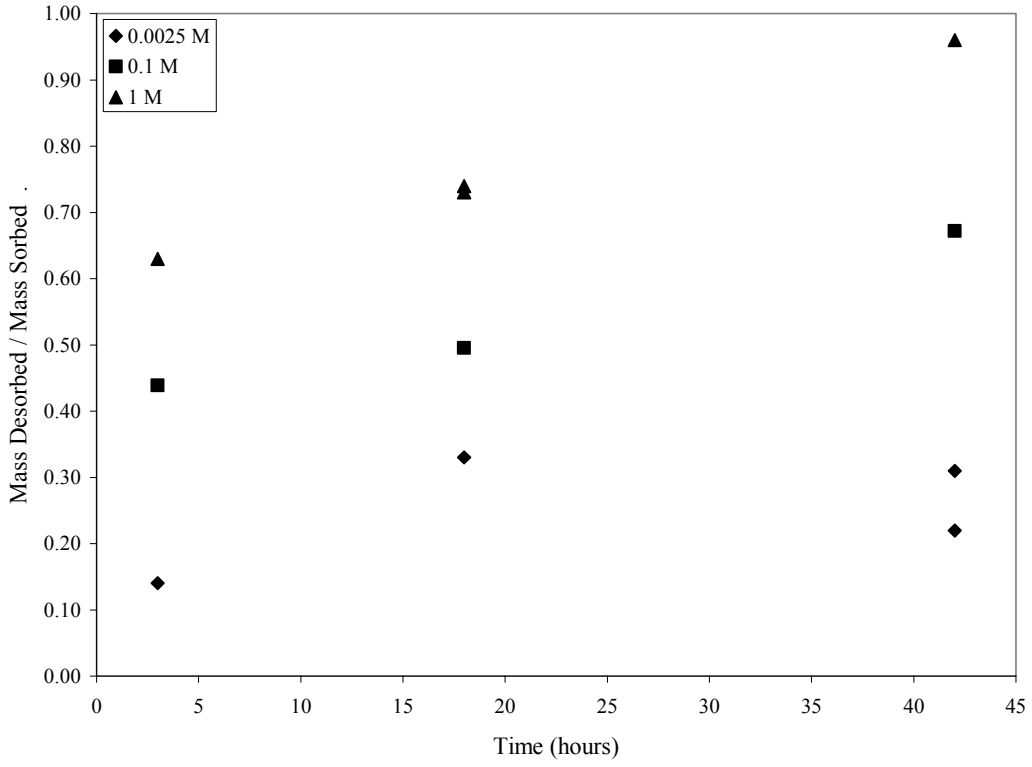

Figure 6.2: Desorption Testing for Kaolinite

It is important to note the different scale between Figure 6.2 and Figure 6.1. Overall desorption for the kaolinite is much higher than that of the natural soil. Values range from 15 – 65% at the three – hour test interval, to 20 – 95% at the 42 hour test interval. The highest ionic strength solutions resulted in the greatest removal rates, and even the moderate ionic strength dramatically increased desorption levels. Contamination binding on the kaolinite

was not as irreversible as on the natural soil, and the presence of moderate to high levels of sodium ions was sufficient to induce ion exchange as evidenced by this increased removal efficiency with the increase in ionic strength.

6.3 Sand Contaminant Testing Results

Unlike the kaolinite and natural soil, sorption levels on the sand were expected to be relatively low, while desorption levels were anticipated to be almost the entire fraction of sorbed contamination. Sand has a low SSA and virtually no CEC, so cesium binding, even for hydrophobic contamination, is more difficult than binding to clay or organic materials. A summary of sorption testing is recorded in Table 6.3.

Table 6.3: Sorption Results for Sand

Desorption Ionic Strength	Sorbed Concentration (mg Cs / g soil)		
	3 hour desorption	18 hour desorption	42 hour desorption
Low (0.0025 M)	0.008	0.007 0.007 *	0.008
Medium (0.1 M)	0.006	0.007	0.006 0.007 *
High (1.0 M)	0.009 0.007 *	0.008	0.009

* Double numbers indicate sample duplicates / all values averages of duplicate runs

Samples undergoing duplicate testing for the sand were different from either the kaolinite or natural samples, allowing each combination of ionic strength and desorption time to be tested in duplicate upon the culmination of testing. When considering all three soils, each ionic strength / time combination was represented in duplicate at least once. The accuracy of sand sorption results was midway between that of the natural soil and the

kaolinite. Relative standard deviation values for testing on sand were between 0.27 and 2.38%. Among tests the standard deviation was 0.001, with a variance of $1.23 \cdot 10^{-6}$, and a coefficient of variation of almost 15%. Sorbed concentrations were comparable to the kaolinite and over an order of magnitude lower than that of the natural soil. These sorption results compare well to those of earlier testing – with the kaolinite and sand having similar sorption results, and the natural soil exhibiting significantly higher sorption levels (Kunberger and Gabr, 2005).

Figure 6.3 presents the desorption results for the sand. The scale is the same as that of the kaolinite (both of which are 4 times greater than the natural soil scale).

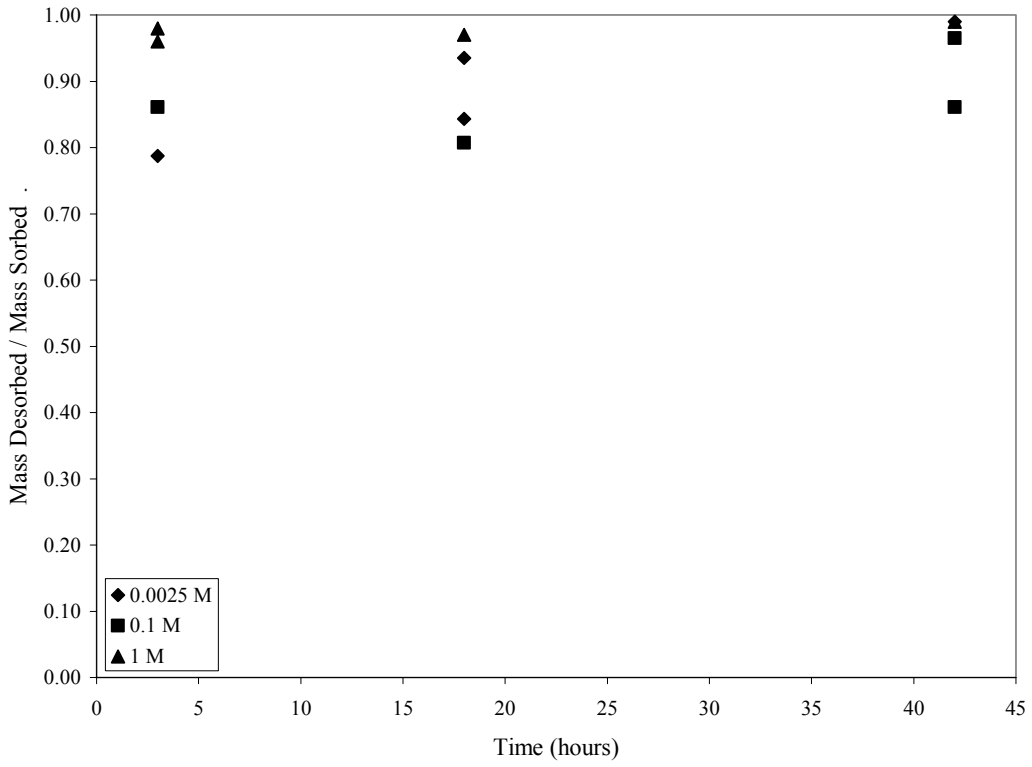

Figure 6.3: Desorption Testing for Sand

Results conform to the expected trend and show desorption levels between 80 – 100% for all ionic strengths at all tested time periods. As with both the natural soil and the kaolinite, the greatest ionic strength induced the greatest fraction of desorbed contamination.

6.4 Summary of Contaminant Testing Results

The outcome of contaminant batch testing was a demonstration of the colloid remediation assumption which attaches the cesium with the fines particles in the subsurface in a manner that reduces or prohibits the removal of the contamination without the removal of the fines themselves. Testing confirmed extensive sorption on the natural soil, with limited desorption for all times tested. For kaolinite, more moderate desorption was found, although on a mass basis these results were analogous to the natural samples. The higher fractional desorption results for the kaolinite were an effect of the lower initial sorption levels. Sand experienced the greatest desorption amounts, with almost complete removal even at the earliest (3 hour) testing time.

One limiting factor in the testing conducted is the lack of time associated with the "contamination period". Most hydrophobic contaminants demonstrate greater affinity for the sorbed phase with increased exposure time and Cs specifically can migrate into interlayers of mica, replacing K and becoming fixed to the minerals. Thus, subsurface contamination that has existed for greater lengths of time is typically more difficult to remediate than newer contamination using a conventional pump and treat system. The benefit of colloid mobility as a remediation measure in this case is that these greater bindings need not be overcome in order to induce remediation. The lab testing performed here illustrates a "best case" scenario in terms of contamination time. Desorption levels are likely to decrease with increased

exposure, or at minimum remain the same. In either case, the use of clay dispersion and piping can be beneficial as a means of increasing remediation efficiencies.

Chapter 7. Model Development

7.1 Comments on Prior Models

Prior research in colloid behavior includes a number of different modeling approaches. Five earlier research programs form the core of modeling evaluation.

Saiers and Hornberger (1996) created the facilitated transport model based on laboratory studies of colloidal and contaminant movement through packed sand columns. While this research did consider a three – phase system, ionic strength variations, and various sorption and desorption processes; the program did not consider the mobilization of colloids, only the deposition. Additionally, the starting point for testing (on which this model was based) was no colloids or contamination in the columns; both the contamination and colloids were injected in the flushing solution.

In their book Migration of Fines in Porous Media, Khilar and Fogler (1998) develop a general model to describe and predict the erosion of fines. The majority of the book focuses on the behavior of colloidal particles, rather than on contamination or contaminated particles, but the incorporation of contamination is proposed in the final chapter. Khilar and Fogler (1998) consider the initial conditions of existing colloids in the soil matrix and look at the effect of fluid physical and chemical, to an extent, characteristics have on both the release and deposition of colloids.

The reasoning behind the incorporation of Schelde's work (described in Section 2.5.3) as a basis for current modeling efforts was twofold. The first was that of the physical variations employed in controlling colloidal release. The two main physical effects that the authors desired to analyze were that of different flow rates and various lengths of flow

interruptions. No chemical deviations were performed, allowing physical differences to be the focus of the results. The second major benefit associated with Schelde's modeling is that of the initial conditions. The laboratory experiments and associated modeling begin with the provision of an infinite number of detachable colloids in the sample and zero colloids in the mobile phase. These are the same initial conditions employed in current modeling, and the work performed by Schelde et. al. is one of few previous tests that consider these initial conditions. However, it only considers this flow through a limited number of larger macropores, not the entire soil matrix. It also does not consider the presence of contamination or any chemical variations in the flushing solution.

In 2001, Sun et. al. discussed their multiple cell balance model, a three – phase system model that considers spatial and chemical variability of the soil system. The model also considers the dynamics of colloid deposition, release, and transportation, but has a number of assumptions that are not valid for the current research. These include initial conditions of zero deposited colloids, the injection of colloidal particles, and the lack of consideration with respect to colloid – associated contamination and ionic strength variations.

Grolimund and Borkovec (2005) present a mathematical transport model in the latest of a series of articles discussing the transport kinetics of colloidal particles. The model considers the transport of dissolved ions in a classical convection dispersion method and "particle transport is modeled according to classical filtration theory [with] the most important ingredient an appropriate description of particle release" (Grolimund and Borkovec, 2005). While the model considers ionic strength variations as well as colloid release and deposition; it does not take into consideration hydrodynamically induced particle release or initially low levels of ionic strength saturation (analogous to natural groundwater

levels). Focus, instead is on the suppression of particle release in two specific, although realistic, situations discussed previously in chapter two.

7.2 Model Considerations

Based on the desired modeling applications, four main factors dominate the issue. The first is the importance of a three – phase system of water, colloids and the soil matrix. Although a relatively new concept in contaminant transport, in contrast to the conventional two – phase (mobile water and immobile soil) system, the three – phase system is the backbone of current research, and has become a more widely accepted modeling approach. The second is that of the initial conditions. Unlike much of the previous research, this research considers the initial deposited colloids (i.e. existing clay content of the soil) and existing contamination as the initial conditions. This also means that the soil flushing solution would possess the initial conditions of no mobile colloids and no contamination. Consideration of release and deposition of colloids from soil as well as sorption and desorption of contamination from colloids and soil matrix is the third area of concern. While mobilization of the colloids is a major focus, the relevance of this mobilization to remediation efforts is entirely based on the level of contamination removal associated with mobilization. Also, increases in deposition over release can become a limiting factor in efficiency considerations. The final point is that of spatial and chemical variability of soil and flushing solution. This includes items such as flow rate variations, pumping schedules for flushing solutions, and ionic strength variations.

The two main goals of model development are 1) to assess the potential means and extent of colloid mobilization on the remediation of saturated systems and 2) to determine the magnitude of the effect of colloidal mobility on overall remediation efforts.

7.3 Model Development

Once these objectives and general features were defined, it was possible to establish a list of pertinent equations that would govern modeling. These equations can be classified as one of four main types: (1) general flow through a soil matrix, (2) colloidal movement, (3) contamination reactions, and (4) permeant variations.

General flow equations include flow rates, head variations, and pumping information. Colloidal transport, deposition, and release, as well as pore clogging and mass loading rates are part of the colloidal movement equations. Advection, dispersion, diffusion, decay, sorption and desorption are factors involved in contaminant reactions, while variations in ionic strength is the main permeant issue. A flow chart illustrating the initial conception of the model is shown in Figure 7.1.

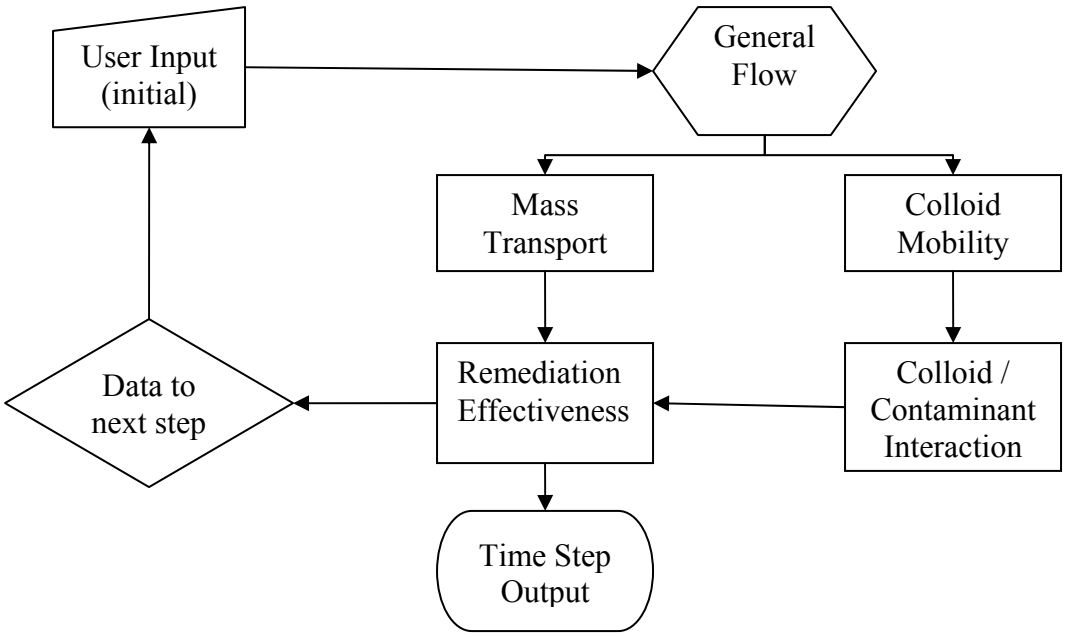

Figure 7.1: Flowchart of Model Conception

Required user input would involve soil and contaminant properties as well as proposed injection and extraction flow rates, pumping schedules, and any proposed chemical applications. Data would first enter the general flow portion of the model in order to develop head variations and velocity profiles for the given time step. Colloid mobility and mass transport would be considered based on the output from the general flow analysis, and coupled with colloid / contaminant interaction in order to determine the overall remediation effectiveness of the system. These results would be exported as the time step output (if desired) and relevant data would be transferred back to the start of the model for subsequent time step intervals.

7.4 Modeling Equations

Equations utilized in the model fall into four main categories discussed above: (1) general flow through a soil matrix, (2) colloidal movement, (3) contamination reactions, and (4) permeant variations.

7.4.1 General Flow Equations

General flow equations are based on the principles of Darcy's Law for flow in porous media and Poiseuille's Law for flow in tubes. These laws are applicable if the soil is approximated as a series of capillary tubes allowing flow only through these tubal areas. This approximation becomes critical later on in the development of colloidal movement equations. The equation for Poiseuille's Law is listed as equation 7.1.

$$\Phi = \frac{\partial V}{\partial t} = \frac{\pi R^4 |\Delta P|}{8 \eta L} \qquad \text{eqn. 7.1}$$

Where:

Φ = voluminal flow of liquid (cm^3 / sec)

V = volume of liquid (cm^3)

t = time (sec)

R = inner radius of tube (cm)

$|\Delta P|$ = pressure difference (dynes / cm)

η = fluid viscosity (poise)

L = tube length (cm)

The inner radius of the tube (R) can be approximated as half the average pore diameter. Pressure difference can be determined by an analysis of head variations as a function of location within the sample or soil profile.

7.4.2 Colloidal Movement Equations

The main focus of colloidal movement equations is on the depletion of clay particles from within the soil matrix. Khilar and Fogler (1998) present a generalized equation for this depletion that is the basis for current work and is presented in equation 7.2:

$$\frac{\partial}{\partial t}\left[V_i n_i C_s\right] = A_{si} r_{ri} - V_i n_i r_{ci} \qquad \text{eqn. 7.2}$$

Where:

V_i = volume of the ith segment (cm^3)

n_i = porosity of the ith segment

C_s = clay content of the soil (gram / cm^3 PV)

A_{si} = surface area of the ith segment (cm^2)

r_{ri} = rate of surface erosion in the ith segment (grams / cm^2 sec)

r_{ci} = volume rate of capture in the ith segment (grams / cm^3 PV)

Volume and porosity of the segments are straightforward values that can be determined based on the soil parameters. Clay content of the soil can also be directly determined if the specific gravity, porosity, and percent of clay by mass of the soil are known. Surface area of segments can be calculated using equation 7.3.

$$A_{si} = \frac{4}{d_0} V_i n_i \qquad \text{eqn. 7.3}$$

Where:

A_{si} = surface area of the ith segment (cm^2)

d_0 = average pore diameter of the ith segment (cm)

V_i = volume of the ith segment (cm^3)

n_i = porosity of the ith segment

These four variables are all relatively simple to calculate if *in situ* values of density are known and specific gravity and grain size distribution tests are performed in the lab. To determine the average pore diameter, "it is common to assume the effective pore diameter is approximately 20% of the effective grain size (d_{10})" (Holtz and Kovacs, 1981). This leave only the rate variables left to determine.

7.4.2.1 Rate into Flushing Solution

The rate of surface erosion in simplified terms relates to the rate in which colloids enter the flushing solution. Important items to consider include how many colloidal particles are available, the permeability of the soil, the rate of flow of the flushing solution, shear force induced by the flushing solution, chemical contributions to particle release or suppression, and the overall likelihood of particle release.

This rate is based both on the properties of the soil, as well as those of the flushing solution and can be calculated using equation 7.4:

$$r_{ri} = \frac{\Phi}{K_0} C_s \Xi \qquad \text{eqn. 7.4}$$

Where:

r_{ri} = rate of surface erosion in ith segment (grams / cm^2 sec)

Φ = volume flow of liquid based on Poiseuille's law (cm^3 / sec)

K_0 = intrinsic permeability (cm^2)

C_s = clay content of the soil (grams / cm^3 PV)

Ξ = correction factor to account for permeant variations

Poiseuille's law was presented earlier in the general flow equations. The intrinsic permeability is determined by multiplying the permeability of the soil by a ratio of the viscosity of the flushing solution divided by its density. Clay content is the same as above, while the correction factor will be discussed in the permeant variations section below.

7.4.2.2 Rate out of Flushing Solution

In the same manner in which the rate of surface erosion in simplified terms equates to the rate in which colloids enter the flushing solution; the volume rate of capture in simplified terms equates to the rate in which colloids exit the flushing solution. Significant factors to bear in mind include the rate of water flow, the concentration of colloids in solution, the principle cause of dispersion and flocculation (e.g. the ratio of pore diameter to particle size and the saturation of the solution in terms of colloids), as well as the total amount of water

under consideration and the chemical composition of that water. The equation is again based on soil and solution properties, and is presented in equation 7.5.

$$r_{ci} = \frac{\Phi}{V_v} C_L \mathrm{X} \qquad \text{eqn. 7.5}$$

Where:

r_{ci} = volume rate of capture in the ith segment (grams / cm^3 PV sec)

Φ = volume flow of liquid based on Poiseuille's law (cm^3 / sec)

V_v = volume of voids in the ith segment (cm^3)

C_L = clay concentration in solution (grams / cm^3 PV)

X = correction factor to account for permeant variations

Clay concentration in solution is a function of the rate of colloidal generation, i.e. the rate of surface erosion, within the soil profile. The correction factor to account for permeant variations is based on similar properties as the correction factor in the previous equation, but has slight variations to account for the differences in erosion versus deposition.

7.4.3 Contamination Reactions

Contamination reactions include those considerations in both the Mass Transport and Colloid / Contaminant boxes of the flowchart depicted in Figure 7.1. In this section the traditional advection, dispersion, diffusion aspects would come into play as well as the sorption and desorption from both the immobile soil matrix and the mobile soil colloids.

From a model development standpoint there are no equations introduced in this subsection that differ from previous modeling efforts.

In specific regard to the research at hand, this section will be largely disregarded. Justification for this stems from two main features: 1) the contaminant of choice and 2) the focus on colloidal movement without contamination in the laboratory testing. The bulk of flow – through testing is conducted without the influence of contamination. For this reason, it is not necessary to incorporate contamination reaction in the modeling of these scenarios. Modeling can be compared on a colloidal basis alone, and contamination can be inserted in subsequent analysis. For the current research, the contaminant of concern is cesium, historically a metal that binds strongly to clay particles in the subsurface. Although soil specific, partition coefficient (K_d) values for cesium have been determined by various test methods to range between 10 and 66,700 mL/g, depending on the CEC and clay content of the soil (EPA, 1999). Even the most modest of these values would indicate the relatively low, to almost inexistent, removal levels of cesium in the soluble phase. For these two reasons, the focus of modeling will be on colloid, rather than on aqueous contaminant, mobility and transport.

7.4.4 Permeant Variations

Physical and chemical differences are the two main types of permeant variations important to modeling development. The primary physical variation is that of changes in hydraulic gradient, while the focus of chemical differences is on the ionic strength of the solution. Each plays its own role in contributing to both the rate of colloidal release, as well as to the rate of capture; and must be considered as independent entities.

7.4.4.1 Physical Permeant Variations

Increases in hydraulic gradient can be a two – edged sword when viewed with respect to colloidal mobility. While the higher hydraulic gradients are more likely to mobilize a greater mass of particles; it is unsure if this greater mass will be due to the mobilization of a larger numerical quantity of particles, or rather the mobilization of larger – sized particles (which would contribute more mass on an individual basis than the same number of smaller particles but perhaps contain less associated cesium). Particle volume, both in the form of larger particles and greater number of particles, can also become a hindrance when considering the limited pore volume diameters through which these colloids must pass. Therefore, while hydraulic gradient considerations must be applied to both the rate of erosion and the rate of capture – the application needs to be in a distinctly different manner for each.

For the rate of erosion it becomes critical to compare the shear force induced by the solution flow with that required to initiate movement of colloidal particles. This can be accomplished by comparing the seepage velocity with that of the critical shear velocity. Seepage velocity can be calculated using the following equation:

$$V_s = \frac{k \cdot i}{n} \qquad \text{eqn. 7.6}$$

Where:

V_s = seepage velocity (cm / sec)

k = permeability (cm / sec)

i = hydraulic gradient

n = porosity

The use of seepage velocity over simply the velocity allows for a more accurate assessment of what is actually occurring in the soil profile. The difference in the two is simply the incorporation of the porosity of the soil, but this incorporation leads to higher velocity values and thus greater induced shear forces within the soil.

The determination of the critical shear velocity is a more complicated process, relying on a set of equations in stepwise manner instead of simply a single equation. It is based on Shields curve for the initiation of motion, which can be described using the following set of equations:

eqn. 7.7

$$
\begin{aligned}
D_* \le 4 \quad &\Rightarrow \quad \theta_{cr} = 0.24 \cdot (D_*)^{-1} \\
4 < D_* \le 10 \quad &\Rightarrow \quad \theta_{cr} = 0.14 \cdot (D_*)^{-0.64} \\
10 < D_* \le 20 \quad &\Rightarrow \quad \theta_{cr} = 0.04 \cdot (D_*)^{-0.10} \\
20 < D_* \le 150 \quad &\Rightarrow \quad \theta_{cr} = 0.013 \cdot (D_*)^{0.29} \\
D_* > 150 \quad &\Rightarrow \quad \theta_{cr} = 0.055
\end{aligned}
$$

This set of equations relates the dimensionless particle parameter, D_*, to the critical mobility parameter, θ_{cr}. Utilizing this relationship, it is possible to determine the critical shear velocity, $u'_{*,cr}$, by first calculating the particle parameter using the equation:

$$D_* = D_p \left[\frac{(s-1)g}{\nu^2} \right]^{1/3} \qquad \text{eqn. 7.8}$$

where:

D_* = particle parameter

D_p = average colloidal particle diameter

s = specific density = (particle density / fluid density)

g = gravitational constant

ν = kinematic viscosity coefficient

= (dynamic viscosity coefficient (μ) / fluid density)

From this particle parameter value, the Shields curve set of equations is utilized to determine the critical mobility parameter. Once this value is established, the critical shear velocity can be calculated from equation 7.9:

$$u'_{*,cr} = \sqrt{\Theta_{cr} \cdot (s-1) \cdot g \cdot D_p} \qquad \text{eqn. 7.9}$$

where:

$u'_{*,cr}$ = critical shear velocity

θ_{cr} = critical mobility parameter

s = specific density = (particle density / fluid density)

g = gravitational constant

D_p = particle diameter

Once these two values are determined, it is a simple matter to compare and create a ratio between what is present and what is necessary. This ratio becomes part of the correction factor (Ξ) for the initiation of movement.

The rate of capture is less concerned with actual initiation of movement, and more with the properties of what is being moved. In this case a comparison is performed between the average pore size diameter, and the average diameter of the mobilized particles. Average pore diameter is based on the grain – size distribution curve of the soil; while the average diameter of the mobilized particles can be determined using the previous equations in a slightly different manner. In this case it is necessary to take the seepage velocity and set it equal to the critical shear velocity in equation 7.9. The critical mobility parameter can then be calculated, followed by the particle parameter, and the average particle diameter. Because of the multiple equations in determining the particle parameter from the critical mobility parameter, extreme caution must be exercised to ensure use of the correct equation based on the restrictions of each. This back calculation can lead to the diameter of the mobilized particles. A ratio between this and the average pore diameter is then determined, and applied as a part of the correction factor (X) for the rate of particle capture.

7.4.4.2 Chemical Permeant Variations

The chemical perturbation focus of this research is the modification of the ionic strength (as NaCl) of the initial pore volume of flushing solution before low ionic strength solution is applied. Not only is this NaCl addition in various concentrations, but it is also for a finite length of time, reverting back to typical groundwater concentrations after a short influx of higher ionic strength. The importance of this finite time span is the understanding

that extended exposure to high ionic strength concentrations has the effect of increasing flocculation and thus decreasing colloidal mobility. Shorter influx times (volumes) of high ionic strength solutions are likely to prove beneficial, rather than harmful, to the dispersion of colloids and thus increase removal rates. Soil cation exchange capacity and activity are likely to play a role in the efficiency of this method, and as such become important properties for consideration.

The ultimate goal is the development of a ratio between the cation exchange capacity of the soil and the quantity of cations present in the flushing solution. This quantity depends on the cation charge, ionic strength of the solution, and total volume of the flushing solution. Both this and the soil CEC can be converted to cmol of charge on a volumetric basis and then compared to form an ionic strength ratio. When combined with the activity of the soil, this becomes an ionic strength normalization parameter. This parameter accounts for the primary properties important in the chemical consideration portion and can be applied to both the rate of erosion, as well as to the rate of capture in similar manners.

A normalization parameter that is very low indicates the ionic strength of the flushing solution is low compared to the CEC of the soil. This low ratio is likely to have no adverse effect on the results, but also likely to have little benefit with regards to colloidal mobility. In contrast, high normalization parameters suggest a greater level of ions in the flushing solution with respect to the CEC of the soil. This excess, whether truly above the CEC or not, can potentially suppress the dispersion of colloids to the point the soil can not recover – even after the introduction of a lower ionic strength concentration of the flushing solution. These values are prone to do more harm than good, and thus should be avoided in remediation situations. Moderate values of the normalization parameter are those most apt to

produce increased benefits with minor costs. These values have sufficient ionic strength levels in the flushing solution, that the change in concentration can initiate particle movement, but are not so large in comparison to the CEC of the soil as to create a condition from which the soil can not recover – causing an overall suppression of colloid mobility.

7.5 Model Flexibility

One of the greatest benefits associated with the model is the flexibility implicit in the design. While it is initially designed for a strongly sorbing contaminant, the addition of a traditional mass transport analysis can make it feasible for a wide variety of contamination. Additionally, it can be incorporated into existing models that currently do not consider colloidal mobility as a means of remediation. Information could be fed to the model as a subroutine, and the results sent back to be integrated with existing model results. For contaminants with little or no transition between phases; this incorporation would not only be extremely valuable, but also relatively simple. Contaminants with greater solubility ratios would increase the complication of the application, but not make it any less important.

7.6 Model Innovation

Although a number of models exist to date, they either differ in focus, or in the primary approach from the one presented herein. Some fail to consider clogging, while others consider either the physical or chemical effects, but not both. A number base the initial conditions on colloids in the flushing solution, but none in the soil matrix. Those that look at it in terms of remediation focus on the inhibition of colloidal mobility to prohibit

migration; rather than the enhancement to encourage removal. This model seeks to determine the efficiency and effectiveness of colloid mobility as a means of remediation and predict results of the application of colloid mobilization to the remediation of select sites.

7.7 Model Evaluation

The comparison of the model with laboratory results will serve to provide values for the parameters of interest. So although these two items will be discussed separately; where appropriate they will also be considered concurrently. The main parameters for the analytical model to predict colloidal mobility fall into two categories – that of soil parameters, and that of solution parameters. The soil parameters that will initially be considered are those of permeability, pore diameter, clay content, and cation exchange capacity. The solution parameters are hydraulic gradient and ionic strength. Since CEC and ionic strength are combined in the model – they will be considered in tandem as simply ionic strength effects. This effect, as well as that of hydraulic gradient, can be seen with the comparison to lab results, and will be discussed in that section. The remaining parameters of permeability, pore diameter, and clay content will be discussed in the following section.

7.8 Parametric Study Results

While permeability, pore diameter, and clay content are three separate parameters, they are however somewhat interconnected. An increase in clay content is likely to decrease the permeability of the soil, possibly with a decrease in the pore diameter. An increase in pore diameter will likely increase the permeability, regardless of whether or not it comes

with a decrease in clay content. For this study, we will assume that each parameter is independent and discuss as such. Model parameters that will be maintained throughout the course of testing include the following: Specific gravity of 2.65, porosity of 0.5, and a hydraulic gradient of 6.

7.8.1 Effect of Permeability

Typical values in permeability for soils can range anywhere from 10^2 cm / sec to as low as $1 \cdot 10^{-9}$ cm / sec. For this study we are not going to consider any value greater than $1 \cdot 10^{-3}$ cm/sec. The reasoning is that values higher than this are unlikely to have any significant levels of clay particles, or more simply put, the level of naturally occurring soil colloids in these soils is expected to be rather low. Clay content will be maintained at 30%, and the effective pore diameter will be $2 \cdot 10^{-4}$ mm. The results of this comparison are presented in Figure 7.2.

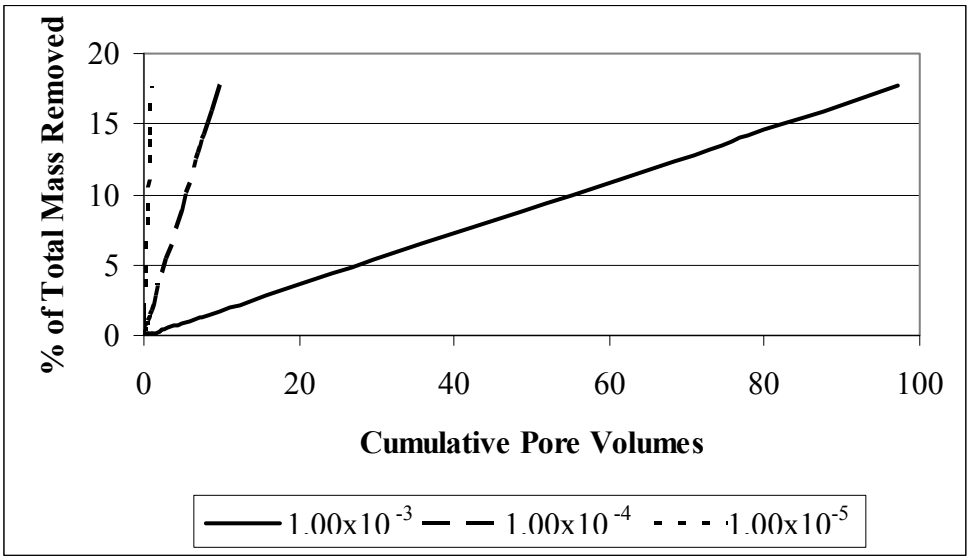

Figure 7.2: Effect of Permeability Variations (values in cm/sec)

Upon initial consideration, the graph appears to be contradictory; in that is suggests that the lower the permeability, the better the results. However, one must note that the graph is in terms of cumulative pore volume, not time, and a decrease in permeability leads to an increase in time needed to flush a set number of pore volumes through the sample. To give a general idea of how time factors into the results, the difference in the length of time to achieve a single pore volume (based on the typical laboratory sample dimensions of 12 cm length and 7 cm diameter) was calculated. For a permeability of $1.00 \cdot 10^{-3}$, a pore volume can be obtained in slightly less than 17 minutes. In contrast, it takes almost 3 hours to obtain the same pore volume with a permeability of $1.00 \cdot 10^{-4}$, and over a day when the permeability is $1.00 \cdot 10^{-5}$. Additionally, the comparisons are all made at the same porosity, average pore diameter, and clay content. Variations of two orders of magnitude in permeability are not likely to occur with these values remaining stationary. It is much more likely that decreases in permeability would be partnered with decreases in average pore diameter, porosity, and increases in clay content.

What can be seen from this graph is the fact that permeability itself does not play a part in the overall total mass removed from the system – it simply adjusts the pore volumes needed for this removal to occur. This implies that the colloidal concentration is greater for the lower permeability. This observation is reasonable considering the implicit increase in residence time without a decrease in pore diameter or applied shear forces. In reality, these combinations are unlikely to occur, but the importance of accurate permeability assessments for model input is clearly visible from the data in Figure 7.2.

7.8.2 Effect of Pore Diameter

No typical values exist for average pore diameters – and even the averages themselves are not necessarily indicative of soil matrix conditions. A value is required, however, in order to perform calculations, and thus we will consider a range which is comparable based on d_{10} values of soils with moderate to high clay levels. If the d_{10} values range from 0.001 to $1 \cdot 10^{-4}$ mm, we obtain a range of pore diameters from $2 \cdot 10^{-4}$ to $2 \cdot 10^{-5}$ mm based on the relationship of average pore diameters equaling approximately 20% of the d_{10} value. A clay content of 30% and a permeability of 10^{-3} cm / sec will be employed. Figure 7.3 graphs the result of this analysis.

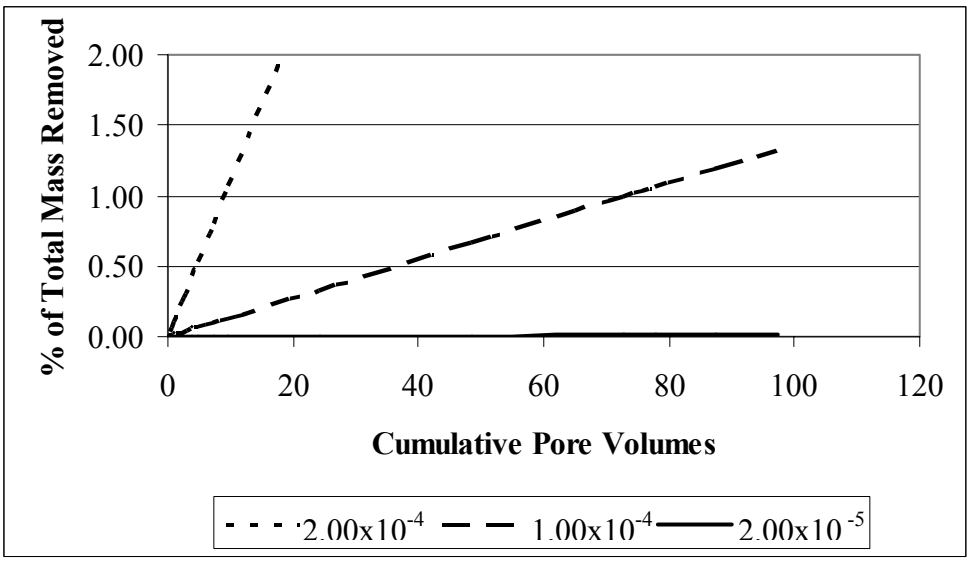

Figure 7.3: Effect of Pore Diameter (values in mm)

The figure plainly shows the important role pore diameter plays on the effectiveness of colloidal remediation. If a cumulative pore volume of 20 is considered, total mass removed is 2.181% for a pore diameter of $2.00 \cdot 10^{-4}$, 0.272% for a pore diameter of $1.00 \cdot$

10^{-4}, and only 0.003% for a pore diameter of $2.00 \cdot 10^{-5}$. A decrease in one order of magnitude can reduce removal rates by almost three orders of magnitude. This is a logical estimation due to the importance the flow path plays in colloid removal. The larger the area for flow, the greater number of particles, as well as the greater the size of particles, that can pass through. Larger flow paths also decrease the opportunities of clogging – a condition which further reduces the colloid removal effectiveness. One of the most significant things this suggests then is that soils that are more gap graded – e.g. those that have very small and large but few moderate sized particles can experience more effective remediation over those that have very fine particles in conjunction with more moderately sized particles. Also, if larger flow paths could be developed in the system, removal rates along those paths would be expected to increase over existing smaller paths.

7.8.3 Effect of Clay Content

Although clay content of a soil can range from 0 – 100 %, for the purpose of this study the range will be limited to 20 – 50 %. Because of the dependence of permeability on clay content, a larger range would result in erroneous data due to the incorporation of unrealistic permeabilities with respect to corresponding clay content. This effect is complicated by structure developed at high soil clay concentration, giving inter-aggregate flow paths (i.e. cracks). For all cases, a permeability of 10^{-3} cm / sec and an effective pore diameter of $2 \cdot 10^{-4}$ mm will be used. As with the permeability comparison, results presented in Figure 7.4 involving the variation of clay content have limitations in their interpretation.

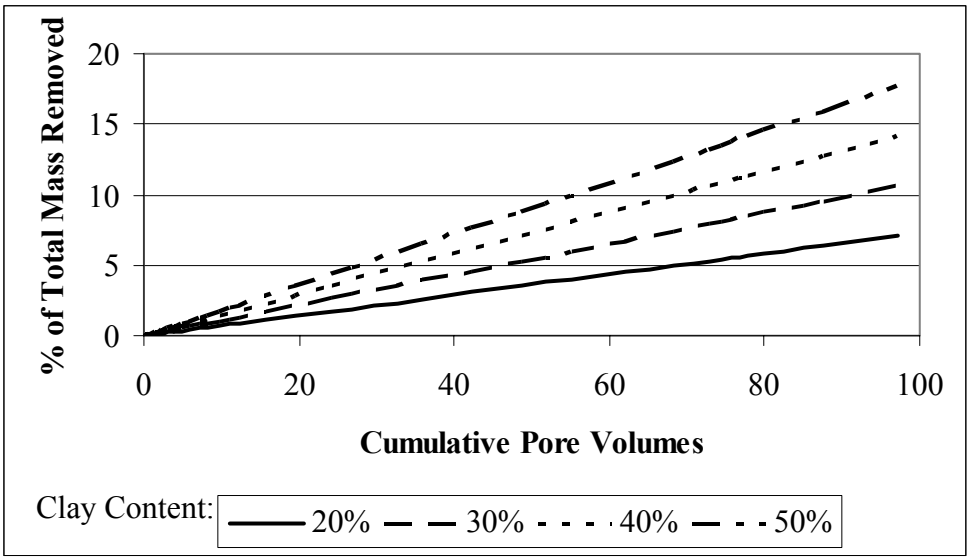

Figure 7.4: Effect of Clay Content (values in percent by mass)

Initial inspection shows that an increase in clay content yields an increase in the total mass removed. This outcome is based mainly on the fact that there are a greater amount of particles to remove in a system with a higher clay content than in one with a lower content. The limitation implicit in the approach however, is that these higher clay contents are assumed to not correspond to a decrease in permeability or, more importantly, a decrease in average pore diameter. While it is possible that a moderate increase in clay content may not affect the average pore diameter, it is unlikely that doubling this value would not significantly affect pore diameter values within the system. These results are more moderate than either those of permeability or pore diameter, suggesting that clay plays a less significant role in colloidal mobility, at least when considered independently.

7.9 Model Application to Laboratory Results

Once model development was complete, it was desirable to validate the developed model utilizing data that was obtained from laboratory testing. To this end, the model was applied to the laboratory testing on the five soil types at different combinations of hydraulic gradient (i = 6, 14.5, and 29) and ionic strength (0.0025 M, 0.1 M, and 1.0 M). Results from the natural soil at the lowest ionic strength (0.0025 M) and all three hydraulic gradients are presented in Figure 7.5. In general, the model and laboratory results follow similar trends. The model itself is a linear prediction, and thus does not possess the variations inherent in the laboratory results. Table 7.1 summarizes the predicted versus actual percent of total mass removed at a cumulative pore volume equal to 40 for all three tests presented in Figure 7.5.

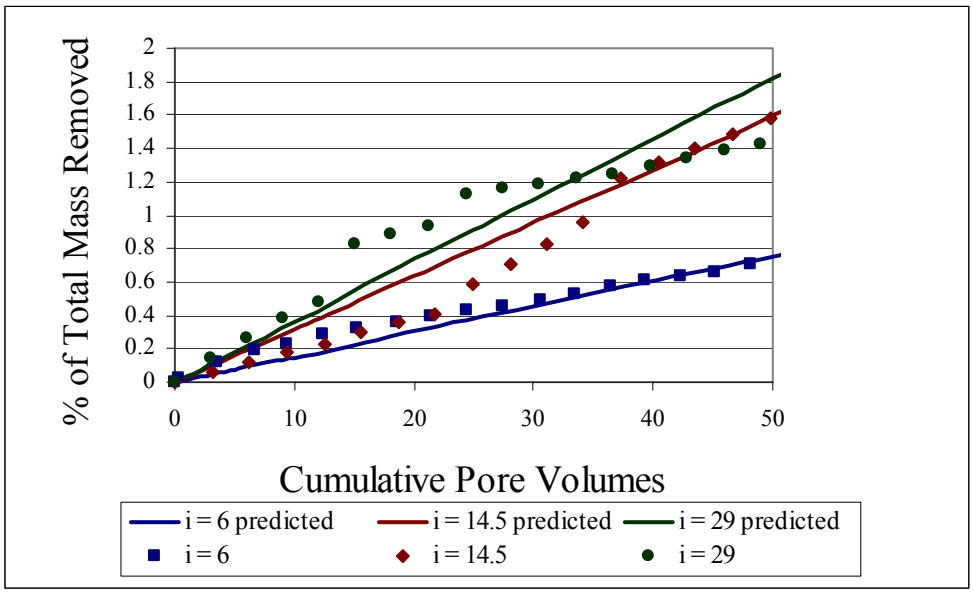

Figure 7.5: Comparison of Model and Laboratory Results for Natural Soil at Low (0.0025 M) Ionic Strength for All 3 Hydraulic Gradient Values

Table 7.1: Comparison of Predicted Versus Actual Total Mass Removed at a Cumulative Pore Volume of 40 (from Data in Figure 7.5)

	Percent of Total Mass Removed		
	i = 6	i = 14.5	i = 29
Predicted (Model)	0.60 %	1.31 %	1.39 %
Actual (Laboratory)	0.61 %	1.32 %	1.30 %

Agreement between the actual and predicted for both the hydraulic gradient of i = 6, and i = 14.5 is much closer than that of the hydraulic gradient of i = 29. The difference in the linearity of the model and the fluctuations in the laboratory results may contribute, in part, to the differences, as a choice of a different cumulative pore volume for comparison could improve (or weaken) the results. In general, however, the differences between predicted and actual results are within about 7% of the total predicted mass.

Model versus laboratory results were also graphed for the natural soil at all three ionic strength variations and the low (i = 6) hydraulic gradient. These results are presented in Figure 7.6.

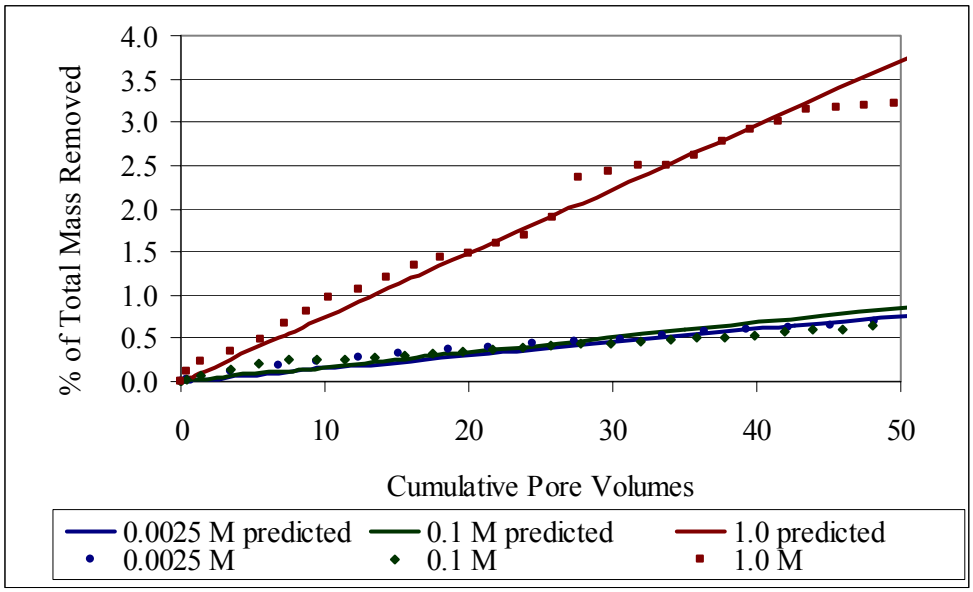

Figure 7.6: Comparison of Model and Laboratory Results for Natural Soil at Low (i = 6) Hydraulic Gradient for All 3 Ionic Strength Values

As with the ionic strength comparison, results of the hydraulic gradient comparison show the similarities in the general trends between the actual versus predicted values. The percent of total mass removed can again be analyzed at the 40 cumulative pore volume mark, the results of which are presented in Table 7.2. Again, general agreement can be seen between the model and laboratory values, with the 0.1 M comparison possessing the largest variation at this particular point. The variation is slightly larger this time, with a difference in approximately 10% of the total mass removed. Both variations err on the model over – predicting removal, although there are points within the analyzed data that show laboratory results greater than those of the model predictions.

Table 7.2: Comparison of Predicted Versus Actual Total Mass Removed at a Cumulative Pore Volume of 40 (from Data in Figure 7.6)

	Percent of Total Mass Removed		
	0.0025 M	0.1 M	1.0 M
Predicted (Model)	0.60 %	0.61 %	2.90 %
Actual (Laboratory)	0.61 %	0.54 %	2.90 %

In addition to the natural soil, laboratory and model comparisons were performed for the other soil types tested as well. Results of select comparisons are presented in Figure 7.7.

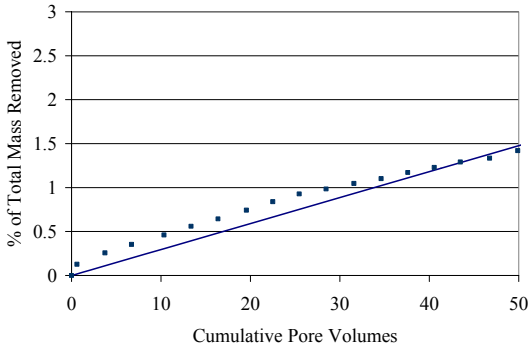

a) Sand + 10% Kaolinite (i = 6, 0.0025 M)

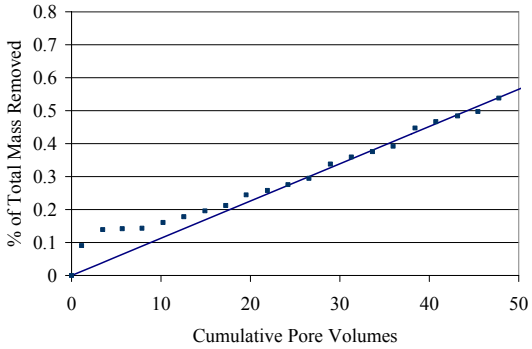

b) Sand + 10% Bentonite (i = 14.5, 1.0 M)

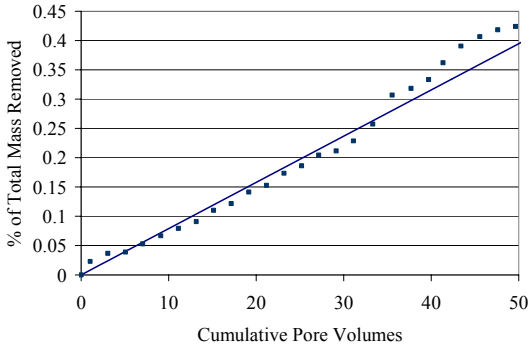

c) Sand + 15% Kaolinite (i = 14.5, 0.1 M)

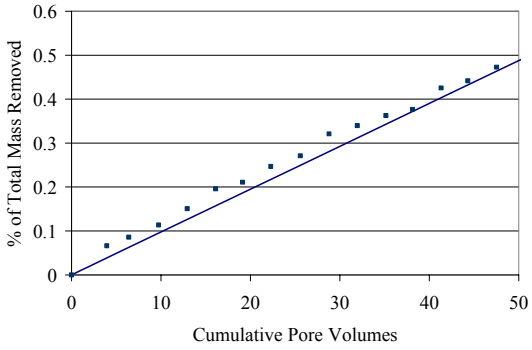

d) Sand+15% Bentonite(i = 29, 0.0025 M)

Figure 7.7: Comparison of Model and Laboratory Results for Select Ionic Strength and Hydraulic Gradient Combinations for Different Soil Types

Although the y – axis scales for each of the four graphs presented in Figure 7.7 are different, the purpose of the figure is not to compare across graphs, but rather between the laboratory actual values (plotted as individual points) and the model predicted values (plotted as solid lines) within each of the individual graphs. Results of the comparisons are similar to those of the natural soil comparisons presented previously.

7.10 Presentation of Correction Factor Parameter Values

Colloidal movement is based on the depletion of clay particles within the soil matrix. As discussed previously, this depletion is a function of both the rate in which colloids enter the flushing solution, as well as the rate at which they exit the flushing solution (e.g. are deposited within the soil matrix). Both of these rates are dependent, to an extent, on permeant variations such as hydraulic gradient and ionic strength. For the rate into the flushing solution, the correction factor to account for these permeant variations is Ξ, while for the rate out of the flushing solution, X is the correction factor.

7.10.1 Factors Included for Ξ Determination

The two factors employed in the calculation of Ξ include the ratio of the seepage velocity to that of the critical shear velocity and the ionic strength normalization parameter. These two values combined for the correction factor for the rate in which colloids enter a flushing solution. The parameter itself is both soil and permeant specific, and will vary depending on soil parameters such as cation exchange capacity, clay content, grain size distribution, and average pore size diameter; as well as on parameters of the flushing solution

including hydraulic gradient and ionic strength. Values for Ξ as a function of hydraulic gradient and ionic strength are presented in Figure 7.8 for the natural soil.

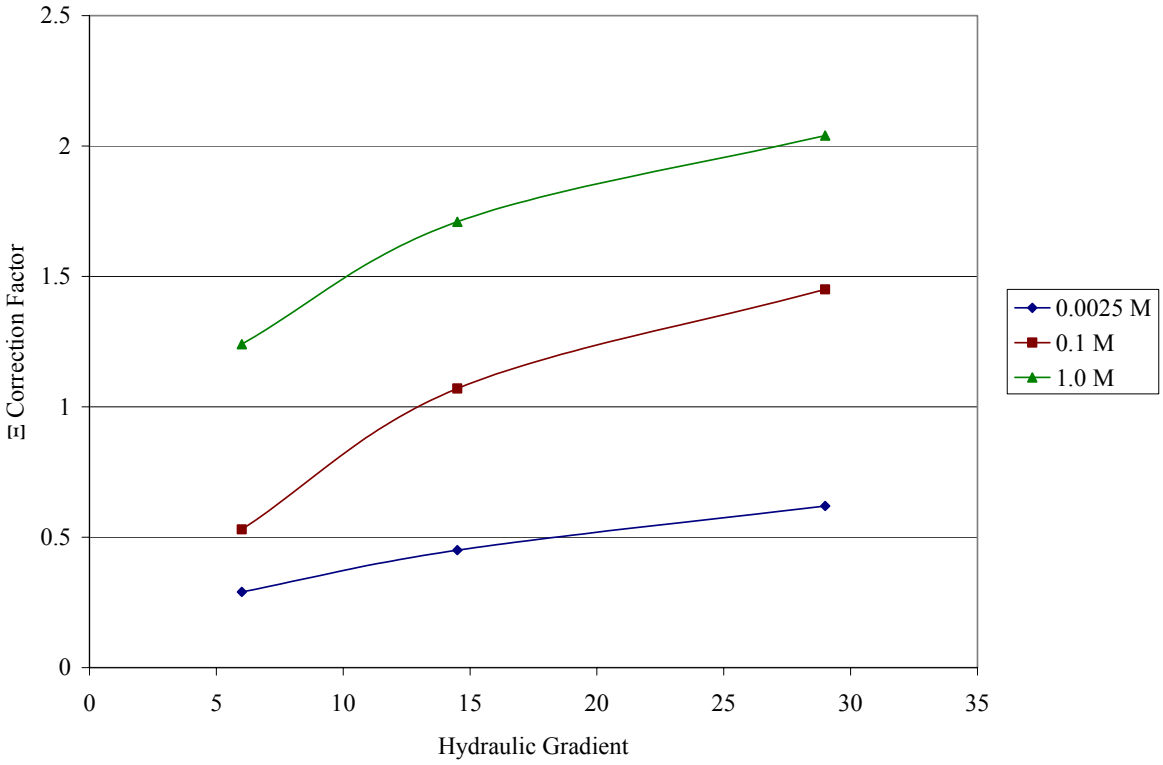

Figure 7.8: Ξ Values for Natural Soil as a Function of Hydraulic Gradient for Different Ionic Strength Flushing Solutions

Increases in both hydraulic gradient and ionic strength result in increases in the value of the correction factor. It is important to note that these values are based on a single pore volume of the specified ionic strength flushing solution. Increases in the number of pore volumes at the given ionic strength (even at the same ionic strength and same hydraulic gradient) would result in different correction factor values due to the adjustment in the ratio between the ionic concentration in the flushing solution and the cation exchange capacity of

the soil. Trends are similar for other soil types, although again exact Ξ values are soil and flushing solution specific.

7.10.2 Factors Included in the Determination of X

Unlike Ξ, which is influenced both by physical and chemical variations, factors included in the determination of X are only physical in nature. The calculation considers the ratio between the diameter of the mobilized colloidal particle and the effective pore diameter of the soil matrix. Larger values indicate a greater tendency toward colloidal particle capture, due to the larger particle size relative to the size of the available openings. Ionic strength is not included directly in the correction factor, but does exert influence in the rate of capture of colloidal particles by contributing to the clay concentration in solution (C_L term of equation 7.5). Figure 7.9 presents X values for the test soils at the three different hydraulic gradients tested.

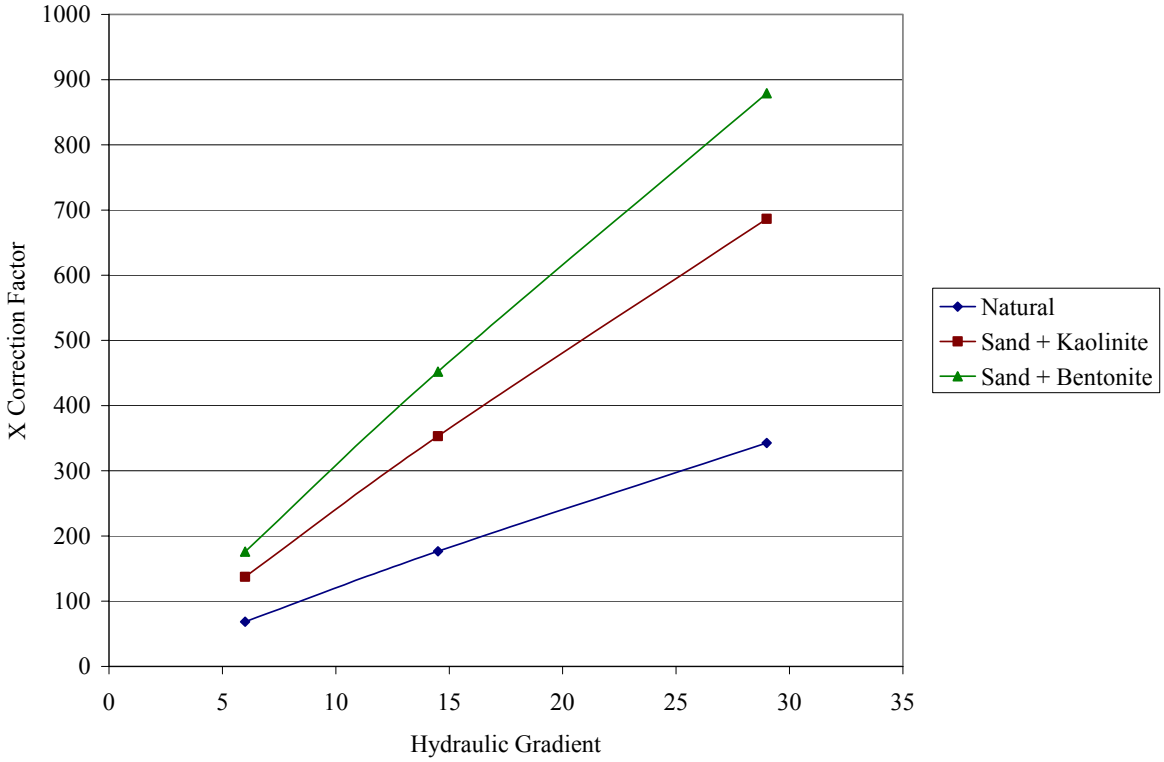

Figure 7.9: X Values for Different Soils at Various Hydraulic Gradient Values

Only three curves are presented on the graph due to the negligible difference between values for the ten and fifteen percent clay content for the sand and kaolinite and bentonite soils respectively. This small difference is due to the small difference in the D_{10} values of the 10% and 15% grain size distribution curves for each of the respective soils. The kaolinite and bentonite used in testing were manufactured with relatively small variations in particle diameter and combined with a sand that possessed virtually no fines, thus the D_{10} for a soil with 10% of the clay is quite similar to that of a soil with 15% of the clay. A larger difference in the total clay content or a more significant variation in the diameter of the clay – sized particles would contribute to a greater difference in the calculated correction factor.

Considering only the correction factor, it would appear that the sand and bentonite soils are most prone to colloidal capture, while the natural soil is the least likely to experience colloidal trapping. Laboratory results confirmed that the natural soil experienced the lowest rate of colloids exiting the flushing solution and remaining in the soil matrix. From experimental testing, the kaolinite experienced the greatest level of colloid removal from the flushing solution. This rate of capture is dependent, not only on the correction factor above, but also on the concentration of clay particles in the flushing solution, as well as several other factors. So, although the sand and kaolinite soils possess a lower correction factor than the sand and bentonite soils, the concentration of clay particles in the flushing solution can outweigh the correction factor and result in greater levels of colloid trapping.

7.11 Summary of Model Development and Limitations

Model development was focused on two main features: 1) the determination of the means and extent of colloid mobilization on the remediation of saturated systems and 2) the determination of the magnitude and effect of colloidal mobility on the overall remediation efforts. Pertinent equations focus on four main areas of concern: 1) general flow through a soil matrix, 2) colloidal movement, 3) contaminant reactions, and 4) permeant variations. General flow equations consider Darcy's and Poiseuille's Laws. Colloidal movement equations were developed from the work of Khilar and Fogler (1985) – who considered the effect of clay particle movement on piping and stability of dams. Rate values were adjusted to better reflect the remediation design criteria over that of dam design criteria. Contaminant reaction equations were ignored for the research at hand due to the contaminant of choice (cesium) and the focus on colloidal movement without contamination in the laboratory

testing. The two main permeant variations under consideration include those of hydraulic gradient and ionic strength.

Model flexibility allows for either the incorporation into existing models that do not consider colloid mobility or the inclusion of traditional mass transport analysis to allow for the consideration of a wider variety of contaminant. The developed model differs in focus and / or primary approach from previously developed models, and seeks to determine the efficiency and effectiveness of colloid mobility as a means of remediation and predict results of the application of colloid mobilization to the remediation of select sites.

The model is currently limited to contaminants that exhibit significant levels of sorption – with the majority of contamination associated with the soil matrix. It does not currently consider dissolved phase contamination, nor does it consider the condition of an unsaturated subsurface. The model assumes contaminant sorption is focused in the mobile colloid phase and does not take into consideration a preferential removal of colloids or contamination. This means that the model assumes even contamination across all colloidal particles and equal release of colloids with different mineralogical properties.

On a more general note, the model does not currently possess a self – check option. The lack of this option means it is up to the user to confirm the validity of input variables. Errors in input of required values can lead to significant over or under prediction of potential results.

With regards to the remediation method in general – colloidal mobility is not a universal solution to subsurface contamination. For sites with high percentages of clay content that require extensive remediation – colloid mobilization would not be an effective alternative. There comes a point where the total required mass to be removed is too great to

allow for an effective remediation. This total mass required is not dependent on clay content alone, but rather on a combination of soil type, grain size distribution, contaminant type, and degree of contamination. Additionally, remediation would depend on peripheral chemical conditions such as pH and soil calcite levels.

Chapter 8. Model Application: Case Study

8.1 General Description

The Battelle Columbus Laboratories Decommissioning Project (BCLDP) desired to remove radioactive contamination from the Battelle-owned facilities and grounds known as the West Jefferson North (WJN) site. This site is located about 17 miles west of Columbus and 3 miles north – northeast of West Jefferson, Ohio in a rural agricultural area on the eastern border of Madison county along Big Darby Creek. A detailed map of the area, as well as a general map of the site, can be found in Appendix B. The site is a retired filter bed area composed of tills that were compacted on site and are characterized by a high clay content and low hydraulic conductivity. Figure 8.1 is an illustration of this area from the main service road.

Figure 8.1: West Jefferson North Abandoned Filter Area

The secondary access road is visible in the picture. Big Darby creek is to the right of the filter beds, at the bottom of the sloping ground outside of the fenced area. Past flood stages have actually raised the creek to a level which floods the fenced area as shown in Figure 8.2.

Figure 8.2: Battelle Site Under Flood Conditions from Big Darby Creek

The only current contamination is radioactive Cesium which is chemically bound, usually via molecular bonding of some sort, to the micaceous/clay minerals of the soil, and is focused mainly at depths less than 15 feet below ground surface. The site area is graded and capped with a one-foot clay layer to prevent storm water from entering or percolating through the contaminated soils.

8.2 Site Geology

General geology of the West Jefferson site is characterized by glacial till and alluvium deposits overlying bedrock, and is typically one of four different types of surficial soil. In the abandoned filter bed area, where the test site is located, the soil is a Medway silty loam formed on recent alluvium derived from upland soil. A soil survey map of the area can be found in Appendix B. Surface soils are approximately 15 inches thick, with 19 – inch thick subsoils. Gravelly loam characterizes the substratum, which may be located at depths greater than two feet. The soil is moderately well drained and often possesses high organic material contents. The bedrock in the site area consists mainly of limestone and dolomite strata of Silurian and Devonian ages and is located at elevations of 791 to 796.5 MSL, which is roughly 100 feet below the ground surface.

8.3 Site Contamination

Contamination at the site is mainly radioactive cesium (^{137}Cs) at levels as high as 200 pCi/g, although trace levels of americium (^{241}Am) have also been detected. The cesium contamination is still above acceptable free release levels (15 pCi/g for ^{137}Cs - negotiated) after the excavation of the leach field tiles and sand. This excavated soil was replaced with a fill material. The cesium is tightly bound to the soil fines, as confirmed by periodic sampling and monitoring well observations.

8.3.1 Contamination Variations as a Function of Location

Figure 8.3 presents a general profile of the cesium concentration as a function of depth and shows soil types as classified by USCS.

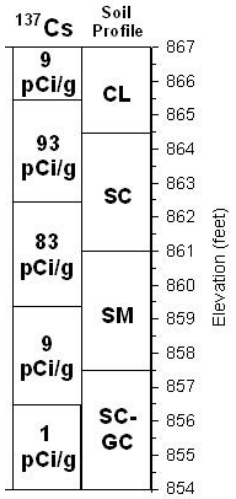

Figure 8.3: Soil and Contaminant Profile

Changes in average cesium concentration are presented on the left, while the soil profile is illustrated on right. Elevation (in feet above mean sea level) is indicated at the far right, with the ground surface at 867 feet. The groundwater table is at an elevation of 863 feet, although not shown in Figure 8.3. From the figure it is possible to see that the greatest contaminant concentrations are from depths of 0.9 – 4.6 meters (3 – 15 feet) below ground surface. The main soils present at these depths are the Low Plasticity Clay (CL) used in the testing program and a Clayey Sand (SC). This SC is similar to the CL soil, but has higher sand and correspondingly lower silt and clay concentrations than the CL. The contamination levels drop rapidly as the depth increases, averaging 9 pCi/g at the 4.6 – 6.4 meter (15 – 21 ft) depth and $\leq$ 1 pCi/g at depths at or below 6.4 meters (21 ft). This decrease in contamination correlates with an increase in the effective particle size of the profile soil and a corresponding

decrease in the percentage of soil fines. The drop in concentrations also confirms the relatively immobile nature of the contaminant, as rainfall infiltration and groundwater table fluctuations have not diffused contamination intensity with depth. A profile view of the site, with cesium concentration variations at the 0.6 – 1.2 meter (2 – 4 foot) depth is presented in Appendix B. Although remediation to levels below 15 pCi/g is acceptable, the preferred level is specified to concentrations at or below 3 pCi/g.

8.3.2 Contamination Variations as a Function of Soil Type

Previous analysis of the soil and associated contamination from the site has found that "almost all of this contaminant [Cs] in these soils is in recalcitrant (immobilized) forms such as interlayer edge and structural sites of micas" (Mattigod et. al., 2002). Gamma spectrometry data has shown that 88% of the cesium is on the silt and clay (~70% by mass of the soil) while only 12% of the cesium is associated with the sand and gravel portion of the soil (~30% by mass). Figure 8.4 illustrates the relative distribution of cesium and soil mass percentage as a function of particle size for the soil at the site.

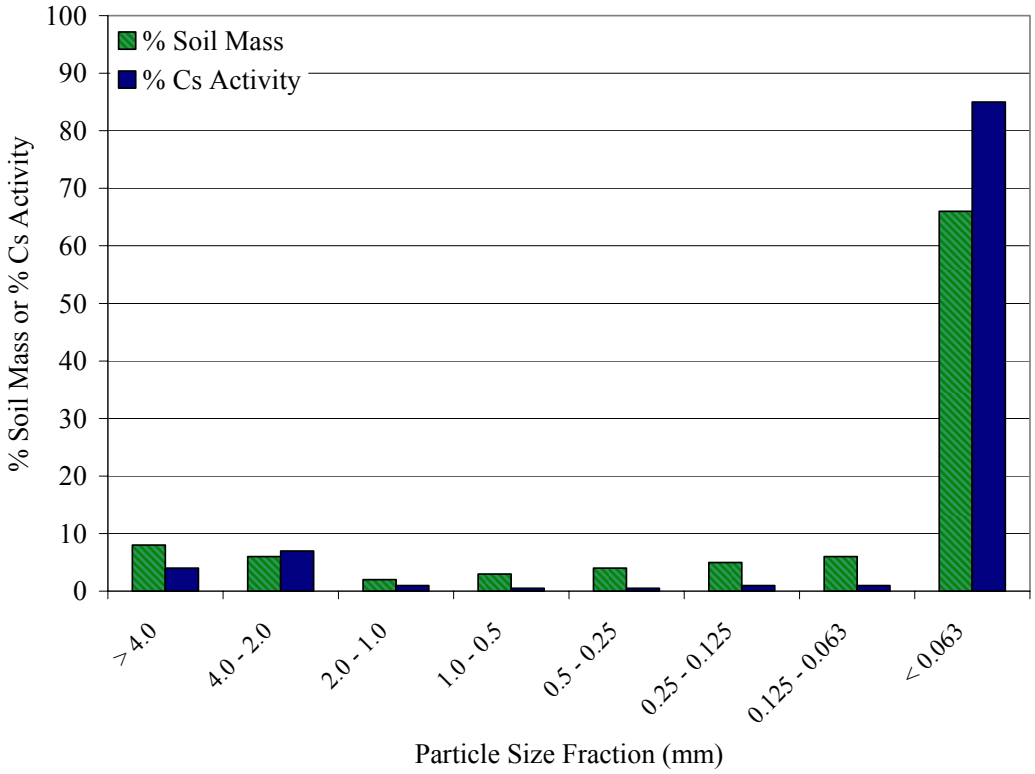

Figure 8.4: Mass and ^{137}Cs Activity Distribution Based on Particle Size (from Mattigod et. al., 2002)

From this figure it is possible to see that the majority of cesium contamination is associated with the fines portion of the soil. Mattigod et. al. (2002) suggest that the manner of this association is based on the soil minerals involved. Table 8.1 summarizes the various minerals present, as well as the types of sites expected to be occupied by cesium.

Table 8.1: Types of ^{137}Cs – Mineral Associations (from Mattigod et. al., 2002)

Type of site occupied by cesium	Minerals
Exchangeable	Smectite, Chlorite, Kaolinite, Fe-oxide, Humates
Interlayer Edge	Micas, Vermiculites
Structural	Feldspars, Micas

This variation in cesium fractionation leads to a difference in the degree of extractability based on the type of contaminant mineralogical association. That portion of cesium occupying exchangeable sites is more likely to be extractable than interlayer edge, which in turn, is more likely to be extractable than structural. This extractability preference is based on the assumption of extraction in the liquid phase, not on the removal of the contaminated particles themselves.

The relatively low organic carbon content (less than 2%) indicates that "the proportion of ^{137}Cs associated with the organic fraction would be low relative to its activity associated with the inorganic mineral fraction" (Mattigod et. al., 2002). Based on this evaluation, it is expected that "any significant reduction (for instance, ~50%) in total ^{137}Cs activity in these soils can be attained only if at least ~42% of the activity associated with the silt and clay size fraction is removed" (Mattigod et. al., 2002).

8.4 Previously Considered Remediation Measure

Prior to lixiviant testing and the implementation of the WIDE system at Battelle Laboratories West Jefferson North Abandoned Filter Bed Facilities, soil excavation and subsequent radioactive disposal was considered as a means of remediation. This remediation measure would involve the excavating, packaging and shipping of approximately 2,380 cubic meters (84,000 cubic feet) of radioactive soil to Utah for radioactive burial. Additionally, it poses significant containment control issues with regards to the release of soil fines into Big Darby Creek.

8.5 Alternative Remediation Approach

Lixiviant testing was conducted as a possible in situ remediation approach. Laboratory testing confirmed removal efficiencies of almost 40% of total Cesium contamination with a contact time of only 3 hours. These promising results however, are tempered with the requirement that the extractions are conducted at 90 ºC. Although easy to maintain in laboratory settings, elevated temperatures are complicated and costly to maintain in a field setting.

8.6 Site Applicability for Modeling

The site was chosen as the field site for modeling testing for a number of reasons. First, extensive characterization of the in situ soil and contamination profiles has been performed. This information provides a valuable picture of the subsurface profile, which allows for depth specific targeting of the most crucial areas. Second, laboratory testing has been conducted on borings taken from the site. This general laboratory testing imparts additional information to further clarify the subsurface profile. Moreover, a wide range of laboratory testing has also been carried out on one of the soils from the main depth where contamination is present. More specific lab testing supplies detailed soil information critical to modeling efforts, and allows for the determination of important parameters and relative sensitivity of parameters for model prediction. Third, actual pilot scale results of WIDE operation at the site are available. While these results are not colloid mobilization tests, they will give a broad idea on rates and volumes, possible limitations of the system in field situations, and overall WIDE performance.

8.7 Model Application

Utilizing data obtained from the field and laboratory testing performed on the Battelle site; it was possible to conduct a case study to assess the effectiveness of colloidal mobilization as a means of remediation of the contaminated subsurface. Field data provided information regarding attainable and maintainable hydraulic gradient values, while soil parameters, such as specific gravity, average pore diameter, porosity, and permeability, were obtained from laboratory testing. Since flow – through column testing was also performed on soil from the site, additional information was also available. Results from the flow – through column testing provided a basis for the choice of hydraulic gradient and ionic strength combinations employed in the case study. Analysis can be performed without column testing results; the limitation being that multiple model runs with various input variations would be necessary in order to optimize the system.

The case study compared three of the most promising options to each other, as well as to a control simulation. The only parameters varied between options were those of hydraulic gradient and ionic strength of the flushing solution. As in laboratory testing, the ionic strength applies only to the first pore volume of flushing solution, subsequent pore volumes are injected at groundwater background ionic strength concentrations. Table 8.2 summarizes the different hydraulic gradient and ionic strength values utilized for each of the various options.

Table 8.2: Hydraulic Gradient and Ionic Strength Values Utilized in Model Runs

	Hydraulic Gradient	Ionic Strength
Control	9	0.0025 M
Option 1	27.9	0.0025 M
Option 2	18.3	0.1 M
Option 3	18.3	1.0 M

The control corresponds to a low hydraulic gradient as well as a low ionic strength. Option 1 also employs a low ionic strength, but uses a high hydraulic gradient. Options 2 and 3 combine a moderate hydraulic gradient with either a moderate or high ionic strength, respectively. The combinations of low ionic strength and high hydraulic gradient, or moderate to high ionic strength with a moderate hydraulic gradient were those that showed the most promising results in the flow – through column testing for the natural soil. Ionic strength values are analogous to those tested in the laboratory – both in strength and the use of sodium chloride. Hydraulic gradients are similar, but not exact, to those from laboratory testing. The discrepancy comes from utilizing actual field data hydraulic gradients attained during WIDE testing over general system estimates used in the lab. All values were able to be achieved and maintained in the actual field setting and thus are viable for analysis. Figure 8.5 summarizes the results of the four study model runs.

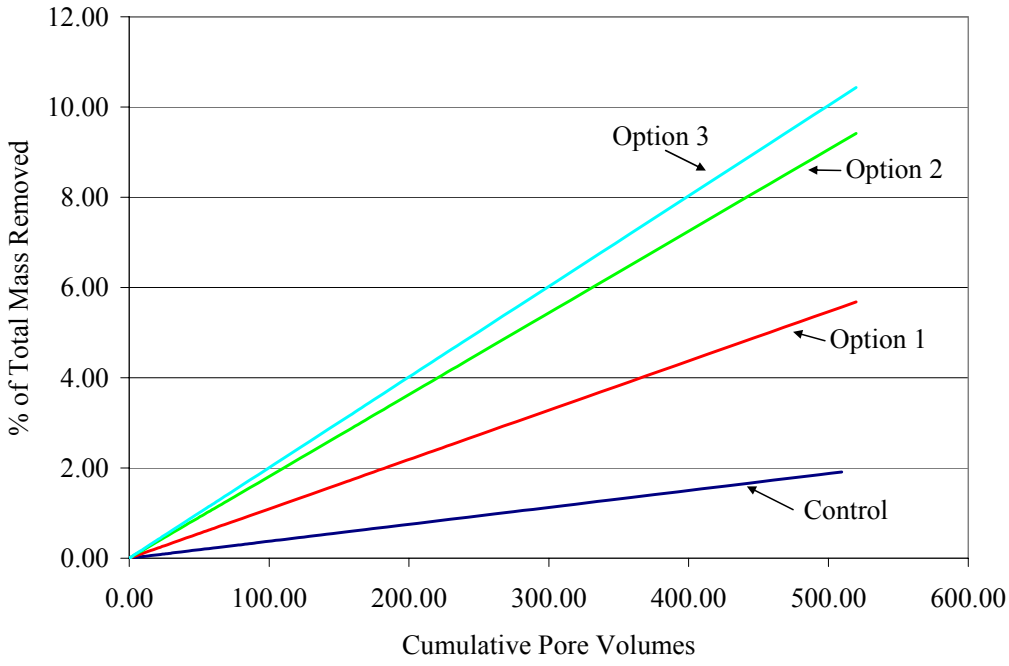

Figure 8.5: Comparison of Various Remediation Options from Model Analysis

From the figure it is obvious that the application of any option will result in a higher percentage of total mass of soil removed over that of the control (i.e. 0.0025 M ionic strength and hydraulic gradient = 9). The most beneficial removal rate (almost 10% of total mass at 500 pore volumes) occurred with the 1.0 M ionic strength and a moderate hydraulic gradient. If the introduction of high levels of sodium chloride are not advisable for the site, the moderate ionic strength and hydraulic gradient (i.e. 0.1 M and i = 18.3) result in roughly 9.5% of total mass of soil removed at the 500 pore volume mark and is only slightly lower than that of the higher ionic strength. Option 1, with the 0.0025 M ionic strength and highest (27.9) hydraulic gradient, has only 5.5% of the total mass removed, but is still almost 3 times as effective as the control, where less than 2% of the total mass is removed after 500 pore volumes.

Figure 8.6 plots the estimated remediation time as a function of WIDE operation and effluent colloidal concentration.

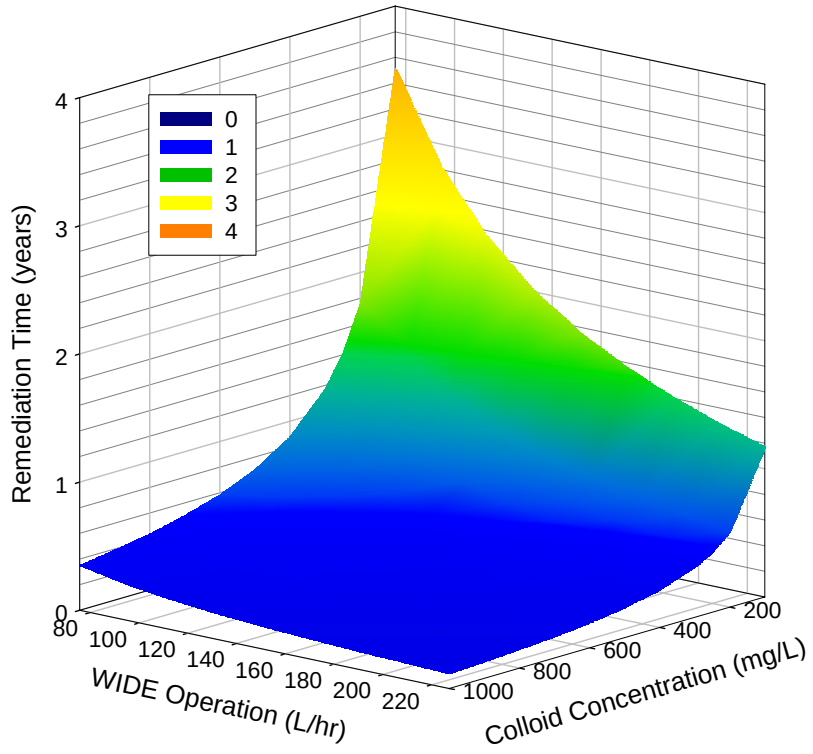

Figure 8.6: Estimation of Remediation Times based on WIDE Operation and Colloid Concentration in Effluent

Values are based on remediation from 93 to 15 pCi/g with 37.5% clay by mass and assuming removal of sorbed contamination only. WIDE operating times are for 8 hour days at rates ranging from 100 – 220 L/hr, all of which were able to be maintained in field conditions. Colloidal concentrations range from 200 – 1000 mg/L. Higher values were shown to have been achieved in the lab, but were not able to be maintained for significant lengths of time (> 2 pore volumes) and thus were not considered in the estimation. With the exception of a combination of low WIDE operating rates (e.g. 120 L/hr or less) and low colloidal concentrations in the effluent (e.g. 300 mg/L or less) remediation are expected to take less than a year.

Since the colloids can be separated from the extracted liquid, and the liquid reused, the only waste source is that of the colloids themselves. Considering the greatest removal (10% by mass), the total waste for the site is roughly 61 m^3 of soil – or a little more than 0.15 m^3 of soil per day.

Chapter 9. Summary and Conclusions

9.1 Summary of Work Performed

One of the principle results in the search for the ideal energy source is the insufficient storage and inadequate disposal practices of power generation by-products, which has led to widespread contamination of the subsurface environment. Regulations have been enacted which now govern the transport, storage, and disposal of these products however; regulations provide only the desired goal or performance expectations, not a roadmap of how to accomplish remediation. It falls then, to professionals in academia and industry to devise techniques effective in reducing / eliminating contamination levels at sites of concern.

The research presented herein addressed dispersion and piping of clay fines – colloid mobilization – as a means of remediation subsurface contamination. While the majority of previous research in colloidal mobility seeks to limit, rather than enhance, movement; this research desires to promote dispersion and encourage colloidal mobility. Additionally, although many models have been developed that assists in predicting the rate and magnitude of colloidal mobility in various subsurface environments, most again focus on the suppression of colloidal mobility as a means of contamination containment rather than augmenting mobility for site remediation.

The experimental program consisted of laboratory work, modeling, and a field case study. Laboratory work included fifty flow – through tests on five different natural or synthetic soil materials, one native field soil from the Ohio site and four manufactured samples consisting of sand and either kaolinite or bentonite at 10 or 15% by mass. Testing

was conducted at three ionic strengths (0.0025 M, 0.1 M, and 1.0 M) and three induced hydraulic gradients (i = 6, 14.5, and 29). Thirty – six tests comprised the cesium contamination batch program, which utilized three individual soil materials – sand, kaolinite, and the natural soil – and all three ionic strength test levels (0.0025 M, 0.1 M, and 1.0 M). Physical and mineralogical characterization of the test soils was conducted prior to laboratory testing, and quality assurance / quality control measures were undertaken at all stages of testing. Post – testing micro – analysis of colloid mobility was conducted for the confirmation of mass balance, as well as for the determination of colloidal properties.

Modeling was applied to link laboratory testing with existing field situations in order to determine the viability of testing at specific field sites. The proposed model includes a three – phase system of water, soil, and colloids. After development and application to laboratory results, the model was utilized in conjunction with field data to predict remediation capabilities of colloid mobilization applied through Well Injection Depth Extraction (WIDE) to an actual site contaminated with radioactive cesium 137.

Although the research scope is limited in extent with regards to the type of contamination, it is anticipated that results will be applicable to numerous types of contamination including light and dense NAPLs and radioactive heavy metals. An additional potential contribution to the Geoenvironmental field includes the applicability of this remediation to low permeability soils. A decrease in the hydraulic conductivity of a soil typically corresponds to a decrease in the effectiveness of existing remediation measures that rely on removal of contaminants via the aqueous phase. Removal of the sorbed phase of contamination, historically the source of most remediation problems, is another area where this procedure could prove beneficial. Probably the greatest potential contribution however,

is the relatively quick remediation times associated with this type of technique relative to previous remediation measures.

9.2 Conclusions

Based on the research performed, the following conclusions can be drawn:

1. Changes in either the hydraulic gradient or the ionic strength mobilized colloids from the soil and sand / clay mixtures studied.
2. Increases in hydraulic gradients resulted in decreased colloidal removal efficiencies for 1:1 clay mineral colloids.
3. Increases in hydraulic gradients from 6 to 14.5 at the low (0.0025 M) ionic strength resulted in a reduction by half of the colloids removed from both the sand and kaolinite soil mixtures. Increases in hydraulic gradients from 14.5 to 29 at the same ionic strength (0.0025 M) showed almost no change in the amount of colloids removed.
4. Increases in hydraulic gradients from 6 to 14.5 and from 14.5 to 29 at the moderate (0.1 M) and high (1.0 M) ionic strengths results in a steady reduction (between 10 and 30%) of the colloids removed from both of the sand and kaolinite soil mixtures.
5. Tested hydraulic gradient (6, 14.5 and 29) increases resulted either in continuous increases (10% bentonite) or initial increases then decreases (15% bentonite and natural soil) in colloidal removal efficiencies for 2:1 clay minerals.

6. For the sand and 10% bentonite soil mixture, hydraulic gradient increases from 6 to 14.5 resulted in modest (~20%) increase in colloid removal efficiency for the low (0.0025 M) and high (1.0 M) ionic strengths, but more than tripled colloid removal efficiencies for the moderate (0.1 M) ionic strength. For the same soil, hydraulic gradient increases from 14.5 to 29 doubled colloidal removal efficiencies in the low and high ionic strengths, while exhibiting a more temperate (<5%) increase for the moderate (0.1 M) ionic strength test.
7. The sand and 15% bentonite mixtures experienced increases in colloidal removal efficiency of roughly 50% for the low (0.0025 M) and moderate (0.1 M) ionic strengths with an increase in hydraulic gradient from 6 to 14.5. This same soil and hydraulic gradient increase showed no benefit to colloid removal in the high (1.0 M) ionic strength test. Greater hydraulic gradient increases (from 14.5 to 29) resulted in decreased colloidal removal efficiencies.
8. The natural soil experienced roughly a twofold increase in removal rates for colloids when the hydraulic gradient was increased from 6 to 14.5 at all ionic strengths. Further increases in hydraulic gradient (to 29) resulted in a general reduction in colloidal removal.
9. Ionic strength effects for the kaolinite were suppressed with increases in hydraulic gradient – although overall trends within each sample were consistent for all ionic strengths and hydraulic gradients.

10. Low (0.0025 M) or moderate (0.1 M) ionic strength values showed the most promise for colloid removal in the sand and kaolinite mixture samples.
11. Ionic strength effects for the bentonite and natural soil were more effective and moderate levels over elevated levels for virtually all hydraulic gradients (natural low gradient the exception).
12. Moderate ionic strength (0.1 M) at hydraulic gradient values of 14.5 or 29 showed the greatest colloidal removal efficiency for both the natural soil and the sand and bentonite mixtures.
13. The developed model on clay dispersion and piping was able to represent colloid mobilization as a function of relevant soil and flushing solution parameters.
14. Effective pore diameter and overall clay content appear to have the greatest influence on the effectiveness of colloidal mobilization.
15. Colloid mobilization is hampered by "more is not always better" – extreme levels of mobilization typically result in colloid trapping and an overall reduction in effectiveness.

9.3 Contributions to State of the Art

The following contributions are imparted based on the performed research and developed model presented herein:

1. Processes associated with seepage forces overcoming shear resistance at grain interfaces were evaluated to determine effect on mobilization of colloids deposited on larger – sized particles.

2. A model was developed to provide the effect of seepage velocity versus critical shear velocities and induced particle diameter values versus average pore diameters on colloid mobilization.
3. The effect of ionic strength variations and adjustments in the ionic strength as it influences the mobilization of colloids by manipulating clay chemistry were explained.
4. The relationship between soil CEC and cation concentration in flushing solution as it affected colloid mobilization were modeled.
5. The research remediation method is applicable to numerous types of contamination (e.g. heavy metals, radioactive elements, and organics).
6. Colloid mobilization acts to remove the sorbed phase, which historically is the source of a majority of contaminant issues.
7. Model flexibility allows for the incorporation of mass transport for the analysis of dissolved phase contamination in addition to the mobile sorbed phase.
8. Clay dispersion and piping utilizing the WIDE system as a delivery method has the potential to reduce remediation times, as well as health and safety concerns associated with contaminant site remediation, relative to previous methods.

Chapter 10. Recommendations for Future Work

Based on the research performed, the following recommendations are made for future research:

1. Flow testing on undisturbed soil samples should be performed in the laboratory to confirm colloidal mobilization for intact soils over a wide range of soil types.
2. Ionic strength pulses of longer duration, as well as repeat introduction of ionic strength pulses followed by low ionic strength solution, should be employed in flow – through testing to determine if increasing benefits can be found for either / both option(s).
3. Field application of hydraulic gradient and ionic strength manipulation to confirm colloidal dispersion and mobilization.
4. Analysis of cesium contaminated soil columns introducing colloidal mica in the influent for preferential exchange of cesium from the column onto the mica colloids for subsequent removal should be applied in flow – through testing.
5. Mass transport should be incorporated into existing model to consider aqueous phase removal of contamination (when applicable).
6. Additional laboratory tests should be conducted to confirm model validity / generalize model applicability.

Chapter 11. References

Aurell, C. A., and A. O. Wistrom, *Coagulation of Kaolinite Colloids in High Carbonate Strength Water*, Colloids and Surfaces A: Physicochemical and Engineering Aspects, 168 (3), 277 – 285, 2000.

Battelle Laboratories, *The Columbus Environmental Management Project West Jefferson Filter Beds Maps and Images*, July 2000.

Beard, Thomas, Neeraj Gupta, *Geology and Hydrogeology of West Jefferson North Site*, September 1990.

Blume, Theresa, Noam Weisbrod, and John Selker, *Permeability Changes in Layered Sediments: Impact of Particle Release*, Groundwater, 40 (5), 466 – 474, 2002.

Brubaker, S. C., C. S. Holzhey, and B. R. Brasher, *Estimating the Water – Dispersible Clay Content of Soils*, Soil Science Society of America Journal, 56, 1227 – 1232, 1992.

Chen, Gang, Markus Flury, James D. Harsh, and Peter C. Lichtner, *Colloid – Facilitated Transport of Cesium in Variably Saturated Hanford Sediments*, Environmental Science and Technology, 39 (10), 3435 – 3442, 2005.

de Jonge, L.W., C. Kjaergaard, and P. Moldrup, *Colloids and Colloid – Facilitated Transport of Contaminants in Soils: An Introduction*, Vadose Zone Journal, 3, 321 – 325, 2004.

Elimelech, Menachem, and Charles O'Mella, *Kinetics of Deposition of Colloidal Particles in Porous Media*, Environmental Science and Technology, 24 (10), 1528 – 1536, 1990.

Essington, Michael E., Soil and Water Chemistry: An Integrative Approach, CRC Press, 2004.

Fell, Robin, et. al., *Time for Development of Internal Erosion and Piping in Embankment Dams*, Journal of Geotechnical and Geoenvironmental Engineering, 129 (4), 307 – 314, 2003.

Fenton, Gordon A. and D. V. Griffiths, *Extreme Hydraulic Gradient Statistics in Stochastic Earth Dam*, Journal of Geotechnical and Geoenvironmental Engineering, 123 (11), 995 – 1000, 1997.

Foster, Mark and Robin Fell, *Assessing Embankment Dam Filters That Do Not Satisfy Design Criteria*, Journal of Geotechnical and Geoenvironmental Engineering, 127 (5), 398 – 407, 2001.

Gabr, M.A., Nadia Sharmin, Tanya Kunberger, and John Quaranta, *WIDE Implementation at Rickenbacker International Airport Area of Concern 3 (AOC-3) Phase III – Final Report*, July 2006.

Gamerdinger, Amy, and Daniel Kaplan, *Colloid Transport and Deposition in Water – Saturated Yucca Mountain Tuff as Determined by Ionic Strength*, Environmental Science and Technology, 35 (16), 3326 – 3331, 2001.

Griffiths, D. V. and Gordon A. Fenton, *Probabilistic Analysis of Exit Gradients Due to Steady Seepage*, Journal of Geotechnical and Geoenvironmental Engineering, 124 (9), 789 – 797, 1998.

Grolimund, Daniel, Michael Borkovec, Kurt Barmettler, and Hans Sticher, *Colloid – Facilitated Transport of Strongly Sorbing Contaminants in Natural Porous Media: A Laboratory Column Study*, Environmental Science and Technology, 30 (10), 3118 – 3123, 1996.

Grolimund, Daniel, Menachem Elimelech, Michael Borkovec, Kurt Barmettler, Ruben Kretzschmar, and Hans Sticher, *Transport of in Situ Mobilized Colloidal Particles in Packed Sand Columns*, Environmental Science and Technology, 32 (22), 3562 – 3569, 1998.

Grolimund, Daniel, and Michael Borkovec, *Long – Term Release Kinetics of Colloidal Particles from Natural Porous Media*, Environmental Science and Technology, 33 (22), 4054 – 4060, 1999.

Grolimund, Daniel, and Michael Borkovec, *Colloid – Facilitated Transport of Strongly Sorbing Contaminants in Natural Porous Media: Mathematical Modeling and Laboratory Column Experiments*, Environmental Science and Technology, 39 (17), 6378 – 6386, 2005.

http://www.epa.gov, US EPA, 2006.

Kaplan, Daniel, T.G. Hinton, Anna Knox, and S.M. Serkiz, *In Situ Remediation of ^{137}Cs Contaminated Wetlands Using Naturally Occurring Minerals*, A Report Prepared for the US DOE under contract number DE-AC09-96SR18500, 1999.

Kaplan, Daniel, T.G. Hinton, and Anna Knox, *Field Deployment of Illite Clay as an In Situ Method for Remediating ^{137}Cs – Contaminated Wetlands*, A Report Prepared for the US DOE under contract number DE-AC09-96SR18500, 2002.

Kersting, A. B., D. W. Efurd, D. L. Finnegan, D. J. Rokop, D. K. Smith, and J. L. Thompson, *Migration of Plutonium in Ground Water at the Nevada Test Site*, Nature, 397, 56 – 59, 1999.

Khilar, K.C., and H.S. Fogler, Migration of Fines in Porous Media, Springer, 1998.

Khilar, K.C., H.S. Fogler, and D.H. Gray, *Model for Piping – Plugging in Earthen Structures*, Journal of Geotechnical Engineering, 111 (7), 833 – 846, 1985.

Klute, A [ed.], Methods of Soil Analysis Part I, ASA – SSSA, 1986.

Kosakowski, George, *Anomalous Transport of Colloids and Solutes in a Shear Zone*, Journal of Contaminant Hydrology, 72, 23– 46, 2004.

Komarneni, Srihar, and Rustum Roy, *A Cesium – Selective Ion Sieve Made by Topotactic Leaching of Phlogopite Mica*, Science, 239 (4845), 1286 – 1288, 1988.

Kunberger, Tanya, John Quaranta, M. A. Gabr, *Remediation of Former Lockbourne Air Force Base Using Well Injection Depth Extraction (WIDE™)*, Proceedings from the 12th Pan-American Conference on Soil Mechanics and Geotechnical Engineering, 1575 – 1581, 2003.

Kunberger, Tanya, M.A. Gabr, *Temperature Effect on Desorption Kinetics of Benzene on Various Soils*, ASCE Geotechnical Special Publication (GSP) 142 Waste Containment and Remediation, Geofrontiers 2005.

Levin, J.M., J.S. Herman, G.M. Hornberger, J.E. Saiers, *Colloid Mobilization from a Variably Saturated, Intact Soil Core*, Vadose Zone Journal, 5 (2), 564 – 569, 2006.

Mattigod, S.V., V.L. Legore, I. Kutnykov, R.D. Orr, *Lixiviant Tests to Assess Leachability of Cesium – 137 from West Jefferson North Site Soils,* November 2002.

McClune, et. al. [eds.], Mineral Powder Diffraction File, JCPDS, 1980.

McGechan, M.B. and D.R. Lewis, *Transport of Particulate and Colloid – Sorbed Contaminants Through Soil, Part 1: General Principles*, Biosystems Engineering, 83 (3), 255 – 273, 2002.

McGechan, M.B., *Transport of Particulate and Colloid – Sorbed Contaminants Through Soil, Part 2: Trapping Processes and Soil Pore Geometry*, Biosystems Engineering, 83 (4), 387 – 395, 2002.

Nimmo, John, Joseph P. Rousseau, Kim S. Perkins, Kenneth G. Stollenwerk, Pierre D. Glynn, Roy C. Bartholomay, and LeRoy L. Knobel, *Hydraulic and Geochemical Framework of the Idaho National Engineering and Environmental Laboratory Vadose Zone*, Vadose Zone Journal 3, 6–34, 2004.

Penrose, William, Wilfred Poizer, Edward Essington, Donald Nelson, and Kent Oriadini, *Mobility of Plutonium and Americium through a Shallow Aquifer in a Semiarid Region*, Environmental Science and Technology, 24 (2), 228 – 234, 1990.

Quaranta, John, M.A. Gabr, and Tanya Kunberger, *Well Injection Depth Extraction Deployment at the Battelle Columbus Laboratories Decommissioning Project*, February 2003.

Ranville, James, David Chittleborough, and Ronald Beckett, *Particle – Size and Element Distributions of Soil Colloids: Implications for Colloid Transport*, Soil Science Society of America Journal, 69, 1173 – 1184, 2005.

Ritvo, Gad, Oded Dassa, and Malka Kochba, *Salinity and pH effect on the colloidal properties of suspended particles in super intensive aquaculture systems*, Aquaculture, 218, 379 – 386, 2003.

Rousseau, M., L. Di Pietro, R. Angulo-Jaramillo, D. Tessier, and B. Cabibel, *Preferential Transport of Soil Colloidal Particles: Physicochemical Effects on Particle Mobilization*, Vadose Zone Journal, 3, 247 – 261, 2004.

Ryan, Joseph, and Menachem Elimelech, *Colloid Mobilization and Transport in Groundwater*, Colloids and Surfaces A: Physicochemical and Engineering Aspects, 107, 1 – 56, 1996.

Ryan, J. N., T. H. Illangasekare, M. I. Litaor, and R. Shannon, *Particle and Plutonium Mobilization in Macroporous Soils during Rainfall Simulations*, Environmental Science and Technology, 32 (4), 476 – 482, 1998.

Saiers, James, and George Hornberger, *The Role of Colloidal Kaolinite in the Transport of Cesium Through Laboratory Sand Columns*, Water Resources Research, 32 (1), 33 – 41, 1996.

Saiers, James, and George Hornberger, *The Influence of Ionic Strength on the Facilitated Transport of Cesium by Kaolinite Colloids*, Water Resources Research, 35 (6), 1713 – 1727, 1999.

Schelde, Kirsten, Per Moldrup, Ole Jacobsen, Hubert de Jonge, Lis Wollesen de Jonge, and Toshiko Komatsu, *Diffusion – Limited Mobilization and Transport of Natural Colloids in Macroporous Soil*, Vadose Zone Journal, 1, 125 – 136, 2002.

Seaman, John, Paul Bertsch, and William Miller, *Chemical Controls on Colloid Generation and Transport in a Sandy Aquifer*, Environmental Science and Technology, 29 (7), 1808 – 1815, 1995.

Seaman, John, T. Meehan, and P.M. Bertsch, *Immobilization of Cesium – 137 and Uranium in Contaminated Sediments Using Soil Amendments*, Journal of Environmental Quality, 30 (4), 1206 – 1213, 2001.

Sen, Tushar Kanti, and Kartic C. Khilar, *Review on Subsurface Colloids and Colloid – Associated Contaminant Transport in Saturated Porous Media*, Advances in Colloid and Interface Science, 119, 71 – 96, 2006.

Seta, A. K., and A. D. Karathanasis, *Water Dispersible Colloids and Factors Influencing Their Dispersibility from Soil Aggregates*, Geoderma, 74, 255 – 266, 1996.

Shoblom, Kurt, Effective Flushing of Naphthalene from Kaolinite Rich Soils, A thesis submitted to West Virginia University, 1994.

Sumner, M.E., and W.P. Miller, *Cation Exchange Capacity and Exchange Coefficients*, in D. L. Sparks (ed.) Methods of Soil Analysis. Part 3. Chemical Methods, SSSA, 1201 – 1229, 1996.

Sun, Ning, Menachem Elimelech, Ne-Zheng Sun, and Joseph Ryan, *A novel two-dimensional model for colloid transport in physically and geochemically heterogeneous porous media*, Journal of Contaminant Hydrology, 49, 173 – 199, 2001.

USDA – SCS, Soil Survey of Madison County Ohio, 1978.

U.S. Department of Energy Office of Environmental Management Office of Science and Technology, Well Injection Depth Extraction (WIDE) Soil Flushing, Innovative Technology Summary Report, May 2001 http://apps.em.doe.gov/ost/pubs/itsrs/itsr2172.pdf

US EPA, http://www.epa.gov/radiation/cleanup/partition.htm, Volume II Geochemistry and Available Kd Values for Selected Inorganic Contaminants, 2003.

Wokasien, Sean, Retrieval of Subsurface Liquid Utilizing Prefabricated Vertical Drains (PVD), A thesis submitted to West Virginia University, 1994.

Special Topics Journal, Colloids and Colloid – Facilitated Transport of Contaminants in Soils, Vadose Zone Journal, 3, 2004.

Appendix A. Visual Minteq Program Output

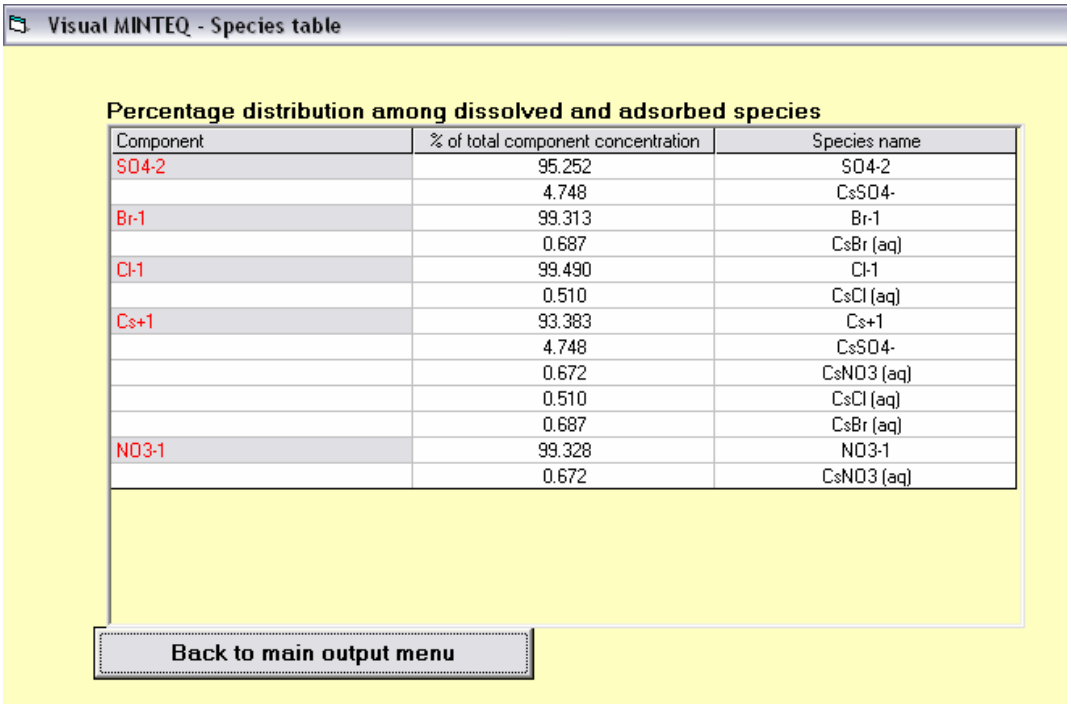

Figure A.1: Visual Minteq Output for Cesium with Bromide, Chloride, Nitrate, and Sulfate (all at equal concentrations)

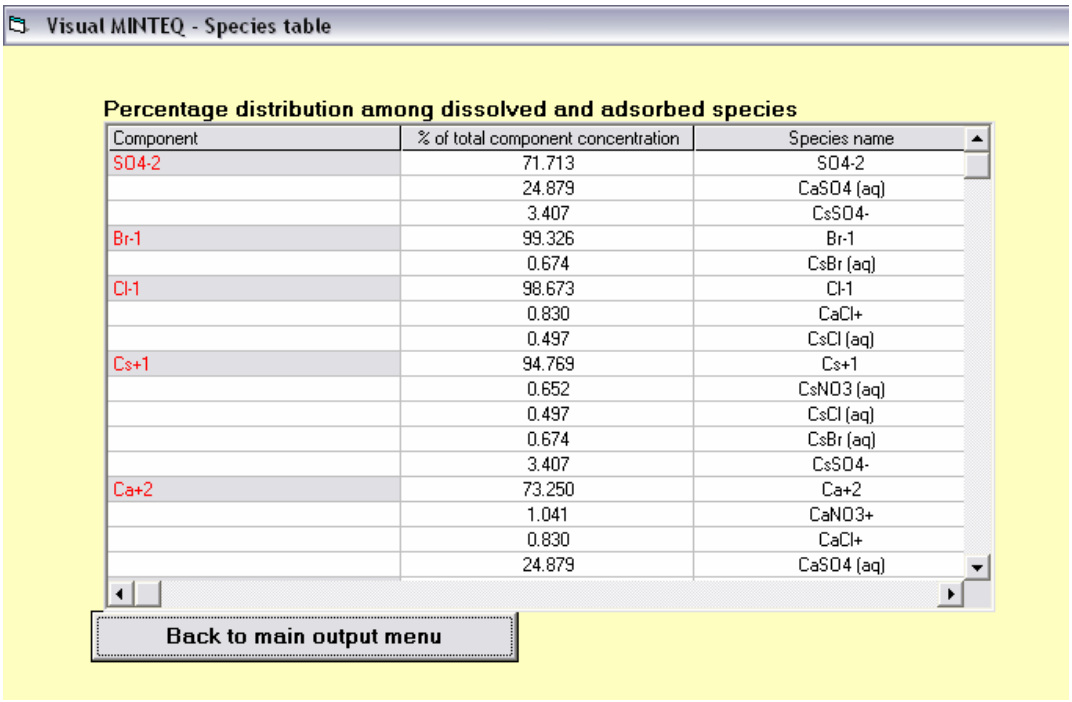

Figure A.2: Visual Minteq Output for Cesium and Calcium (as competing ion) with Bromide, Chloride, Nitrate and Sulfate (all at equal concentrations)

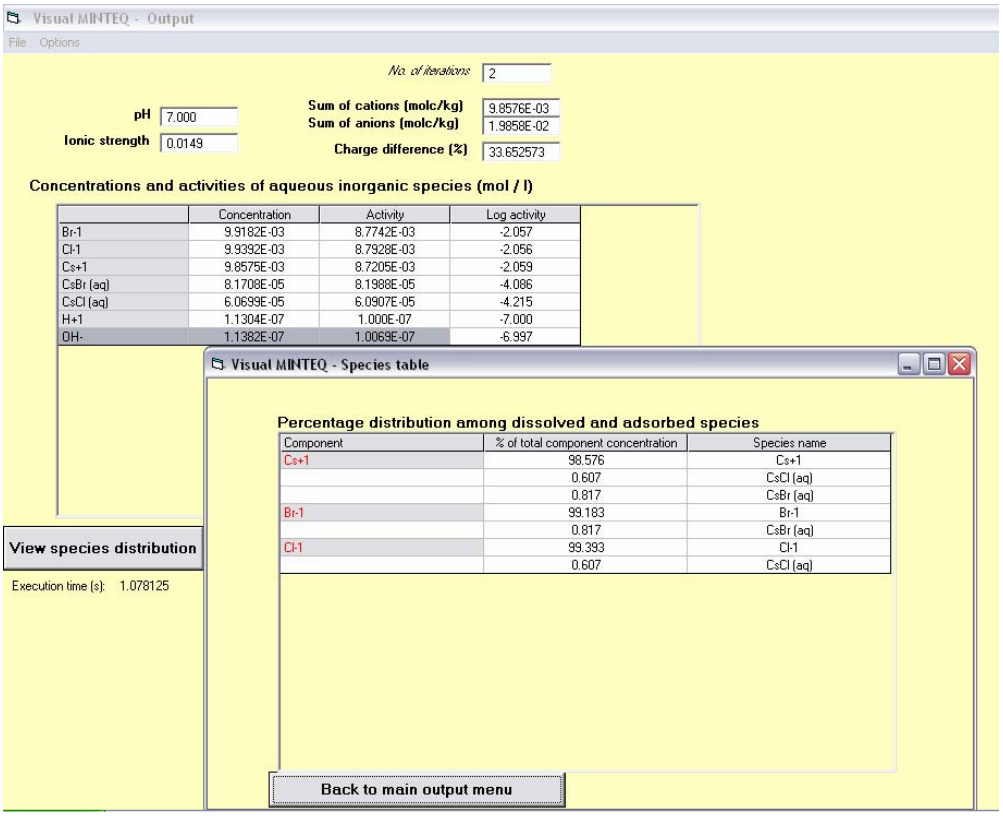

Figure A.3: Visual Minteq Output of Cesium with Bromide and Chloride

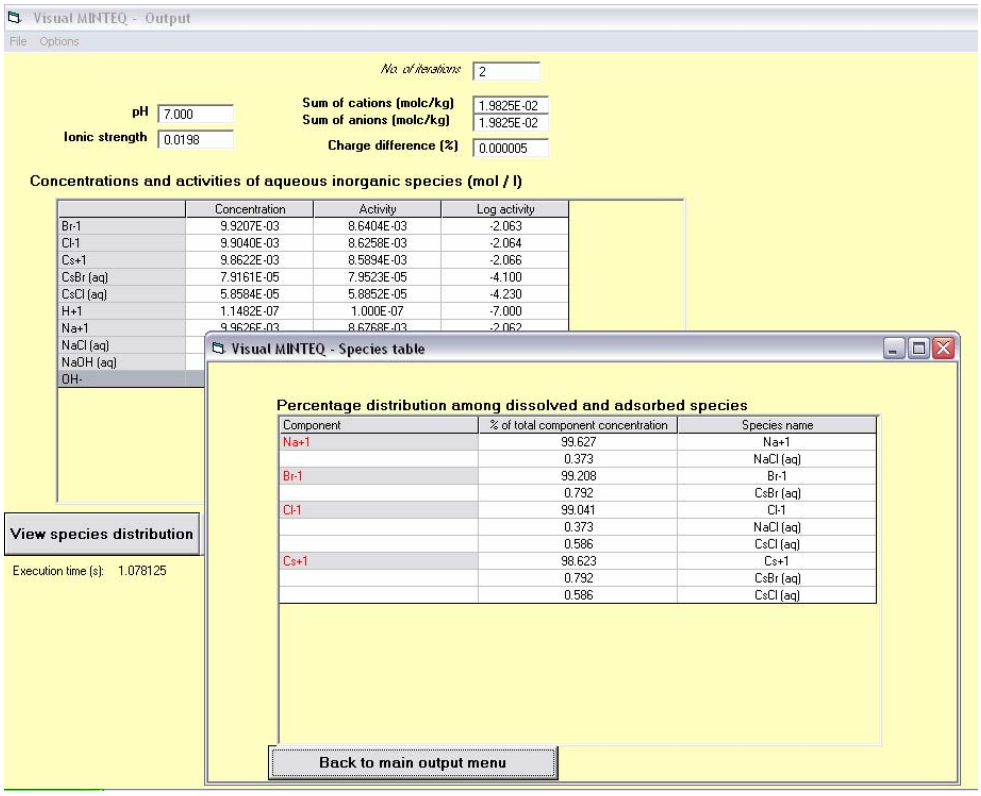

Figure A.4: Visual Minteq Output of Cesium and Sodium with Bromide and Chloride

Appendix B. Field Site Maps and Information

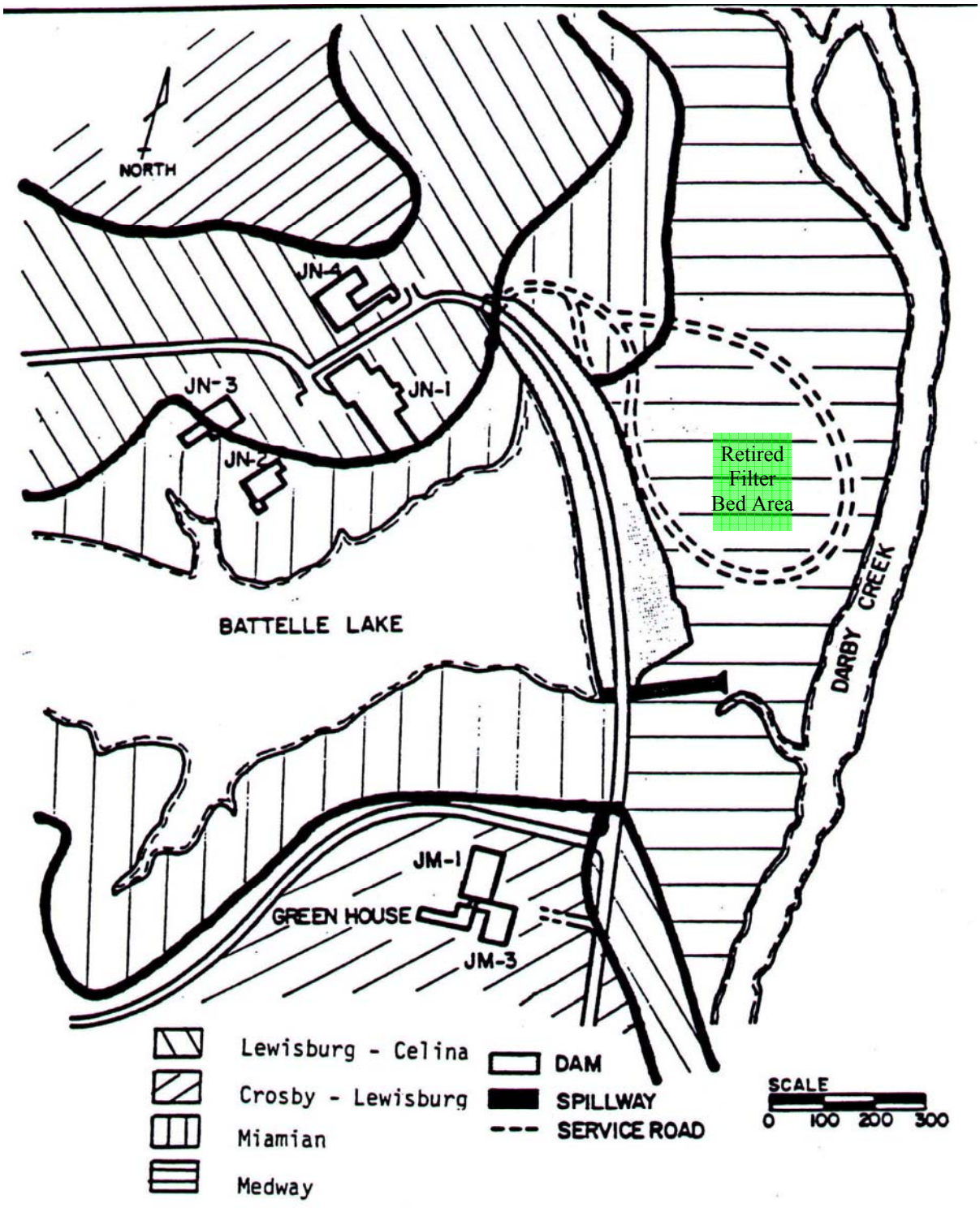

Figure B.1: Soil Survey Map of Battelle West Jefferson North Site (from Beard, 1990)

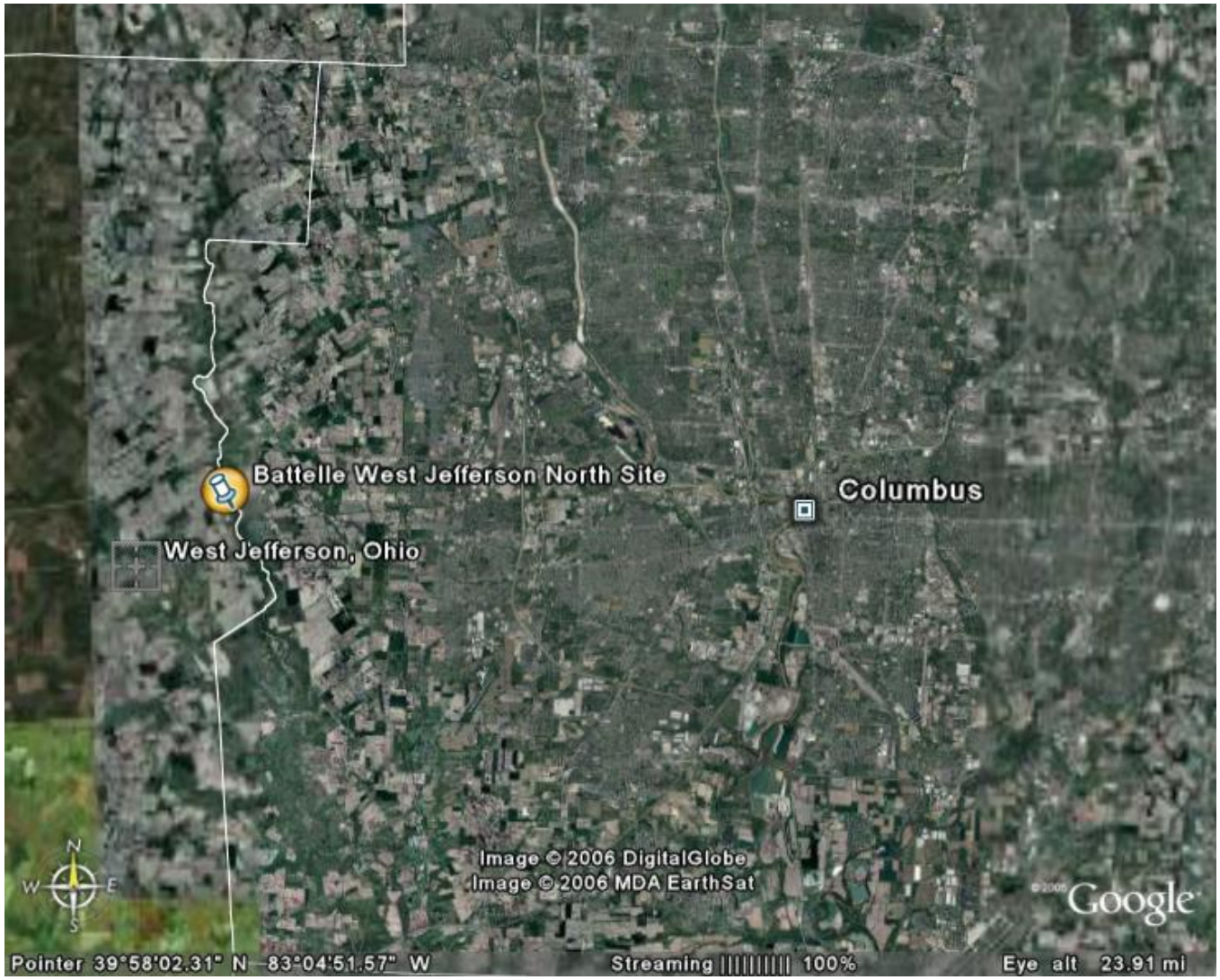

Figure B.2: Location of Battelle West Jefferson North Site (from Google Earth)

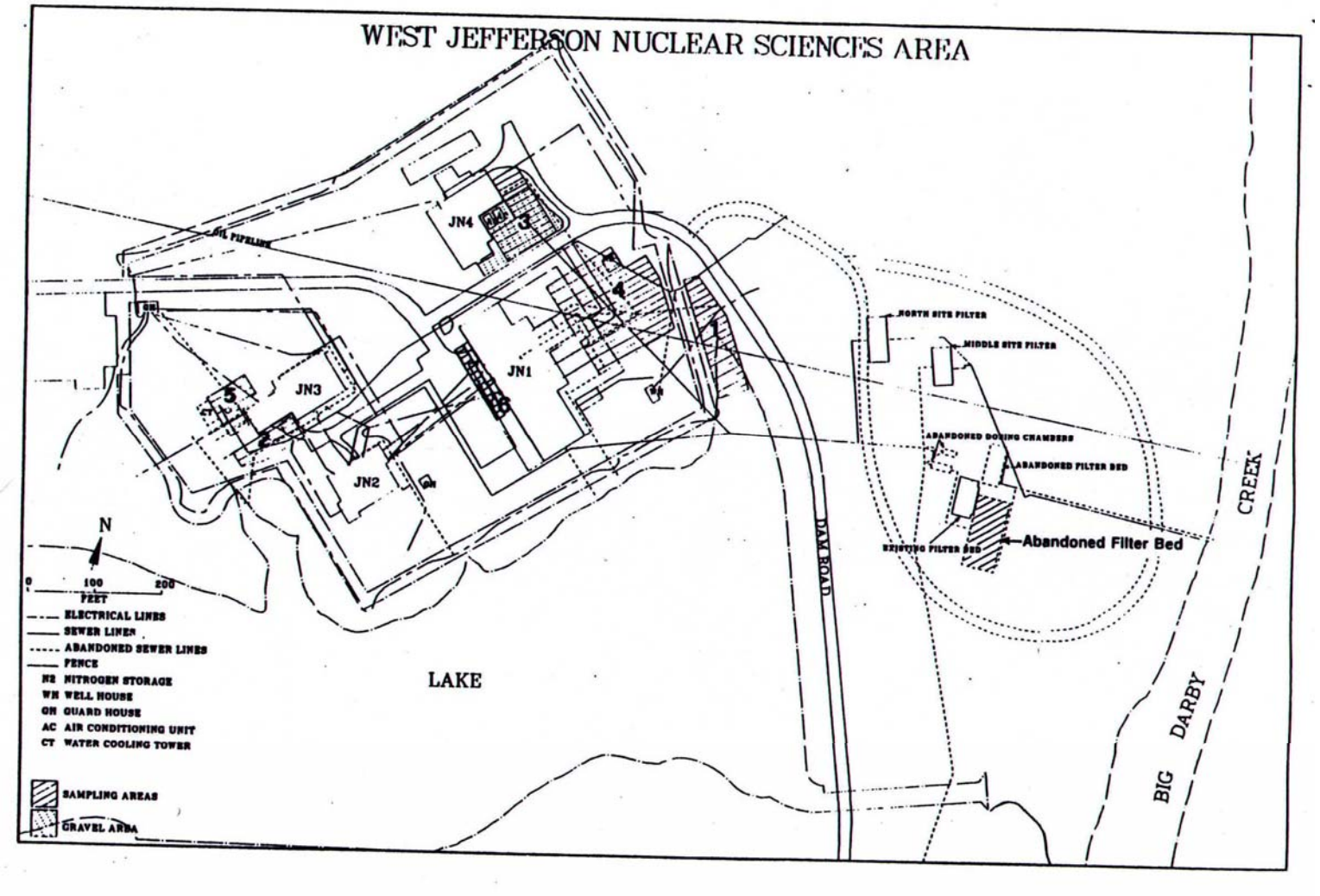

Figure B.3: General Map of Battelle West Jefferson North Site (from Beard, 1990)

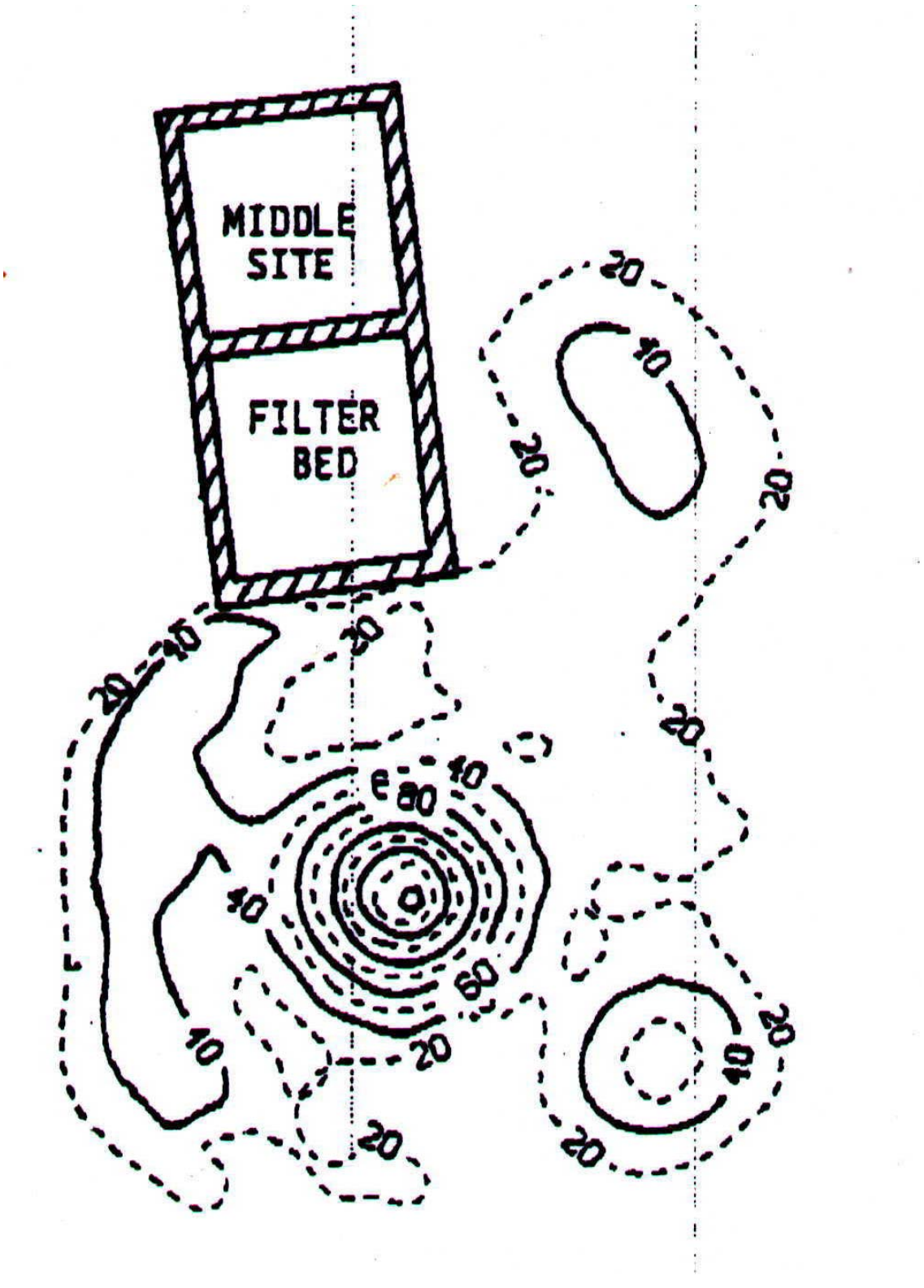

Figure B.4: Cesium Concentration Levels at Retired Filter Bed Area 0.6 – 1.2 meter (2 – 4 foot) Depth (from Beard, 1990)

Appendix C. Soil Mineralogy Testing Procedures

C.1 Soil Fractionation

Before undergoing soil mineralogy testing, the soil sample was subjected to a number of pretreatments in order to remove any rock fragments larger that 2-mm, correct for soil moisture content, and remove any carbonates and organic matter that may have been present. Rock fragment removal was accomplished by passing the soil sample through a 2-mm (#10) sieve. Moisture content was determined by placing a known mass of soil in a clean and dry beaker, placing the beaker in a 105 ºC oven overnight, allowing it to cool in a desiccator, and obtaining a dry mass of soil. The amount of water was then calculated, and the total mass of soil corrected for this hydroscopic moisture content.

Carbonate and organic matter removal was performed in order to enhance dispersion of the soil sample. Removal was accomplished first by the addition of 50 mL pH 5, 1 M NaOAc solution to each of a number of centrifuge bottles containing a portion (roughly 20 grams) of soil sample. The resulting mixture was stirred, placed in a hot water bath, and heated to 90 °C for 10 minutes. Excessive frothing was prevented by periodic monitoring and removal from heat when necessary, and when frothing ceased the sample was centrifuged and the clear supernatant discarded. An additional 100 mL of 1 M NaOAc to each of the bottles was performed to promote Na saturation of the sample, the solution was dispersed with a sonicator, centrifuged, and the clear supernatant was again discarded.

Organic matter removal was accomplished with the addition of 5 – 10 mL of 1 M NaOAc (for buffering) and 10 mL 30% H_2O_2. The samples were then placed in a large clean beaker and covered with a watch glass. These measures inhibited H_2O_2 loss and prevented loss of the sample if accidental frothing over occurred. Samples were allowed to stand overnight, then centrifuged and the procedure repeated until light colored samples, indicating

removal of much of the organic matter, were obtained. Afterwards, fresh aliquots of hydrogen peroxide were added, and the samples heated to almost 100 ºC to decompose the H_2O_2 into H_2O and O_2. Upon subsidence of the effervescence, samples were washed down with NaOAc, centrifuged, and the supernatant discarded. Samples were then washed with NaOAc, and subsequently with NaCl and stored in the refrigerator until needed.

To perform sample fractionation, 100 mL of pH 10 Na_2CO_3 solution was added to each of the samples stored in the refrigerator from the pretreatment above. The samples were sonicated for dispersion and then wet-sieved through a 52-μm opening sieve. That portion of the sample which remained on the sieve was washed into a beaker and placed in a 110 ºC oven to dry overnight. After allowing it to cool in a desiccator, the mass of this sample was weighed, and this was recorded as the sand portion of the soil sample. Silt and clay fractionation was performed utilizing a series of centrifugation steps and employing Stoke's Law (adapted for centrifugation).

For silt separation, samples were placed in 250-mL centrifuge bottles, filled to a depth of 8 cm and centrifuged for 3.9 minutes at 750 rpm using a GSA fixed angle rotor. The supernatant suspension was collected after each run (saved for clay separation) and additional Na_2CO_3 solution was added to bring the depth to the 8 cm mark. Samples were sonicated and the entire process repeated until the supernatant solution is turbid, but able to be seen through. The suspension remaining at the bottom of the bottles was washed into a beaker and placed in a 110 ºC oven to dry overnight. After allowing it to cool in a desiccator, the mass of this sample was weighed, and this was recorded as the silt portion of the soil sample.

For coarse and fine clay separation, samples (from the saved supernatant from silt separation) were again placed in 250-mL centrifuge bottles, filled to a depth of 8 cm and centrifuged for 13.8 minutes at 4000 rpm. The supernatant suspension containing the fine clay portion was collected after each run and additional deionized water was added to bring the depth to the 8 cm mark. Samples were sonicated and the entire process repeated until the supernatant solution was almost clear. The remaining suspension at the bottom of the bottles was freeze-dried and the mass of this sample was weighed, and this was recorded as the coarse clay (2 – 0.2 μm) portion of the sample. The fine clay suspension was flocculated to reduce the volume, dialyzed to remove salt, then also freeze-dried and the mass of this samples was weighed and recorded as the fine clay (< 0.2 μm) portion of the sample.
Soil fractionation results, on a mass basis, can be found in Table C.1.

Table C.1: Percent Fractionation of Soil Sample (by mass)

Soil Type	Percent (by mass)
Sand (2 mm – 50 μm)	31.6%
Silt (50 μm – 2 μm)	30.9%
Coarse Clay (2 μm – 0.2 μm)	16.4%
Fine Clay (< 0.2 μm)	21.1%

This fractionation shows a relatively equal percentage by mass of soil particles in the sand, silt, and clay fractions respectively. The slightly higher concentration of clay particles (37.5%) confirms the clay designation obtained from engineering properties and the USCS classification. Fractionation results help separate different minerals in addition to being

useful from an engineering standpoint in the determination of the effectiveness of various remediation measures under consideration. Fractionation plays a large role in the hydraulic conductivity of a soil, and thus influences the time factors associated with many remediation measures. Fractionation can also help determine a rough estimate of a required removal mass when considering dispersion and piping for the removal of fines as a remediation measure for reducing free release levels of radioactive cesium in the subsurface environment.

C.2 Specific Surface Area Determination

Both external and total specific surface area analyses were performed on the soil samples to provide detailed mineralogical interaction of the fine particles. For external surface area analysis, N_2 adsorption in a Quantachrome Monosorb surface area analyzer was employed. This analyzer saturates the sample with the calibrated N_2/He gas then cools the sample in order to preferentially adsorb the N_2 molecules to the sample. The sample is then exposed to heat, causing a net release of N_2 from the sample surface. This excess is measured directly and the calibrated surface area analyzer gives a direct output of surface area results. Once this value is divided by the known mass of the sample, the specific surface area is known. External surface area analysis was performed on the sand and silt fractions, as well as in duplicate on the coarse and fine clay fractions. Total specific surface area was performed in duplicate only on the coarse and fine clay fractions of the soil using EGME. In this analysis, known masses of samples are placed in clean and dry aluminum weighing dishes. These samples are then saturated with ethylene glycol monoethyl ether (EGME) to form a slurry. The cans are placed in a desiccator containing $CaCl_2$-EGME mix, the desiccator is evacuated, and the samples are allowed to reach an equilibrium weight. In order

to determine when this equilibrium has been obtained, periodic weighing of samples must occur. Once the weights are considered to no longer be fluctuating, the quantity of EGME retained by each sample can be calculated by mass balance. The specific surface area of the samples is then calculated by dividing the mass of EGME retained by the sample by the mass of the sample times 0.000286 (the monolayer surface coverage of EGME in g/m^2).

Like fractionation, specific surface area can not directly contribute to the mineralogical determination of soil samples, but can, to some extent, confirm results obtained from X-ray diffraction analysis. Table C.2 lists external and total specific surface area results for each of the soil types tested.

Table C.2: Specific Surface Area by Soil Type from Natural Sample

Soil Type	External SSA (m^2/g)	Total SSA (m^2/g)
Sand	1.32	--*
Silt	3.52	--*
Coarse Clay	21.32	59.10
Fine Clay	94.48	208.70

* Testing not performed

For samples where duplicate testing occurred, presented results are the mean of tests performed. Total SSA was not performed on sand and silt samples due to the fact that internal surface area is unlikely to be present in the minerals from which these fractions are composed. The large differences between total and external SSA for both the coarse and fine clay fractions suggests the presence of different 2:1 clay minerals with available interlayer

space. The relatively low values for the coarse clay may imply the presence of mica-like minerals, where the higher values for the fine clay hint at a composition of vermiculites or smectites. XRD analysis will provide a more definitive determination of mineralogical composition.

C.3 Cation Exchange Capacity Determination

Cation Exchange Capacity (CEC) determination was performed on the coarse and fine clay portions of the soil sample, as well as the silt portion. Due to the mineralogical composition of the sand portion, the CEC values were expected to be relatively low, and thus testing was not performed. The method utilized is based on measuring the loss of magnesium from a magnesium sulfate solution during $Mg^{2+} - Ba^{2+}$ exchange driven by $BaSO_4$ precipitation as described by Sumner and Miller (1996). In this method, samples are weighed out in duplicate or triplicate into plastic centrifuge tubes. $BaCl_2$ solution is then added to the samples, which are shaken, centrifuged, and washed repeatedly with successively lower ionic strength $BaCl_2$ solutions. Between $BaCl_2$ washes, pH is measured and adjusted to match the naturally occurring pH of the soil. After pH adjustment and $BaCl_2$ washing, centrifuging, and decanting, 0.005 M $MgSO_4$ solution is added to the samples. Samples are sonicated, if necessary, shaken, and subjected to electrical conductivity (EC) adjustment, before being shaken gently overnight. EC is adjusted again, if necessary, and samples are centrifuged, decanted, and subjected to Mg analysis. CEC is determined by calculating the amount of Mg^{2+} lost from solution as the exchanged Ba^{2+} precipitates with SO_4^{2-}. Table C.3 lists the Cation Exchange Capacity and standard deviations for the various fractions of the natural soil sample.

Table C.3: Cation Exchange Capacity Determination by Soil Type for Natural Sample

Soil Type	CEC (cmol/kg)	Standard deviation
Silt	6.60	0.585
Coarse Clay	20.73	0.398
Fine Clay	48.49	2.060

As expected, CEC values of the clay portions of the soil were significantly greater than that of the silt portion, with the fine clay fraction possessing the highest overall cation exchange capacity. The relatively low CEC value in the silt portion suggests the possible presence of larger – sized clay minerals (i.e. phyllosilicates), although in fairly low amounts. The majority of the silt fraction, by mass, is most likely quartz or other minerals (e.g. feldspars) and is unlikely contributors to contamination retention. CEC values imply the presence of smectite or vermiculite minerals in both the coarse and fine clay fractions. With a value of approximately 20 cmol/kg, the CEC of the coarse clay fraction is in the moderate range for clay minerals. The fine clay CEC value of roughly 50 is more in the mid-range, but still somewhat low when considering many secondary clay minerals boast CEC values in the low hundreds. Still, the existence of even moderate levels of CEC can impart significant complications when considering contamination remediation.

Cation exchange capacity is a result of isomorphic substitution during mineral formation, and thus is considered a constant charge for the soil. Because of the permanent nature of this charge, it is usually unaffected by typical pH variations, ionic strength variations, or other changes commonly occurring in the natural environment. Thus, this constant charge is an important component affecting the retention of various organic and inorganic contaminants. As with specific surface area, CEC values can not directly classify

mineralogical composition, but can serve as general guidelines and confirmation of X-ray diffraction analysis results.

C.4 X-ray Diffraction Analysis

Sample mounts for X-ray Diffraction (XRD) analysis were performed differently depending on if it was the coarse or fine-grained portion of the soil sample. For coarse-grained portions (i.e. sand and silt) random powder mount samples were prepared, while for the fine-grained portions (i.e. coarse and fine clay) a paste or slurry method will be employed to make oriented mounts.

C.4.1 Sample Preparation

In order to prepare a random powder mount sample, the particle size should be < 0.1 mm. The silt fraction already meets this standard, however the sand fraction must be ground, using a mortar and pestle, and passed through a 180-mesh sieve. Double sided tape is attached to the XRD slides, and the sand and silt fractions are individually shaken onto these slides. Complete coverage is assured, and the slides are then tapped clear of any excess particles and are ready for analysis.

Clay slide preparation is a more involved process due to the number of analyses that must be performed. For both the coarse and fine grained portions, the following steps must be performed. Place roughly 0.3 g of each clay into each of two 50-mL centrifuge tubes. For XRD analysis, it is necessary to Mg and K saturate for each clay. To obtain Mg saturation, add 35 mL of DI water and solid $Mg(Cl)_2$ to obtain a 0.5 M Mg concentration. Shake

vigorously, sonicate, and centrifuge at 7500 rpm for 10 minutes. Decant clear supernatant, add 0.5 M $Mg(Cl)_2$ solution, sonicate, centrifuge and decant again. To obtain K saturation, add 35 mL of DI water and solid KCl to obtain a 1 M K concentration. Shake vigorously, sonicate, and centrifuge at 7500 rpm for 10 minutes. Decant clear supernatant, add 1 M KCl solution, sonicate, centrifuge, and decant again. To wash excess salt from all samples, add deionized water, sonicate, centrifuge at 15000 rpm for 15 minutes, decant supernatant and repeat process until sample remains dispersed during centrifugation. To prepare slurry mounts, pipette enough of the clay suspension onto a slide to completely cover the slide and allow to dry. For those slides where this slurry mount, once dried, resulted in cracked specimens, the soil sample was mixed into a thick paste and smeared onto the slide in a thin, smooth layer. A Mg and K slide was made for each of the coarse and fine clay samples.

C.4.2 X-ray Diffraction Analysis

X-ray diffraction analysis was performed through the Marine Earth and Atmospheric Department, located in Jordan Hall on the Main Campus of North Carolina State University. The XRD equipment was set up by Dr. Skip Stoddard, and the author would like to gratefully acknowledge his assistance in testing. XRD was performed on a Rigaku machine utilizing Cu Kα radiation. For the sand and silt samples, the 2θ data range for the goniometer was 2 – 80 degrees, at a rate of 1 degree / minute. For the clay samples, the 2θ data range for the goniometer was 2 – 30 degrees, at a rate of 2 degrees / minute. Clay samples were initially run at room temperature. Upon completion, the Mg saturated slides were then sprayed with glycol, allowed to dry overnight, and retested. The K saturated slides were heated to 350 ºC, allowed to cool and retested, then heated to 550 ºC, allowed to cool and retested. This course

of testing resulted in 12 data files, one each for sand and silt, and five (Mg, Mg-gly, K-rt, K-350, and K-550) for each of the coarse and fine clay fractions.

C.4.3 X-ray Diffraction Interpretation

X-ray diffraction analysis results were interpreted utilizing Whittig and Allardice's Phyllosilicate Equivalent Plane Spacing found in Methods of Soil Analysis and the JCPDS Mineral Powder Diffraction File. Output results for all soil types can be found in Appendix D. The main component for both the sand and silt fractions of the sample was determined to be quartz. This was a rather unsurprising result considering the typical composition of sand, visual inspection of the sample, and the low SSA values obtained for both fractions. The effect of the quartz mineral in the sand and silt fraction with regards to remediation of the site assists in confirming the belief that the cesium contamination is focused in the fines fraction of the soil. Cesium binds typically by means of cation exchange, and quartz is not a mineral typically known for a high CEC value. Thus the amount of cesium associated with the sand and silt fractions of this soil is expected to be low to negligible.

From XRD analysis, the coarse clay fraction appears to be composed of mica, kaolinite, and a hydroxy – interlayered vermiculite. The latter was indicated by the shift in the 1.4 nm peak that occurs with heating. These minerals are types that can be expected to be found in the area and conform to SSA and CEC determination results. The presence of mica in the soil sample will provide an interesting addition to remediation analysis. Previous studies have shown that the presence of mica creates an adsorption hysteresis with cesium, that is the rate at which adsorption occurs is much greater than the rate at which desorption occurs. The reason for this slow rate of desorption is the fact that the ditrigonal cavity on the

octahedral layers of mica minerals are the perfect size for a cesium ion. Once the ion is fit into place in this layer, even high concentrations of other ions is not sufficient to displace it. This suggests that typical pump and treat, or any flushing measure, would not be an effective remediation treatment. However, the mobilization and subsequent removal of these mica particles by dispersion and piping could remove the contaminated cesium and provide a more effective remediation measure.

The fine clay fraction of the soil contains vermiculite, smectite, kaolinite, and mica, in order of relative abundance. Again, these minerals are reasonable ones for the sample location, as well as for the measured SSA and CEC. As with the coarse clay fraction, the presence of a mica mineral will provide the same remediation challenge discussed above. Additionally, the smectite and vermiculite, with a high CEC value, would also be a contributing factor to the sorption of cesium in the fines fraction of the soil. The vermiculite is probably the most important in terms of remediation, in that it is very abundant and possesses a high charge.

Appendix D. X-Ray Diffraction Patterns

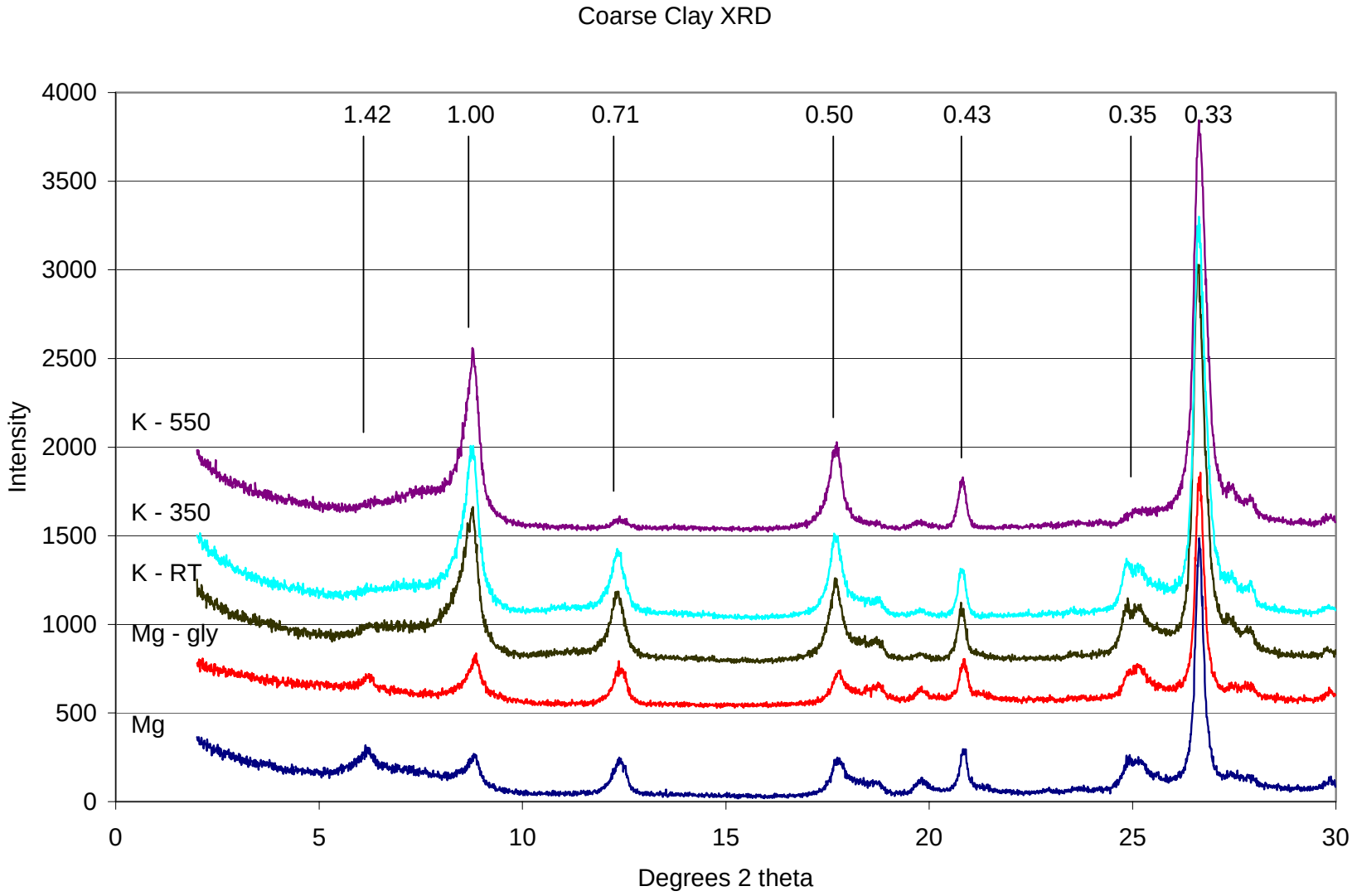
Coarse Clay XRD
1.42
1.00
0.71
0.50
0.43
0.35
0.33
K - 550
K - 350
K - RT
Mg - gly
Mg
Intensity
Degrees 2 theta
0
500
1000
1500
2000
2500
3000
3500
4000
0
5
10
15
20
25
30

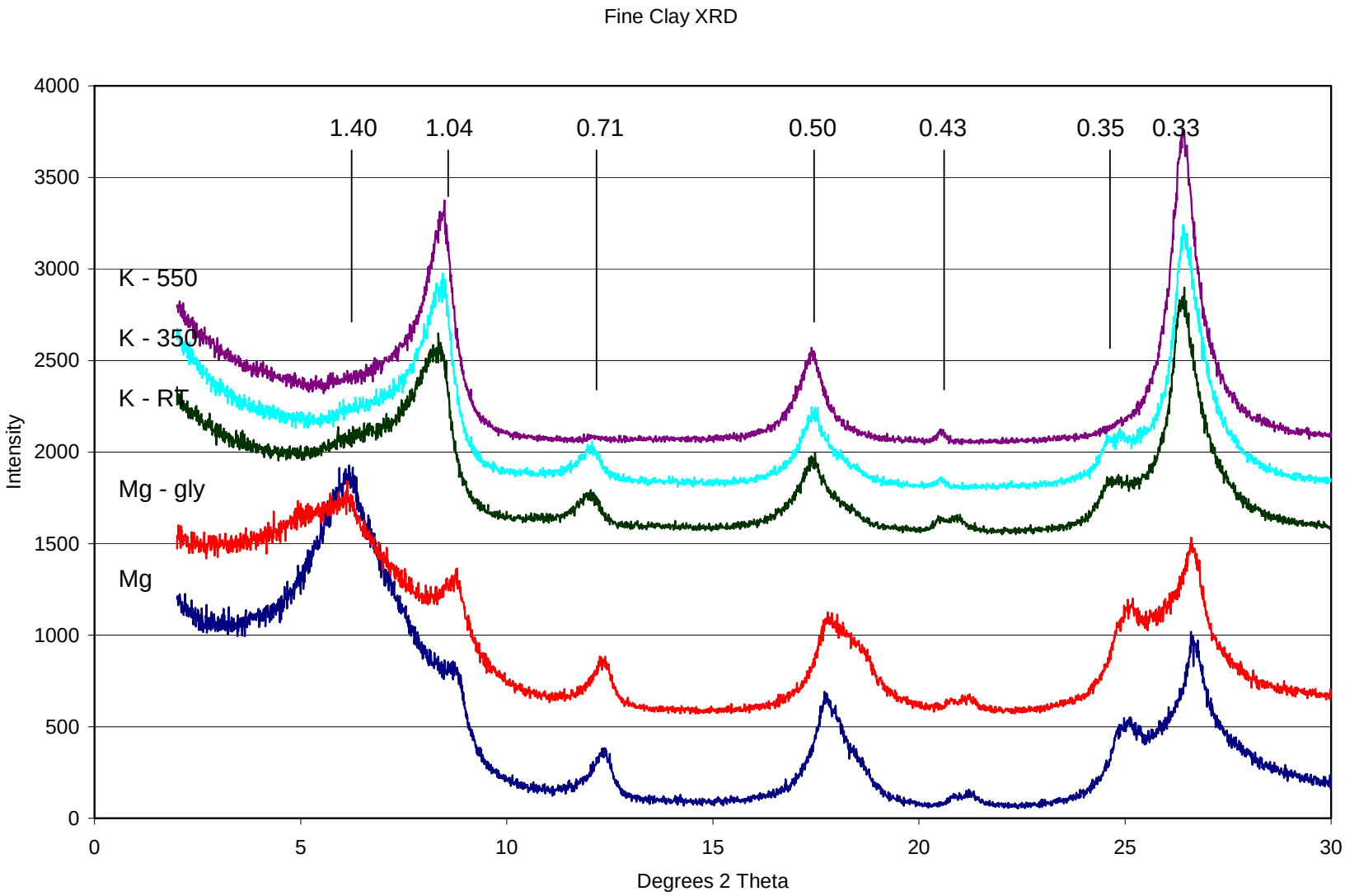
Fine Clay XRD
1.40
1.04
0.71
0.50
0.43
0.35
0.33
K - 550
K - 350
K - RT
Mg - gly
Mg
Intensity
Degrees 2 Theta
0
500
1000
1500
2000
2500
3000
3500
4000
0
5
10
15
20
25
30

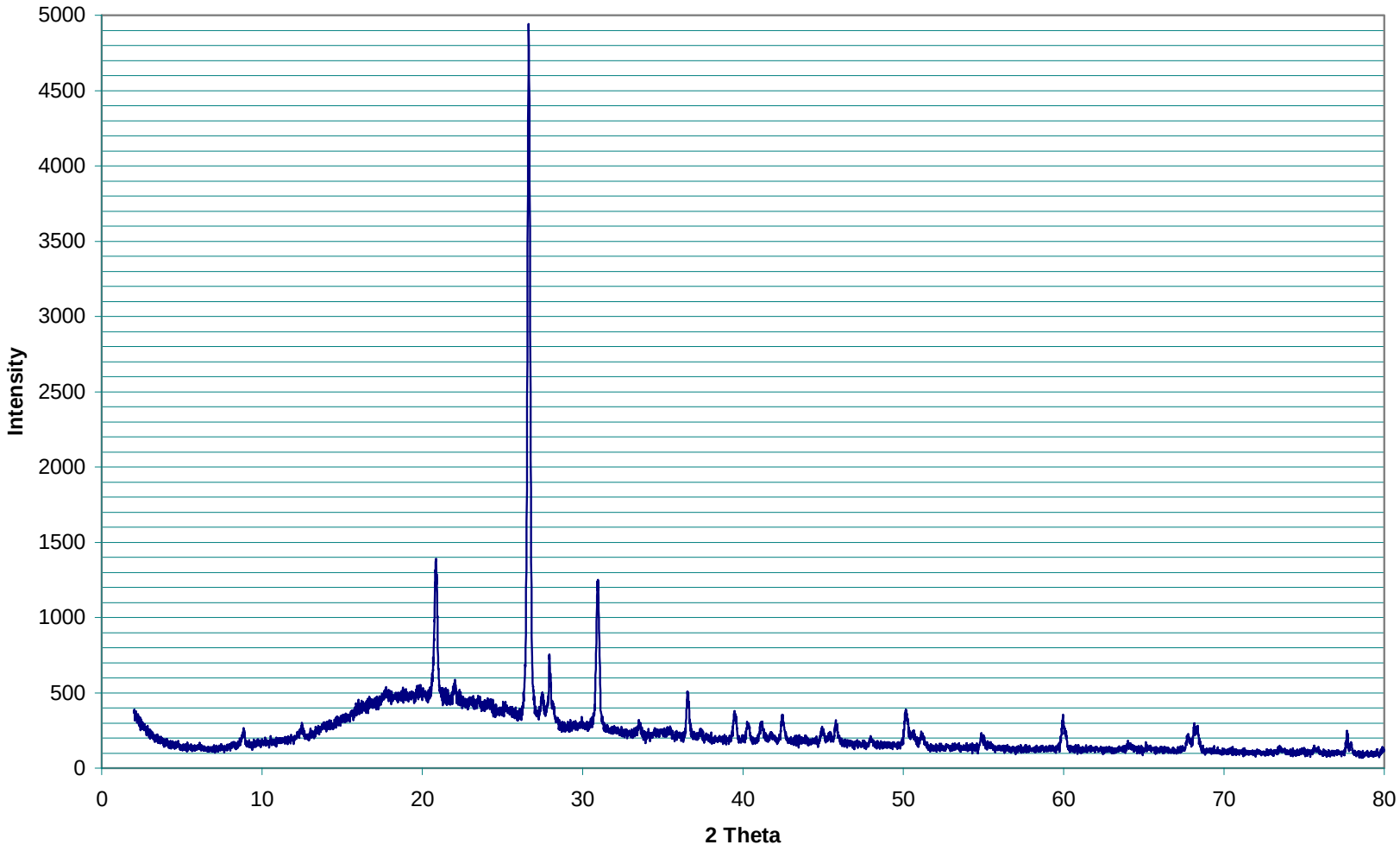
Silt XRD
Intensity
5000
4500
4000
3500
3000
2500
2000
1500
1000
500
0
0
10
20
30
40
50
60
70
80
2 Theta

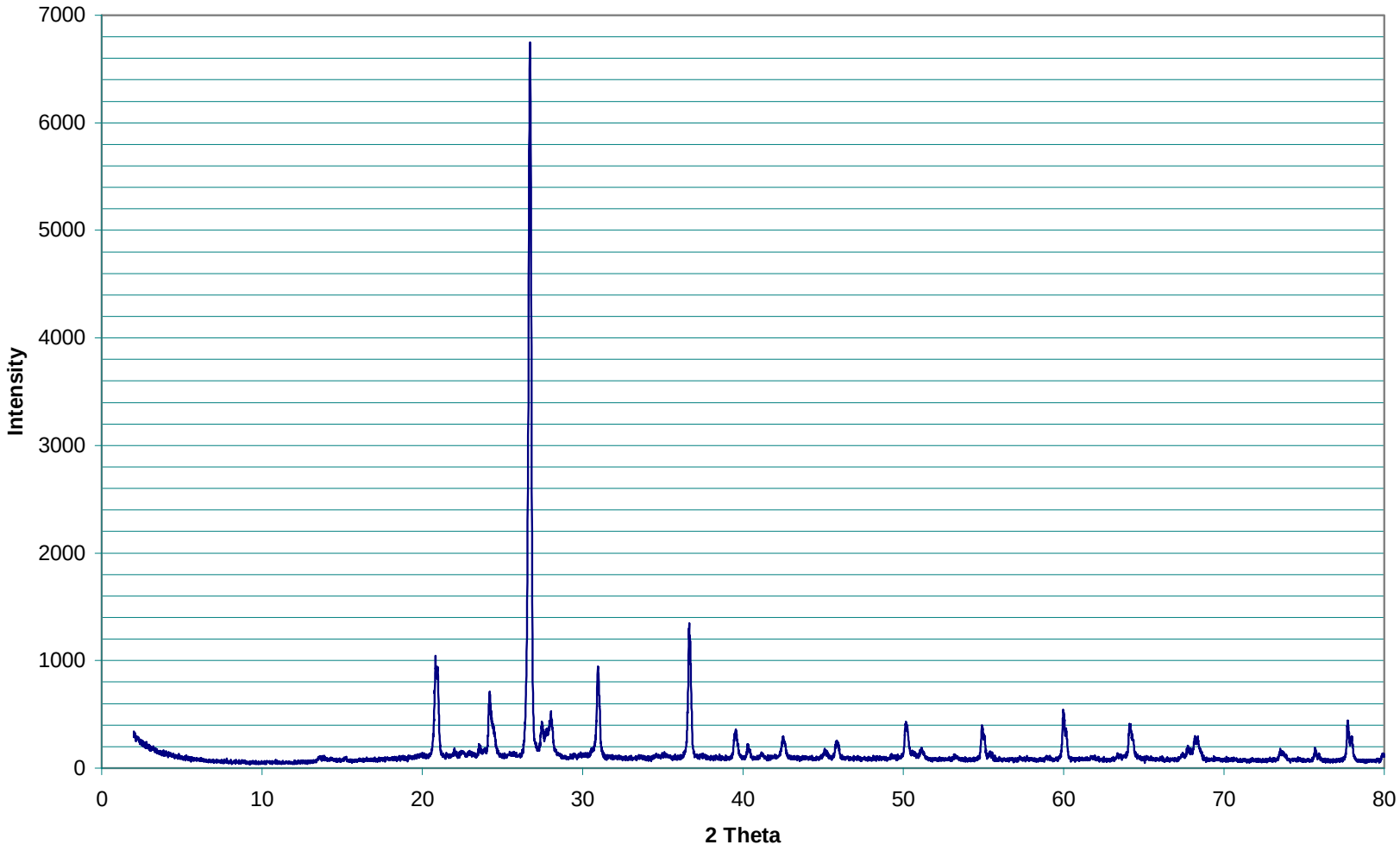
Sand XRD
Intensity
7000
6000
5000
4000
3000
2000
1000
0
0
10
20
30
40
50
60
70
80
2 Theta

Appendix E. Permeability Versus Pore Volume Graphs

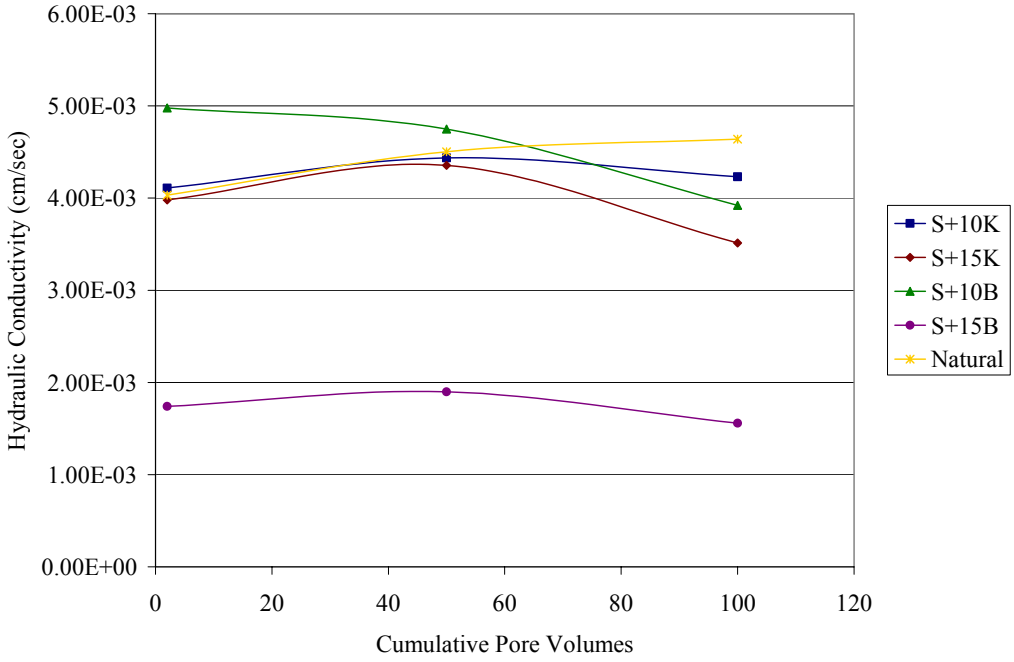

Figure E.1: Permeability as a Function of Cumulative Pore Volume for the Moderate Hydraulic Gradient (i = 14.5) and 0.1 M Ionic Strength Tests

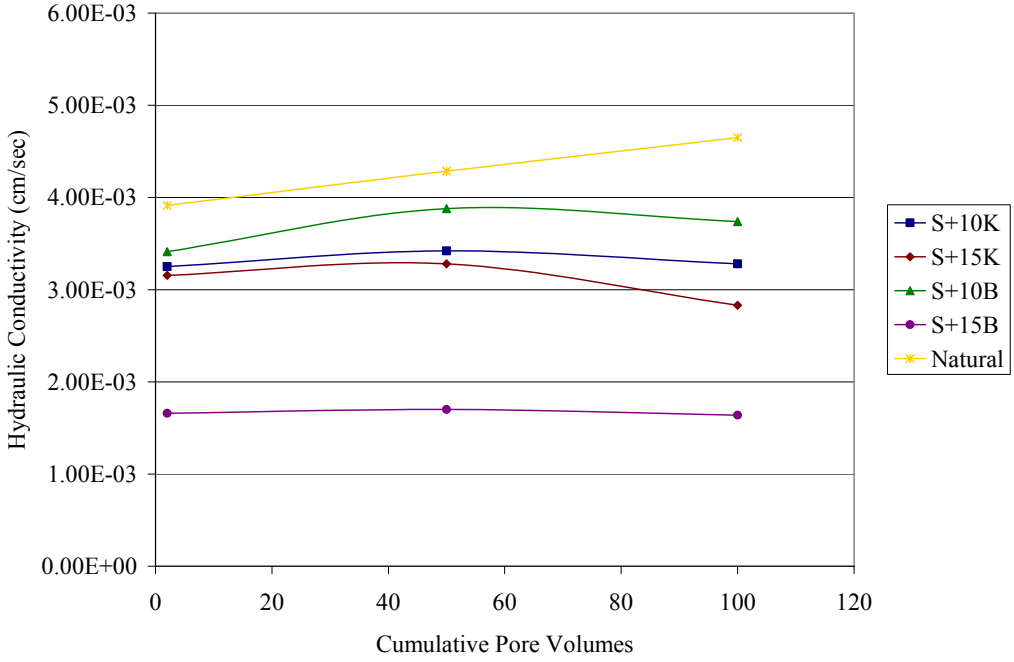

Figure E.2: Permeability as a Function of Cumulative Pore Volume for the High Hydraulic Gradient (i = 29) and 0.1 M Ionic Strength Tests

Appendix F. Flow Through Lab Results

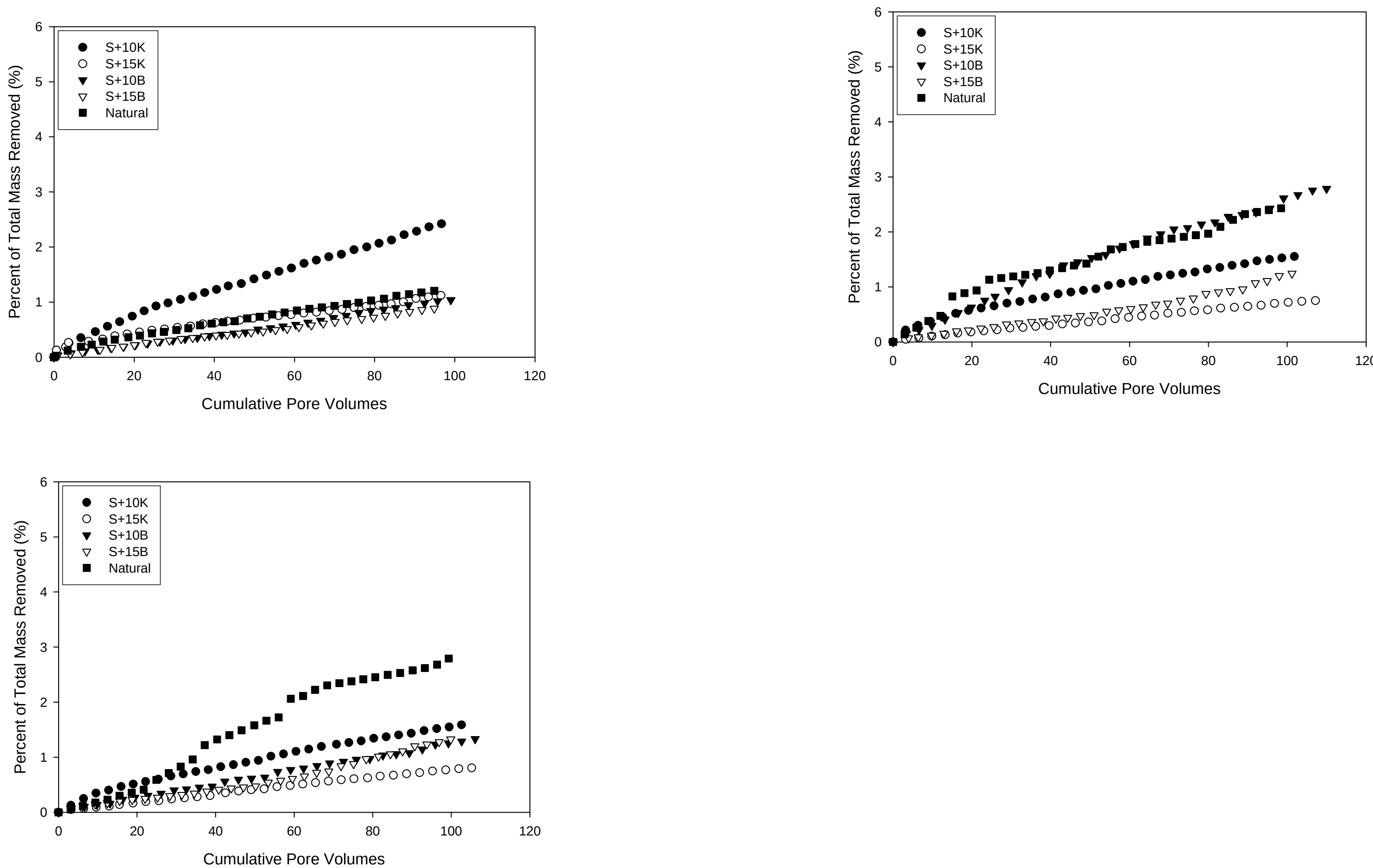

Figure F.1: Colloidal Removal Efficiencies for Low (0.0025M) Ionic Strength for All Soils at Low (top left), Medium (bottom left), and High (top right) Hydraulic Gradient Variations

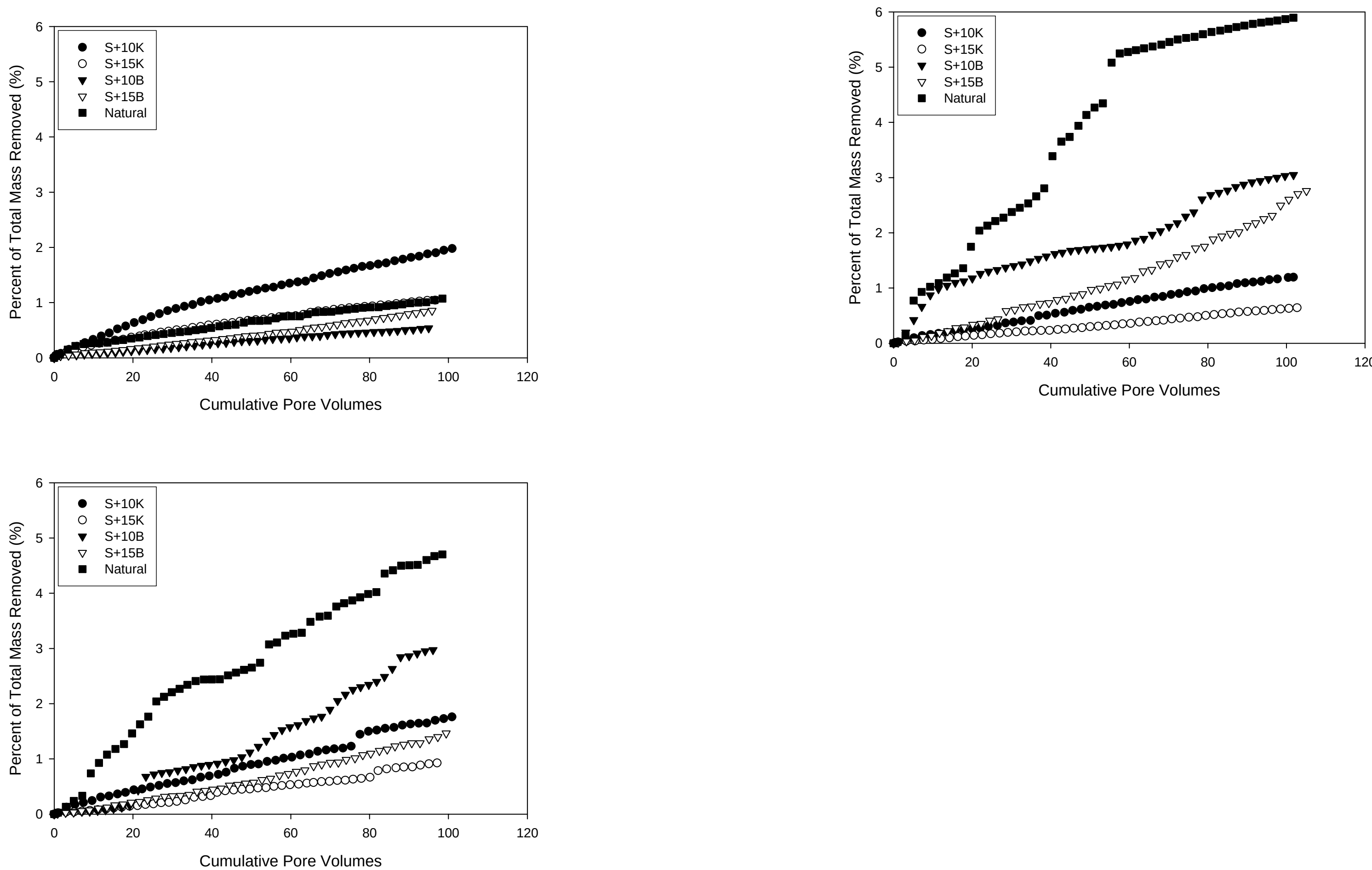

Figure F.2: Colloidal Removal Efficiencies for Medium (0.1M) Ionic Strength for All Soils at Low (top left), Medium (bottom left), and High (top right) Hydraulic Gradient Variations

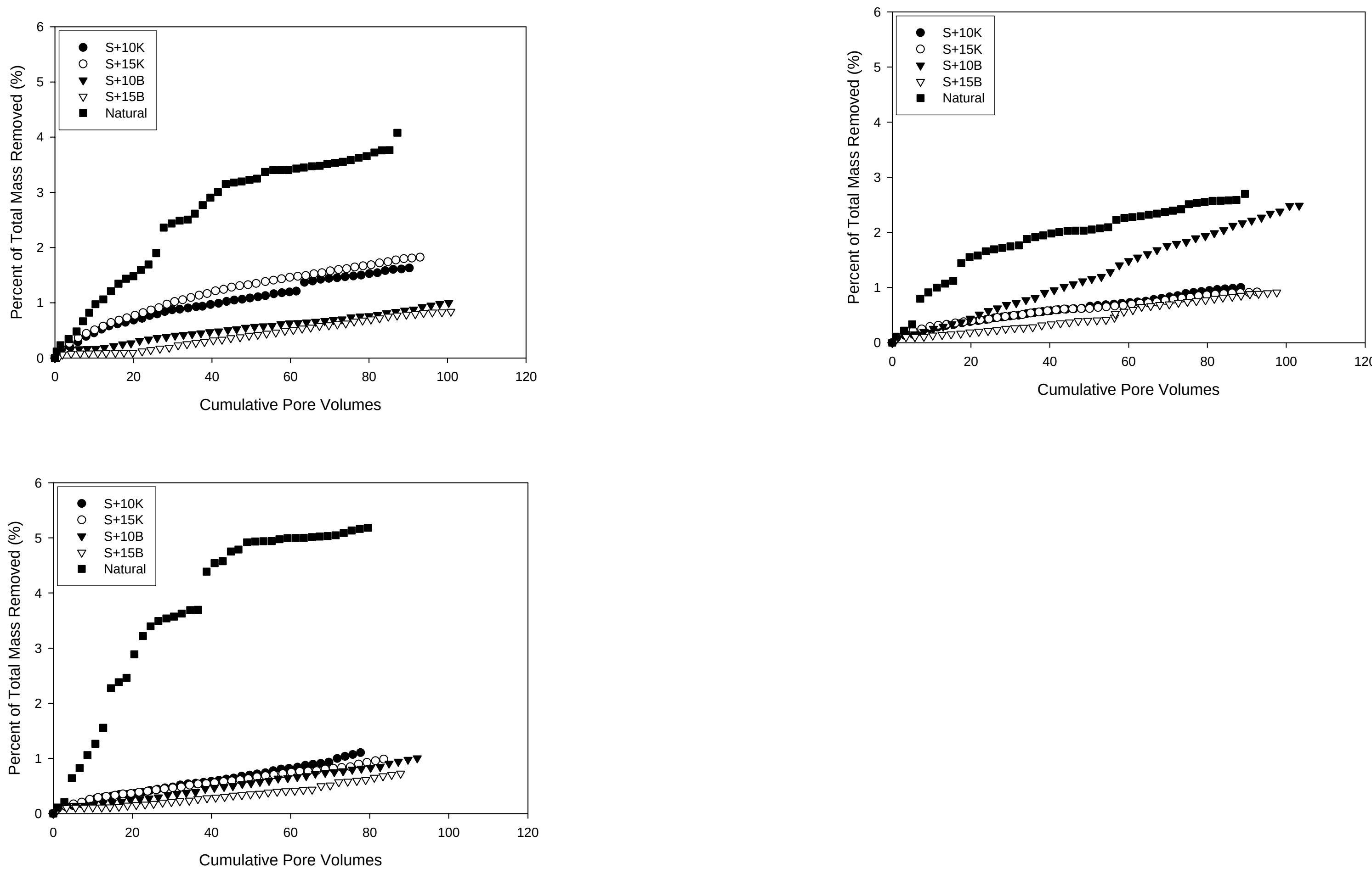

Figure F.3: Colloidal Removal Efficiencies for High (1.0M) Ionic Strength for All Soils at Low (top left), Medium (bottom left), and High (top right) Hydraulic Gradient Variations